
REINFORCEMENT LEARNING UNDER MODEL RISK FOR BIOMANUFACTURING FERMENTATION CONTROL

Bo Wang¹, Wei Xie^{*1}, Tugce Martagan², and Alp Akcay²

¹Northeastern University, Boston, MA 02115

²Eindhoven University of Technology, 5612 AZ Eindhoven, Netherlands

ABSTRACT

In the biopharmaceutical manufacturing, fermentation process plays a critical role impacting on productivity and profit. Since biotherapeutics are manufactured in living cells whose biological mechanisms are complex and have highly variable outputs, in this paper, we introduce a model-based reinforcement learning framework accounting for model risk to support bioprocess online learning and guide the optimal and robust customized stopping policy for fermentation process. Specifically, built on the dynamic mechanisms of protein and impurity generation, we first construct a probabilistic model characterizing the impact of underlying bioprocess stochastic uncertainty on impurity and protein growth rates. Since biopharmaceutical manufacturing often has very limited batch data during the development and early stage of production, we derive the posterior distribution quantifying the process model risk, and further develop the Bayesian rule based knowledge update to support the online learning on underlying stochastic process. With the prediction risk accounting for both bioprocess stochastic uncertainty and model risk, the proposed reinforcement learning framework can proactively hedge all sources of uncertainties and support the optimal and robust customized decision making. We conduct the structural analysis of optimal policy and study the impact of model risk on the policy selection. We can show that it asymptotically converges to the optimal policy obtained under perfect information of underlying stochastic process. Our case studies demonstrate that the proposed framework can greatly improve the biomanufacturing industrial practice.

Keywords Biopharmaceutical manufacturing, model-based reinforcement learning, model risk, cell culture, process control, online learning

1 Introduction

The biopharma industry is growing rapidly and is increasingly able to cure severe health diseases, such as cancer and adult blindness. However, the current systems are unable to rapidly produce new drugs when needed when there is major public health issue. Drug shortages have occurred at unprecedented rates over the past decade, especially during the COVID-19 pandemic. For example, even after COVID-19 vaccines are developed (such as the bio-drugs discovered by Moderna and Pfizer-BioNTech), manufacturing and distributing the billions of doses needed to immunize the world's population is very challenging and time-consuming using existing technologies, lengthening the time period of human and economic distress. *To overcome those challenges, it is critical to accelerate the production process development, improve productivity and production reliability, and shorten the time to market.*

Biopharmaceutical manufacturing processes are typically divided into upstream cell culture, downstream purification, and filling/formulation process. Among the operations, the bioreactor fermentation process plays a critical role, where living cells are mixed with appropriate medium under carefully controlled conditions to grow and produce the target drug substance or protein (e.g., Monoclonal antibodies and antigens). Since the target protein is mainly produced in this operation unit, the fermentation process directly determines the productivity of the whole process. In addition, as byproducts, metabolic wastes, unwanted proteins and mixtures, i.e., impurities, will also be generated at the meantime, better control of fermentation can efficiently reduce the metabolic waste generation, decrease the cost of downstream purification, and support the sustainable biomanufacturing.

*Corresponding author: w.xie@northeastern.edu

The fermentation process control faces critical challenges, including complexity, high variability, and limited process observations. Different with the classical small molecular chemical based pharmaceutical manufacturing, biotherapeutics are manufactured in living cells whose biological processes are complex and have highly variable outputs. The productivity and product critical quality attributes (CQAs) are usually determined by complex interactions of many factors (e.g., raw materials, media compositions, critical process parameters (CPPs)) from each phase of cell culture life cycle. Since a small change in one input factor, such as media composition, gene expression, and cell culture conditions, could cause huge impact on the production trajectories of protein and impurity, the fermentation usually involves high inherent bioprocess *stochastic uncertainty*. In addition, living cells dynamically adjust to their environments and there is lack of complete knowledge on underlying bioprocess mechanisms. Thus, the *customized decision making* is needed to account for process stochastic uncertainty, adapt to the production process state (i.e., protein and impurity levels) evolution, and further improve biomanufacturing flexibility, productivity, production reliability and sustainability.

In this paper, we consider batch-based production, e.g., batch or fed-batch bioreactors, which is widely used in current biopharmaceutical manufacturing industry. The average value of one batch of biopharma product exceeds \$1 million [1]. Even though biomanufacturing process is complex and has high stochastic uncertainty, there are often limited batch data, especially during process development and early stage of manufacturing. For example, during process development, biomanufacturing companies often need to optimize the process based on three batch runs. Estimating the bioprocess model parameters (e.g., cell growth rate, protein production rate), especially with limited batch replication data, will induce high model estimation error, called *model risk*. Ignoring the model risk can lead to high overconfidence bias, which will impact the robustness and reliability of process decision making. Therefore, it is critical to develop a mode-based control strategy, accounting for model risk, to simultaneously facilitate bioprocess learning to reduce the model risk and guide the optimal, intensified and reliable decision making, which can improve productivity and production stability.

For biomanufacturing fermentation processes, various control strategies have been developed to support dynamic decision making, such as manipulating feed rate [2], deciding fermentation stopping time [3], fault detection and diagnosis [4]. Existing methodologies can be categorized into: (1) open loop control where predetermined strategies are calculated based on initial/operating conditions [5, 6]; (2) adaptive control where parameters of controller are adapted to non-linear dynamics or uncertainties over operation [7, 8]; (3) fuzzy control based on fuzzy logic describing the process state evolution [9]; and (4) model-based predictive control which requires predictive process model, such as mechanistic models, flux balance, simulations, multivariate statistical models, neural networks, and the control strategies are carried out through optimization over certain process variables [10, 11, 12, 13]. However, existing studies typically either ignore or do not explicitly quantify the impact of model risk on the process control decision making.

In this paper, we consider a fermentation process model that can capture the kinetics mechanism as well as the inherent process stochastic variability. Then, we develop the Bayesian rule based inference to support the online learning of interpretable model coefficients (i.e., cell, protein and impurity growth rates) and derive the posterior distribution quantifying the model coefficient estimation uncertainty, called model risk. Further built on that, we create the model-based reinforcement learning to guide the “when to harvest” decision for fermentation process. It explicitly accounts for the impact of model risk on prediction risk and models the dynamic update of posterior hyper parameters as “knowledge states”, which allows us to simultaneously guide process learning and decision making, and balance exploration and exploitation. After that, we perform structural and sensitivity analyses to study the properties of value function and optimal policy, and analyze how they are impacted by model risk. Our case study demonstrates the proposed framework can outperform the existing approaches and industry practice.

The key contributions and benefits of this paper can be summarized as following: (1) the bioprocess model-based reinforcement learning can rigorously account for the impact of model risk on fermentation process control decision making; (2) we derive the structural and sensitivity analyses to quantify the impact of model risk on value function and optimal policy, which can provide useful insights to guide the reliable decision making; (3) the proposed model based reinforcement learning under model risk can automatically balance exploration and exploitation, which can simultaneously facilitate process learning and guide the cost-efficient, intensified, reliable, and customized stopping decision for fermentation. Therefore, the proposed reinforcement learning framework can support biomanufacturing automation, enhance productivity, and improve production stability. It can provide a reliable and robust decision guidance for production process at different stages of development with various amounts of historical data.

2 Background

Here, we review the most related literature studies, including bioprocess model-based predictive control and reinforcement learning methodologies for biomanufacturing. For model-based predictive control, models are built to capture and predict bioprocess dynamics, which can be used to guide the search for optimal control strategies. The bioprocess

models are usually built based on deterministic ordinary or partial differential equations (ODE/PDE) mechanistic models, machine learning models (such as neural networks), and stochastic models. For example, [10] constructed the dynamic flux balance models for bioreactor fermentation. Then, they developed the closed-loop control for feed rate and dissolved oxygen concentration profiles to maximize the production. [12] constructed a neural network to model the nonlinear relationship between time-dependent fermentation parameters and antibiotic effects linking to cell growth. Then, the trained neural network is used to support the optimization of fermentation control parameters. Besides the deterministic models, stochastic models were developed to model the bioprocess inherent stochastic uncertainty for fermentation [3] and chromatography [14]. By using the fitted model to characterize the underlying true state transition, they further constructed Markov decision process (MDP) to guide the fermentation harvest decisions [3], dynamic pooling window selections for chromatography [14], or both [15]. However, those studies ignore model risk, which could lead to suboptimal decision policy, especially under the situations with limited bioprocess data.

Recently, various reinforcement learning approaches have been developed for bioprocess control. For example, [16, 17] developed model-free deep-Q-network based reinforcement learning approaches to maintain cells at target populations by controlling the feeding profiles and to maximize the yield by controlling the feeding flow rate. [18] constructed a model-based reinforcement learning for biomanufacturing control, with predictive distribution of system response accounting for both inherent stochastic uncertainty and model risk. After that, they proposed a green simulation assisted policy gradient algorithm that can efficiently reuse the previous process output trajectories to improve the estimation accuracy of policy gradient and speed up the search for the optimal policy. Our methodology is different with [18], in terms of: (1) we incorporate posterior hyper parameters as knowledge states, that both value function and policy will be based on; and (2) they focus on developing new optimization solution algorithm instead of modeling bioprocess mechanism model-based reinforcement learning and providing a comprehensive study on how model risk impacts on the bioprocess control.

In reinforcement learning literature, the model-based Bayesian Reinforcement learning, or the Bayes-Adaptive Markov decision process (BAMDP), explicitly takes a posterior of model parameters as knowledge state and the optimal policy depends on both physical and knowledge states. A comprehensive review of Bayesian reinforcement learning methodologies can be found in [19]. Notice that we can also take unknown model parameters as unobservable states of the system, which can be formulated as a partially observable Markov decision process (POMDP) [20]. Since solving the original model-based Bayesian Reinforcement learning is notoriously complex due to potential huge state space, various approximation algorithms have been developed, including offline value approximation computing the policy a priori through POMDP planning [21]; online near-myopic value and tree search approximation that focus on observed/realized knowledge states in planning [22, 23, 24]; and exploration bonus based methods where an agent acts according to an optimistic model of MDP under uncertainty [25, 26, 27]. Motivated by those studies, in this paper, we develop the model based Bayesian reinforcement learning, accounting for model risk, to guide the harvest decisions for fermentation process. Then, we provide structural and sensitivity analyses to study how the model risk impacts on value function and optimal policy.

3 Problem Description

In Section 3.1, we briefly introduce the background of biomanufacturing fermentation process. Then, in Section 3.2, we summarize the proposed model-based reinforcement learning framework, accounting for model risk, and present the insights why it can facilitate the fermentation process development and guide the customerized, optimal and robust harvest decision making.

3.1 Biomanufacturing Fermentation Process Description

We are interested in process development and operational decision making for bioreactor fermentation being the heart of typical biopharmaceuticals manufacturing; see more information on fermentation in [28, 3, 14, 15]. During fermentation process, cell culture goes through several metabolic phases. First, the cells adjust to their new environment (lag phase). Next, their growth rate steadily increases for a period of time (exponential growth phase), after which it slows down (deceleration phase) and reaches a steady state (stationary phase) followed by cell death (death phase); see Figure 1. Notice that the durations for lag, acceleration and deceleration phases are relatively short, and the fermentation process will stop once entering the stationary phase. In this paper, we consider the most critical exponential growth and stationary phases for simplification. During exponential growth, the target protein and unwanted impurities will both accumulate. Waiting too long to stop the process, in anticipation of a higher yield of target protein, may result in a larger amount of impurities. In turn, this could increase the difficulty and cost of downstream purification operations. This phenomenon is referred to as the *purity-yield trade-off* in the fermentation process. *Thus, our objective is to find the optimal and customized "when to stop" decision for batch-based fermentation production process so that we can*

maximize the expected profit for each batch. Notice that given the times staying in each phase can be estimated in advance, the proposed framework can be extended to multi-phase fermentation processes.

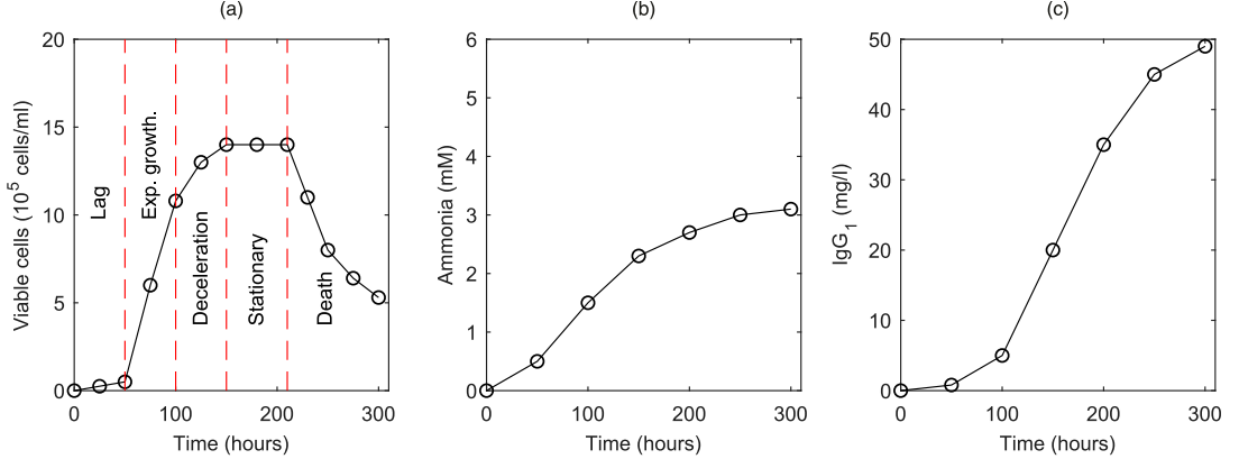


Figure 1: The cell culture goes through several metabolic phases during fermentation [28].

The bioprocess state transitions quantify how the batch critical attributes (i.e., protein and impurity levels) dynamically evolve during the production process, which is often characterized by PDE/ODE based kinetic mechanism models in biomanufacturing. The existing bioprocess modeling studies, see for example [29, 30, 31], typically assume that the structure of mechanistic models is known and coefficients are estimated from data. In this paper, we assume the parametric distribution families, characterizing the state transitions, are known. The model parameters are estimated from finite process data, which introduces *model risk* (MR). Thus, the bioprocess state transition model leverages the mechanism of cell culture and also facilitates the learning of interpretable bioprocess model parameters (i.e., protein and impurity growth rates) from real-world data. We are interested in how MR impacts on the optimal decision making. *Given very limited historical batch data, we develop the model-based reinforcement learning (RL), accounting for model risk, to simultaneously learn the underlying stochastic process model coefficients or bioprocess underlying mechanisms, and accelerate the search for the optimal decisions for biomanufacturing fermentation, which can balance exploration and exploitation and speed up the process development.*

3.2 Summary of Proposed RL Framework to Support Fermentation Harvest Automation

Here, we summarize the proposed model-based reinforcement learning framework accounting for model risk to guide the optimal harvest decision for fermentation or cell culture process. Suppose we can measure the status of each batch at discrete time points $\mathcal{T} = \{t : 0, 1, \dots, \bar{T}\}$, and the end time of the exponential growth phase \bar{T} can be determined in advance. Let T ($0 \leq T \leq \bar{T}$) denote the random stopping time determined by the customized fermentation harvest decision, which considers the purity-yield trade-off. At each decision time point t , based on the current measurements of protein and impurity levels, or “physical state” denoted by $\mathcal{S}_t = (p_t, i_t)$, the agent can take action $a_t \in \{C, H\}$ either to harvest (i.e., $a_t = H$) or continue fermentation (i.e., $a_t = C$). If continuing fermentation, the protein and impurity will further accumulate and evolve to next state, $\mathcal{S}_{t+1} = (p_{t+1}, i_{t+1})$, following the underlying unknown physical states transition model, denoted by $F^c \equiv \Pr(\mathcal{S}_{t+1} | \mathcal{S}_t, a_t = C)$. Suppose the “correct” model F^c , characterizing the fermentation process kinetics and intrinsic stochastic uncertainty, can be specified by parameters θ^c . If the action is harvest $a_t = H$, we stop the fermentation process, set the stopping time $T = t$, and collect a batch with protein and impurity levels (p_t, i_t) . In the paper, we use the superscript “c” to represent the decision and response obtained under the situation when there is perfect information on the underlying state transition model F^c .

Suppose that the reward function $R(\mathcal{S}_t, a_t)$ corresponds to the operational cost for one period fermentation $R(\mathcal{S}_t, a_t = C)$, and gross profit at harvest $R(\mathcal{S}_t, a_t = H)$, which accounts for revenue from protein value, purification and other costs. Thus, under the situation with the perfect information on the correct model F^c , “when to stop” decision making for each batch fermentation run can be formulated as an markov decision problem (MDP). A non-stationary policy, denoted by $\pi^c \equiv \{\pi_t^c(\cdot); t = 0, 1, \dots, T\}$ guiding the harvest decisions, is a collection of time dependent functions, that map from any physical states to an action, i.e., $a_t = \pi_t^c(\mathcal{S}_t)$.

Given any policy π^c , the total expected discounted reward is,

$$\rho^c(\pi^c) = \mathbf{E}_{\tau^c} \left[\sum_{t=0}^T \gamma^t R(\mathcal{S}_t, a_t) \middle| \mathcal{S}_0, \pi^c \right], \quad (1)$$

where $\gamma \in (0, 1]$ is the discount factor and the expectation takes with respect to the stochastic decision process trajectory $\tau^c \equiv (\mathcal{S}_0, a_0, \mathcal{S}_1, a_1, \dots, \mathcal{S}_{T-1}, a_{T-1}, \mathcal{S}_T)$. The objective is to find the optimal policy maximizing the expected overall reward, $\pi^{c*} = \arg \max_{\pi^c} \rho^c(\pi^c)$. At any time period t , the value function $V_t^c(\mathcal{S}_t)$ is defined as the expected total reward achievable starting in state \mathcal{S}_t following the optimal policy π^{c*} , i.e.,

$$V_t^c(\mathcal{S}_t) = \mathbb{E}_{\tau_t^c} \left[\sum_{\ell=t}^T \gamma^\ell R(\mathcal{S}_\ell, a_\ell) \middle| \mathcal{S}_t, \pi^{c*} \right],$$

where $\tau_t^c = (\mathcal{S}_t, a_t, \dots, a_{T-1}, \mathcal{S}_T)$ represents possible trajectory starting at \mathcal{S}_t . Further, to search for the optimal policy, given any policy π^c , we evaluate its performance by taking action $a_t = \pi_t^c(\mathcal{S}_t) \in \{C, H\}$ at state \mathcal{S}_t and calculate the Q -function based on the Bellman equation as follows,

$$Q_T^c(\mathcal{S}_T, a_T = H) = R(\mathcal{S}_T, a_T = H),$$

and

$$Q_t^c(\mathcal{S}_t, a_t = C) = R(\mathcal{S}_t, a_t = C) + \gamma \mathbb{E}_{F^c} \left[\max_{a_{t+1}} Q_{t+1}^c(\mathcal{S}_{t+1}, a_{t+1}) \right].$$

When there is perfect information of underlying process state transition model F^c , the optimal policy obtained by Markov decision process is represented as $\pi_t^{c*}(\mathcal{S}_t) = \arg \max_{a_t} Q_t^c(\mathcal{S}_t, a_t)$.

However, the underlying bioprocess model parameters θ^c , characterizing the dynamic evolution of physical state, are unknown and estimated from limited fermentation process data, which can induce the model parameter estimation uncertainty, called *model risk*. Therefore, in this paper, we first develop a process model, denoted by $p(\mathcal{S}_{t+1} | \mathcal{S}_t, a_t, \theta)$, that can leverage the ODE/PDE-based mechanisms and characterize the bioprocess inherent stochastic uncertainty in Section 4. Then, we provide the Bayesian inference to support the online learning of model coefficients and derive the posterior distribution $p(\theta | \mathcal{X}_t)$, quantifying the model risk, where \mathcal{X}_t denotes the fermentation process historical data. Then, the physical state evolution *prediction risk* is quantified by the posterior predictive distribution $p(\mathcal{S}_{t+1} | \mathcal{S}_t, a_t, \mathcal{X}_t) = \int p(\mathcal{S}_{t+1} | \mathcal{S}_t, a_t, \theta) p(\theta | \mathcal{X}_t) d\theta$ accounting for both stochastic uncertainty and model risk. We derive the variance decomposition to measure the contributions from stochastic uncertainty and model risk on the prediction variance in Section 6.1.

Then, we create the model-based reinforcement learning, accounting for model risk, to simultaneously guide the underlying bioprocess mechanism online learning and dynamic decision making in Section 5. Specifically, we consider the system “hyper states” $\mathcal{H}_t \equiv (\mathcal{S}_t, \mathcal{I}_t)$, where \mathcal{I}_t is the “knowledge state” characterizing the current belief of underlying bioprocess coefficients, specified by hyper-parameters of posterior distribution $p(\theta | \mathcal{X}_t)$. Then, the hyper state transitioning $\Pr(\mathcal{S}_{t+1}, \mathcal{I}_{t+1} | \mathcal{S}_t, \mathcal{I}_t, a_t) = \Pr(\mathcal{S}_{t+1} | \mathcal{S}_t, \mathcal{I}_t, a_t) \Pr(\mathcal{I}_{t+1} | \mathcal{S}_{t+1}, \mathcal{S}_t, \mathcal{I}_t, a_t)$ models the evolution of physical and knowledge states. Thus, the policy and value functions of proposed model-based reinforcement learning (RL) will depend on both physical and knowledge states, denoted by $a_t = \pi_t(\mathcal{S}_t, \mathcal{I}_t)$ and $V_t(\mathcal{S}_t, \mathcal{I}_t)$. The objective is to find policy $\pi \equiv \{\pi_t(\cdot); t = 0, 1, \dots, T\}$ maximizing the expected total reward $\pi^* = \arg \max_{\pi} \rho(\pi)$,

$$\rho(\pi) = \mathbb{E}_{\tau} \left[\sum_{t=0}^T \gamma^t R(\mathcal{S}_t, a_t) \middle| \mathcal{H}_0, \pi \right],$$

where $\tau \equiv (\mathcal{H}_0, a_0, \mathcal{H}_1, a_1, \dots, \mathcal{H}_{T-1}, a_{T-1}, \mathcal{H}_T)$ is the trajectory of hyper states decision process. The Q -function of taking action $a_t = \pi_t(\mathcal{S}_t, \mathcal{I}_t) \in \{C, H\}$ at state \mathcal{H}_t is

$$Q_t(\mathcal{H}_t, a_t = C) = R(\mathcal{S}_t, a_t = C) + \gamma \mathbb{E}_{\Pr(\mathcal{S}_{t+1}, \mathcal{I}_{t+1} | \mathcal{S}_t, \mathcal{I}_t, a_t)} \left[\max_{a_{t+1}} Q_{t+1}(\mathcal{H}_{t+1}, a_{t+1}) \right].$$

Therefore, the optimal policy obtained by model-based reinforcement learning is represented as $\pi_t^*(\mathcal{S}_t, \mathcal{I}_t) = \arg \max_{a_t} Q_t(\mathcal{S}_t, \mathcal{I}_t, a_t)$. *Since the prediction risk of the state $\{\mathcal{S}_t\}$ sample trajectories considers both process stochastic uncertainty and model risk, the proposed model-based reinforcement learning will lead to the optimal and robust decision equally hedging both sources of uncertainties.*

To study the structural properties of value function $V_t(\mathcal{S}_t, \mathcal{I}_t)$ with respect to both physical state \mathcal{S}_t and knowledge state \mathcal{I}_t , we derive the structural analysis in Sections 6.2 and 6.3. In addition, we provide the sensitivity analysis to study the impact of model risk on the selection of the optimal policy in Section 6.4 by: (1) studying the change of optimal policy $\pi_t^*(\mathcal{S}_t, \mathcal{I}_t)$ with respect to knowledge states \mathcal{I}_t , under different levels of model risk; and (2) comparing optimal policy $\pi_t^*(\mathcal{S}_t, \mathcal{I}_t)$ with the optimal policy $\pi_t^{c*}(\mathcal{S}_t)$ with perfect information on F^c , and proving the asymptotic consistency. *We can show that under higher model risk, the optimal policy tends to be more conservative, i.e., we will harvest with smaller amount of protein and impurity, to proactively hedge against higher prediction risk.*

Given any policy π , we could implement in the real process with underlying model F^c and *evaluate* its performance in terms of the total expected discounted reward,

$$\rho^c(\pi) = \mathbb{E}_{\tau^c} \left[\sum_{t=0}^T \gamma^t R(\mathcal{S}_t, a_t) \middle| \mathcal{S}_0, \pi \right].$$

The standard deviation (SD) of the total reward can be used to measure the *process stability* or *batch-to-batch variation*,

$$\text{SD}^c(\pi) = \text{SD}_{\tau^c} \left[\sum_{t=0}^T R(\mathcal{S}_t, a_t) \middle| \mathcal{S}_0, \pi \right].$$

For comparison, we also consider a reinforcement learning ignoring the model risk, which relies on the point estimator of the model parameters $\hat{\theta}$ from limited fermentation data \mathcal{X}_t . The optimal policy is then solved by Q-learning under the estimated model,

$$\hat{Q}_t(\mathcal{S}_t, a_t = C) = R(\mathcal{S}_t, a_t = C) + \gamma \mathbb{E}_{\hat{F}} \left[\max_{a_{t+1}} \hat{Q}_{t+1}(\mathcal{S}_{t+1}, a_{t+1}) \right],$$

where $\hat{F} = \Pr(\mathcal{S}_{t+1} | \mathcal{S}_t, a_t = C; \hat{\theta})$, and the optimal policy is represented as $\hat{\pi}_t^*(\mathcal{S}_t) = \arg \max_{a_t} \hat{Q}_t(\mathcal{S}_t, a_t)$. *Our study indicates that the proposed model-based reinforcement learning accounting for model risk can outperform the optimal policy ignoring the model risk in term of providing higher expected reward and reducing the batch-to-batch variation.*

4 Fermentation Process Modeling and Online Learning

In Section 4.1, we propose a fermentation process model to capture the kinetics mechanism as well as the inherent bioprocess stochastic uncertainty. It can leverage the information from existing ODE-based bioprocess mechanism model and facilitate the learning of *interpretable model coefficients* from real-world process data. Given limited historical data, in Section 4.2, we apply the Bayesian inference and derive the posterior distribution quantifying the model estimation uncertainty, called *model risk* (MR). With more process data collected, the Bayesian rule based knowledge update is derived to support the online learning.

4.1 Fermentation Process Modeling

Suppose we can measure the status of protein and impurity during fermentation process at discrete time points $\mathcal{T} = \{t : 0, 1, \dots, T\}$ with T denoting the stopping time of this batch. Here the unit time depends on the process-specific characteristics and it could be days. For the fermentation process, the cell growth kinetics is often represented by the ordinary differential equation (ODE) based mechanism model [28], i.e., $dX/dt = \mu X$. It can give the kinetics of cell concentration in one time period, $X_{t+1} = X_t e^{\mu}$, where X_t and X_{t+1} represent the starting and ending concentrations, and μ is the *specific growth rate*. Therefore, in the experiential growth phase, the dynamic evolution of protein and impurity in each time period can be modeled as a hybrid model,

$$\begin{cases} p_{t+1} = p_t \cdot e^{\Phi_t}, & \Phi_t \sim \mathcal{N}(\mu_c^{(p)}, \sigma_c^{(p)2}) \\ i_{t+1} = i_t \cdot e^{\Psi_t}, & \Psi_t \sim \mathcal{N}(\mu_c^{(i)}, \sigma_c^{(i)2}) \end{cases} \quad (2)$$

where (p_t, i_t) and (p_{t+1}, i_{t+1}) are the starting and ending protein and impurity levels during the t -th time period. Since the protein and impurity generation rates depend many factors, e.g., working cell viability, gene expression, and media compositions, we model the specific growth rates Φ_t and Ψ_t for protein and impurity by independent random variables, accounting for the *bioprocess inherent stochastic uncertainty*. Notice that the growth rates model the population behaviors of many cells in one batch. By applying central limit theory (CLT), Normal distribution is used to characterize the variability of protein and impurity growth rates, i.e., $\Phi_t \sim \mathcal{N}(\mu_c^{(p)}, \sigma_c^{(p)2})$ and $\Psi_t \sim \mathcal{N}(\mu_c^{(i)}, \sigma_c^{(i)2})$. This normality assumption is often used in the existing biopharmaceutical manufacturing studies; see for example [32]. It also makes the online learning, structural and sensitivity analyses tractable and further provides good and interpretable insights on how the model risk impacts on the optimal harvest decision policy.

4.2 Bayesian Inference for Bioprocess Online Learning and Model Risk Quantification

Let $\theta^c \equiv \{\mu_c^{(p)}, \sigma_c^{(p)2}, \mu_c^{(i)}, \sigma_c^{(i)2}\}$ denote the underlying true mean and variance coefficients for protein and impurity growth rates in the exponential growth phase (see eq. (2)), which are unknown and estimated by limited real-world data.

Here, we provide the Bayesian inference to derive the posterior distribution quantifying the bioprocess model estimation uncertainty and facilitate the online learning. We model the prior beliefs on the mean and variance coefficients by a noninformative normal-inverse-gamma,

$$\begin{cases} \mu^{(p)}, \sigma^{(p)2} \sim \mathcal{N}(\alpha_0^{(p)}, \sigma^{(p)2}/\nu_0^{(p)}) \cdot \text{Inv}\Gamma(\lambda_0^{(p)}, \beta_0^{(p)}) \\ \mu^{(i)}, \sigma^{(i)2} \sim \mathcal{N}(\alpha_0^{(i)}, \sigma^{(i)2}/\nu_0^{(i)}) \cdot \text{Inv}\Gamma(\lambda_0^{(i)}, \beta_0^{(i)}) \end{cases} \quad (3)$$

In each time period, we collect a sample and record the data $(p_t, i_t) \rightarrow (p_{t+1}, i_{t+1})$ to track the dynamic evolution of protein and impurity. We can compute the independent increments, denoted by $\phi_t \equiv \ln(p_{t+1}/p_t)$ and $\psi_t \equiv \ln(i_{t+1}/i_t)$. At the beginning of any time period t , let $\mathcal{X}_t \equiv \mathcal{X}_0 \cup \{\phi_0, \psi_0, \dots, \phi_{t-1}, \psi_{t-1}\}$ represent the historical data collected so far, where \mathcal{X}_0 denotes the data from previous batches.

We quantify the model risk with the posterior $p(\boldsymbol{\theta}|\mathcal{X}_t)$. Let $J_t \equiv |\mathcal{X}_t|/2$ be the size of all the historical growth data collected so far for protein or impurity until t . For notation simplification, we can rewrite all the observed data as $\mathcal{X}_t = \{\phi^{(j)}, \psi^{(j)}; j = 1, \dots, J_t\}$. Similarly, $J_0 = |\mathcal{X}_0|/2$ denotes the size of data collected before the current batch of fermentation process. Given the prior beliefs as shown in eq.(3), by following the derivation in [33], the posterior of protein and impurity growth rate distribution coefficients can be specified as following,

$$\begin{cases} \mu^{(p)}, \sigma^{(p)2} \sim \mathcal{N}(\alpha_t^{(p)}, \sigma^{(p)2}/\nu_t^{(p)}) \cdot \text{Inv}\Gamma(\lambda_t^{(p)}, \beta_t^{(p)}) \\ \mu^{(i)}, \sigma^{(i)2} \sim \mathcal{N}(\alpha_t^{(i)}, \sigma^{(i)2}/\nu_t^{(i)}) \cdot \text{Inv}\Gamma(\lambda_t^{(i)}, \beta_t^{(i)}), \end{cases}$$

with the hyper-parameters for protein accumulation,

$$\begin{cases} \alpha_t^{(p)} = \frac{\nu_0^{(p)}\alpha_0^{(p)} + J_t\bar{\phi}}{\nu_0^{(p)} + J_t}, \nu_t^{(p)} = \nu_0^{(p)} + J_t, \lambda_t^{(p)} = \lambda_0^{(p)} + \frac{J_t}{2}, \\ \beta_t^{(p)} = \beta_0^{(p)} + \frac{1}{2} \sum_{j=1}^{J_t} (\phi^{(j)} - \bar{\phi})^2 + \frac{\nu_0^{(p)}(\bar{\phi} - \alpha_0^{(p)})^2}{2(\nu_0^{(p)} + J_t)}, \end{cases} \quad (4)$$

where $\bar{\phi} = \sum_{j=1}^{J_t} \phi^{(j)}/J_t$ is the sample mean. Similar results also apply to the impurity accumulation, and we can obtain the posterior hyper-parameters $\alpha_t^{(i)}, \nu_t^{(i)}, \lambda_t^{(i)}, \beta_t^{(i)}$.

In addition, we can show the asymptotic consistency. As the sample size increases to infinity $J_t \rightarrow \infty$, the posterior expected values of model coefficients, $E[\mu^{(p)}|\mathcal{X}] = \alpha_t^{(p)} \rightarrow \bar{\phi}$ and $E[\sigma^{(p)2}|\mathcal{X}] = \frac{\beta_t^{(p)}}{\lambda_t^{(p)} - 1} \rightarrow \frac{1}{J_t - 1} \sum_{j=1}^{J_t} (\phi_j - \bar{\phi})^2$, are equal to the sample mean and variance, which further converge to the underlying true coefficients, denoted by $\mu_c^{(p)}$ and $\sigma_c^{(p)2}$. The model estimation uncertainty, quantified by posterior variance, converges to zero, $\text{Var}[\mu^{(p)}|\mathcal{X}] = \frac{\beta_t^{(p)}}{(\lambda_t^{(p)} - 1)\nu_t^{(p)}} \rightarrow 0$ and $\text{Var}[\sigma^{(p)2}|\mathcal{X}] = \frac{\beta_t^{(p)2}}{(\lambda_t^{(p)} - 1)^2(\lambda_t^{(p)} - 2)} \rightarrow 0$ as more data collected $J_t \rightarrow \infty$.

Then, we focus the current batch fermentation run and derive the posterior update as the new data are collected, which can support the *online learning*. Once the new data (ϕ_t, ψ_t) are collected, the Bayesian rule is used for posterior updating $p(\boldsymbol{\theta}|\mathcal{X}_{t+1}) \propto p(\boldsymbol{\theta}|\mathcal{X}_t)p(\phi_t, \psi_t|\boldsymbol{\theta})$ and supporting the online learning,

$$\begin{cases} \mu^{(p)}, \sigma^{(p)2} \sim \mathcal{N}(\alpha_{t+1}^{(p)}, \sigma^{(p)2}/\nu_{t+1}^{(p)}) \cdot \text{Inv}\Gamma(\lambda_{t+1}^{(p)}, \beta_{t+1}^{(p)}) \\ \mu^{(i)}, \sigma^{(i)2} \sim \mathcal{N}(\alpha_{t+1}^{(i)}, \sigma^{(i)2}/\nu_{t+1}^{(i)}) \cdot \text{Inv}\Gamma(\lambda_{t+1}^{(i)}, \beta_{t+1}^{(i)}), \end{cases} \quad (5)$$

where the hyper-parameters will update as follow,

$$\begin{cases} \alpha_{t+1}^{(p)} = \alpha_t^{(p)} + \frac{\phi_t - \alpha_t^{(p)}}{\nu_{t+1}^{(p)}}, \nu_{t+1}^{(p)} = \nu_t^{(p)} + 1, \lambda_{t+1}^{(p)} = \lambda_t^{(p)} + \frac{1}{2}, \beta_{t+1}^{(p)} = \beta_t^{(p)} + \frac{\nu_t^{(p)}(\phi_t - \alpha_t^{(p)})^2}{2\nu_{t+1}^{(p)}}, \\ \alpha_{t+1}^{(i)} = \alpha_t^{(i)} + \frac{\psi_t - \alpha_t^{(i)}}{\nu_{t+1}^{(i)}}, \nu_{t+1}^{(i)} = \nu_t^{(i)} + 1, \lambda_{t+1}^{(i)} = \lambda_t^{(i)} + \frac{1}{2}, \beta_{t+1}^{(i)} = \beta_t^{(i)} + \frac{\nu_t^{(i)}(\psi_t - \alpha_t^{(i)})^2}{2\nu_{t+1}^{(i)}}. \end{cases} \quad (6)$$

The bioprocess prediction risk is quantified by the posterior predictive distribution, accounting for both bioprocess inherent stochastic uncertainty and model risk, i.e., $\tilde{\Phi}_{t'} \sim p(\phi_{t'}|\mathcal{X}_t) = \int p(\phi_{t'}|\boldsymbol{\theta})p(\boldsymbol{\theta}|\mathcal{X}_t)d\boldsymbol{\theta}$ for protein and $\tilde{\Psi}_{t'} \sim p(\psi_{t'}|\mathcal{X}_t) = \int p(\psi_{t'}|\boldsymbol{\theta})p(\boldsymbol{\theta}|\mathcal{X}_t)d\boldsymbol{\theta}$ for impurity prediction with $t' = t, t + 1, \dots, T$. Given the normal-inverse-gamma

conjugate prior, the prediction uncertainty of protein growth rate at t' is specified by $(\alpha_t^{(p)}, \nu_t^{(p)}, \lambda_t^{(p)}, \beta_t^{(p)})$. The predictive distribution of $\tilde{\Phi}_{t'}$ follows generalized t-distribution, see [34],

$$\{\tilde{\Phi}_{t'} | \mathcal{X}_t\} \sim t_{2\lambda_t^{(p)}} \left(\alpha_t^{(p)}, \frac{\beta_t^{(p)}(1 + \nu_t^{(p)})}{\nu_t^{(p)} \lambda_t^{(p)}} \right), \quad (7)$$

with the density function,

$$f_t^{(p)}(\phi_{t'} | \mathcal{X}_t) = \pi^{-1/2} \frac{\Gamma\left(\lambda_t^{(p)} + \frac{1}{2}\right)}{\Gamma(\lambda_t^{(p)})} \left[\frac{\nu_t^{(p)}}{2\beta_t^{(p)}(1 + \nu_t^{(p)})} \right]^{1/2} \left[1 + \frac{\nu_t^{(p)}(\phi_{t'} - \alpha_t^{(p)})^2}{2\beta_t^{(p)}(1 + \nu_t^{(p)})} \right]^{-\lambda_t^{(p)} - 1/2}. \quad (8)$$

Similar results can be obtained for the predictive distribution of the impurity growth rate.

5 Model-based Reinforcement Learning Accounting for Model Risk

In this section, we will present the bioprocess model based reinforcement learning, accounting for model risk, to guide the optimal and robust customized decision making for fermentation process.

Decision Epoch: For fermentation process, we consider the decision epochs for each batch production, i.e., the finite time horizon $\mathcal{T} = \{t : 0, 1, \dots, T\}$.

Physical State: At decision epoch t , the physical state is specified by the current protein and impurity levels, i.e., $\mathcal{S}_t = (p_t, i_t)$. Suppose that $p_t \in (0, \bar{P}]$, where \bar{P} denotes the maximum amount of protein due to the capacity of bioreactor. The impurity state space $i_t \in (0, \bar{I}] \cup \{I_f\}$, where \bar{I} is a predefined threshold value in accordance with FDA standards on batch quality and $\{I_f\}$ denotes a batch failure state whenever the impurity level is greater than threshold \bar{I} . In other words, once we have $i_t > \bar{I}$, the impurity state will transit to the failure state I_f .

Action Space: At decision epoch t before reaching to the stationary phase, we can take action $a_t \in A$ with the decision set $A \equiv \{C, H\}$, where C denotes to continue fermentation and H denotes the action to harvest. In this paper, we focus on the ‘‘when to stop’’ decision, i.e., at what condition we should stop the batch fermentation and harvest so that we can maximize the expected profit. We will directly harvest and terminate the episode: (1) once either protein or impurity level reaches the limits \bar{P} and \bar{I} ; (2) we have batch failure (i.e., the impurity level reaching the failure state I_f); or (3) the production reaches to the stationary phase (i.e., $t = \bar{T}$), which also defines the stopping time T .

Underlying Physical State Transition: At any time period t starting with physical states (p_t, i_t) , if the action is to continue fermentation $a_t = C$, the physical state transition for $(p_t, i_t) \rightarrow (p_{t+1}, i_{t+1})$ follows the bioprocess probabilistic hybrid model presented in eq.(2) with true model coefficients $\theta^c = \{\mu_c^{(p)}, \sigma_c^{(p)2}, \mu_c^{(i)}, \sigma_c^{(i)2}\}$.

Knowledge State: Since the bioprocess underlying model true coefficients θ^c are unknown and estimated with limited real-world data, the *knowledge state*, specified by the posterior distribution coefficients or moments, is used to quantify our current belief of θ^c characterizing the dynamic growth behaviors of protein and impurity. Following the derivation in Section 4.2 for Bayesian online learning, at any time period t , we specify the knowledge state with the hyper-parameters, $\mathcal{I}_t = \{\alpha_t^{(p)}, \nu_t^{(p)}, \lambda_t^{(p)}, \beta_t^{(p)}, \alpha_t^{(i)}, \nu_t^{(i)}, \lambda_t^{(i)}, \beta_t^{(i)}\}$.

Hyper State and State Transition: In this model-based reinforcement learning with model risk, we consider the *hyper states* $\mathcal{H}_t \equiv (\mathcal{S}_t, \mathcal{I}_t)$, including both physical state \mathcal{S}_t and knowledge state \mathcal{I}_t . If the action at time period t is to continue the fermentation, i.e., $a_t = C$, the hyper state transition probability for $(\mathcal{S}_t, \mathcal{I}_t) \xrightarrow{a_t=C} (\mathcal{S}_{t+1}, \mathcal{I}_{t+1})$ can be specified by,

$$\Pr(\mathcal{S}_{t+1}, \mathcal{I}_{t+1} | \mathcal{S}_t, \mathcal{I}_t, a_t) = \Pr(\mathcal{S}_{t+1} | \mathcal{S}_t, \mathcal{I}_t, a_t) \Pr(\mathcal{I}_{t+1} | \mathcal{S}_{t+1}, \mathcal{S}_t, \mathcal{I}_t, a_t), \quad (9)$$

where $\Pr(\mathcal{S}_{t+1} | \mathcal{S}_t, \mathcal{I}_t, a_t = C) = p(\phi_{t'}, \psi_t | \mathcal{I}_t)$ is the posterior predictive distribution following eq.(7)–(8) with $t' = t + 1$, and $\Pr(\mathcal{I}_{t+1} | \mathcal{S}_{t+1}, \mathcal{S}_t, \mathcal{I}_t, a_t)$ provides the knowledge state update by applying eq.(6). Therefore, since this hyper state transition accounts for both bioprocess inherent stochastic uncertainty and model risk, the proposed model-based reinforcement learning framework can equally proactively hedge against both sources of uncertainty, simultaneously guide the optimal reliable decision making and support the underlying process model learning.

Reward: We assume the fermentation operating cost for each time period is constant, denoted by c_u . Denote the penalty cost associated with batch failure by r_f . Suppose that the harvest reward only depends on the protein and impurity levels (p, i) at the harvest time (for $i \leq \bar{I}$), i.e., $r_h(p, i)$. Basically, more protein production gives more profit and more

impurity implies more cost required for downstream purification. Thus, suppose that the harvest reward $r_h(p, i)$ is non-decreasing in protein level p and non-increasing in impurity level i . Further, in this paper, we assume the harvest reward is a linear function of protein and impurity levels [3],

$$r_h(p, i) = c_0 + c_1 p - c_2 i, \quad c_1, c_2 > 0. \quad (10)$$

At any time period t , if the decision is continue $a_t = C$, we have the operating cost or the immediate reward $-c_u$. Otherwise, if the decision is harvest $a_t = H$, we stop the batch fermentation and obtain the harvest reward $r_h(p_t, i_t)$. If at any time $i_t = I_f$, we have the batch failure and get the failure penalty as the immediate reward $-r_f$. Thus, given the hyper states $(\mathcal{S}_t, \mathcal{I}_t)$ and the action a_t , the reward $R(\mathcal{S}_t, a_t)$ can be written as,

$$R(\mathcal{S}_t, a_t) = R(p_t, i_t, a_t) = \begin{cases} -r_f, & i_t = I_f, a_t = H \\ -c_u, & i_t \leq \bar{I}, a_t = C \\ r_h(p_t, i_t), & i_t \leq \bar{I}, a_t = H. \end{cases} \quad (11)$$

Policy: Here we define the nonstationary policy $\pi \equiv \{\pi_t(\cdot); t = 0, 1, \dots, T\}$ for the model-based reinforcement learning accounting for model risk, which maps from any hyper state $\mathcal{H}_t \equiv (\mathcal{S}_t, \mathcal{I}_t)$ to an action a_t , i.e., $a_t = \pi_t(\mathcal{S}_t, \mathcal{I}_t)$. Given a policy π , the total expected discounted reward is,

$$\rho(\pi) = \mathbb{E}_\tau \left[\sum_{t=0}^T \gamma^t R(\mathcal{S}_t, a_t) \middle| \mathcal{H}_0, \pi \right], \quad (12)$$

where $\gamma \in (0, 1]$ is the discount factor and the expectation takes with respect to the stochastic decision process trajectory $\tau \equiv (\mathcal{H}_0, a_0, \mathcal{H}_1, a_1, \dots, \mathcal{H}_{T-1}, a_{T-1}, \mathcal{H}_T)$. Our objective is to find the optimal policy maximizing the expected overall reward, $\pi^* = \arg \max_\pi \rho(\pi)$. *Since this stochastic optimization considers both bioprocess inherent stochastic uncertainty and model risk through the evolution of hyper state $\Pr(\mathcal{H}_{t+1} | \mathcal{H}_t, a_t)$ in eq. (9), the optimal policy π^* will automatically balance the exploration and exploitation trade-off and facilitate simultaneously learning and searching for the optimal reliable policy for the underlying fermentation process.*

Value Function: At any time period t , the value function $V_t(\mathcal{S}_t, \mathcal{I}_t)$ is defined as the expected total reward achievable starting from the hyper state $\mathcal{H}_t = (\mathcal{S}_t, \mathcal{I}_t)$ following the optimal policy π^* , i.e.,

$$V_t(\mathcal{S}_t, \mathcal{I}_t) = \mathbb{E}_{\tau_t} \left[\sum_{\ell=t}^T \gamma^\ell R(\mathcal{S}_\ell, a_\ell) \middle| \mathcal{H}_t, \pi^* \right],$$

where $\tau_t = (\mathcal{H}_t, a_t, \dots, a_{T-1}, \mathcal{H}_T)$ represents possible trajectory starting at \mathcal{H}_t . The *stopping time* is defined as, $T \equiv \min\{t : 0 \leq t \leq \bar{T} \text{ s.t. } a_t = H, \text{ or } p_t = \bar{P}, \text{ or } i_t = \bar{I}, \text{ or } i_t = I_f, \text{ or } t = \bar{T}\}$; if (1) we reach to stationary phase $t = \bar{T}$, or (2) we reach to the protein or impurity limit $p_t = \bar{P}$ or $i_t = \bar{I}$, or (3) we have batch failure $i_t = I_f$, or (4) we decide to harvest $a_t = H$. At the stopping time T , the value function is,

$$V_T(p_T, i_T, \mathcal{I}_T) = \begin{cases} r_h(p_T, i_T), & \text{if } i_T \neq I_f \\ -r_f, & \text{if } i_T = I_f. \end{cases}$$

Then, we have the corresponding Bellman optimality equations,

$$V_t(p_t, i_t, \mathcal{I}_t) = \begin{cases} \max \{r_h(p_t, i_t), -c_u + \gamma \mathbb{E}[V_{t+1}(p_{t+1}, i_{t+1}, \mathcal{I}_{t+1})]\}, & \text{if } t < T \\ V_T(p_T, i_T, \mathcal{I}_T), & \text{if } t = T \end{cases}$$

where the expectation is taken with respect to the hyper state transitioning $\Pr(\mathcal{S}_{t+1}, \mathcal{I}_{t+1} | \mathcal{S}_t, \mathcal{I}_t, a_t)$.

6 Structural and Sensitivity Analysis of Optimal Policy

Since the prediction risk accounts for both bioprocess inherent stochastic uncertainty and model risk, in Section 6.1, we will develop the prediction variance decomposition quantifying the contributions from both sources of uncertainties. Then, we study the structural analysis of value function $V_t(\mathcal{S}_t, \mathcal{I}_t)$ over the physical and knowledge states in Sections 6.2 and 6.3, where the knowledge state is specified by the process model posterior distribution parameters, $\mathcal{I}_t = \{\alpha_t^{(p)}, \nu_t^{(p)}, \lambda_t^{(p)}, \beta_t^{(p)}, \alpha_t^{(i)}, \nu_t^{(i)}, \lambda_t^{(i)}, \beta_t^{(i)}\}$. After that, we study the impact of model risk on the selection of optimal policy in Section 6.4. Since the proposed model-based reinforcement learning appropriately considers both stochastic uncertainty and model risk, higher model risk or less knowledge of underlying stochastic process can lead to more conservative fermentation stopping decision to proactively hedge against higher prediction risk. For analytical tractability, in this section, we consider the protein and impurity growth rates following non-truncated predictive distributions given in eq.(7), and we assume the probability of out-of-boundary realizations of physical states is ignorable.

6.1 Prediction Risk and Variance Decomposition

Suppose at any time epoch $t \leq T$, the knowledge states are given by hyper parameters $\mathcal{I}_t = \{\alpha_t^{(p)}, \nu_t^{(p)}, \lambda_t^{(p)}, \beta_t^{(p)}, \alpha_t^{(i)}, \nu_t^{(i)}, \lambda_t^{(i)}, \beta_t^{(i)}\}$. The prediction uncertainties of protein and impurity growth rates are characterized by the posterior predictive distribution as shown in eq.(7)–(8), accounting for both bioprocess inherent stochastic uncertainty and model risk. Since the predictive distribution follows generalized t -distribution [35, 34], we have the posterior predictive variances $\tilde{\sigma}_t^{(p)2} \equiv \text{Var}[\tilde{\Phi}_{t'} | \mathcal{X}_t] = \frac{\beta_t^{(p)}(1 + \nu_t^{(p)})}{(\lambda_t^{(p)} - 1)\nu_t^{(p)}}$ and $\tilde{\sigma}_t^{(i)2} \equiv \text{Var}[\tilde{\Psi}_{t'} | \mathcal{X}_t] = \frac{\beta_t^{(i)}(1 + \nu_t^{(i)})}{(\lambda_t^{(i)} - 1)\nu_t^{(i)}}$ for protein and impurity growth rates respectively. Then, we derive the variance decomposition to quantify the prediction variance contributions from bioprocess inherent stochastic uncertainty and model risk in Proposition 1. Notice that the model risk can be reduced by collecting more real-world process data.

Proposition 1. *Given the knowledge state \mathcal{I}_t , we can decompose the predictive variances $\tilde{\sigma}_t^{(p)2}$ and $\tilde{\sigma}_t^{(i)2}$ for protein and impurity,*

$$\tilde{\sigma}_t^{(p)2} = \hat{\sigma}_t^{(p)2} + \check{\sigma}_t^{(p)2}; \quad \tilde{\sigma}_t^{(i)2} = \hat{\sigma}_t^{(i)2} + \check{\sigma}_t^{(i)2};$$

where $\hat{\sigma}_t^{(p)2} = \frac{\beta_t^{(p)}}{\lambda_t^{(p)} - 1}$, $\hat{\sigma}_t^{(i)2} = \frac{\beta_t^{(i)}}{\lambda_t^{(i)} - 1}$ measure the prediction risk contribution from bioprocess inherent stochastic uncertainty; and $\check{\sigma}_t^{(p)2} = \frac{\beta_t^{(p)}}{(\lambda_t^{(p)} - 1)\nu_t^{(p)}}$, $\check{\sigma}_t^{(i)2} = \frac{\beta_t^{(i)}}{(\lambda_t^{(i)} - 1)\nu_t^{(i)}}$ measure the contribution from model risk, for protein and impurity growth rates respectively.

Based on this result, the practitioner can estimate the inherent stochastic uncertainty and model risk of protein and impurity growth rates at any time period t , by $\hat{\sigma}_t^{(p)2}$, $\hat{\sigma}_t^{(i)2}$ and $\check{\sigma}_t^{(p)2}$, $\check{\sigma}_t^{(i)2}$. Notice that under the normal-inverse-gamma prior assumption, the estimated ratio of model risk to inherent stochastic uncertainty, i.e., $\frac{\check{\sigma}_t^{(p)2}}{\hat{\sigma}_t^{(p)2}} = \frac{1}{\nu_t^{(p)}}$ and

$\frac{\check{\sigma}_t^{(i)2}}{\hat{\sigma}_t^{(i)2}} = \frac{1}{\nu_t^{(i)}}$, only depend on the shape parameters $\nu_t^{(p)}$ and $\nu_t^{(i)}$. As size of bioprocess data increase, both $\nu_t^{(p)}$ and $\nu_t^{(i)}$ will increase, the ratios will decrease, and the impact of model risk will decrease.

6.2 Structural Analysis of Value Function Related to Physical State

Here, we analyze the structural properties of value function and optimal policy related to physical state $\mathcal{S}_t = (p_t, i_t)$ under given knowledge state \mathcal{I}_t . We will first show the monotonicity over physical state, and then present sufficient conditions for the existence of *control limit policies* (CLPs). The detailed proofs are included in Appendix B and Appendix C respectively.

Theorem 1. *Given the knowledge state \mathcal{I}_t , the value function $V_t(\mathcal{S}_t, \mathcal{I}_t)$ with $\mathcal{S}_t = (p_t, i_t)$ is a non-increasing function in the impurity level i_t and a non-decreasing function in the protein level p_t .*

Based on the monotonicity properties presented in Theorem 1, we can derive sufficient conditions for the existence of control limit policies as following.

Theorem 2. *At any time period t , given any feasible protein level p_t , there exists a threshold i_t^* such that the optimal decision is to harvest if the impurity level $i_t \geq i_t^*$ and following condition holds for all $i_t^+ > i_t^- \geq 0$:*

$$\begin{aligned} r_h(p_t, i_t^-) - r_h(p_t, i_t^+) &\leq \gamma r_f [\Pr(i_{t+1} \leq \bar{I} | i_t^-) - \Pr(i_{t+1} \leq \bar{I} | i_t^+)] \\ &\quad + \gamma \int_0^{\ln \bar{I} - \ln i_t^-} [r_h(p_t, i_t^- e^{\psi_t}) - r_h(\bar{P}, i_t^- e^{\psi_t})] f_t^{(i,n)}(\psi_t) d\psi_t, \end{aligned} \quad (13)$$

where $\Pr(i_{t+1} \leq \bar{I} | i_t) = \Pr(i_t e^{\psi_t} \leq \bar{I}) = \int_0^{\ln \bar{I} - \ln i_t} f_t^{(i,n)}(\psi_t) d\psi_t$ is the probability that the batch failure doesn't happen in next period given the current impurity level i_t .

Theorem 2 presents the existence of the optimal threshold i_t^* with respect to impurity level. It indicates that given the same protein and knowledge states, if we harvest at smaller impurity level denoted by i_t^- , we will also harvest at any higher level of impurity, denoted by i_t^+ , under the conditions listed in Theorem 2. Notice that the harvest reward $r_h(p_t, i_t)$ is non-increasing in impurity level i_t , the left hand side of condition in inequality (25) is the reward

difference by harvesting at current time with different impurity levels i_t^- or i_t^+ . The right hand side is the discounted additional reward difference of harvesting one-period ahead. The term $r_f [\Pr(i_{t+1} \leq \bar{I}|i_t^-) - \Pr(i_{t+1} \leq \bar{I}|i_t^+)] = r_f [\Pr(i_{t+1} = I_f|i_t^+) - \Pr(i_{t+1} = I_f|i_t^-)]$ quantifies the additional risk and cost of batch failure when the impurity level increases from i_t^- to i_t^+ . The second term on the right hand side considers the maximum reward difference when the fermentation operates at physical states (p_t, i_t^-) and the batch does not fail. Inequality (25) ensures that the additional risk and cost of batch failure dominant the potential additional reward of going forward when impurity level increases from i_t^- to i_t^+ . Thus, the optimal policy for i_t^+ is harvest at current step.

6.3 Structural Analysis of Value Function Related to Knowledge State

Given the physical state \mathcal{S}_t , in this section, we further study the structural properties of value function and show the monotonicity related to knowledge state $\mathcal{I}_t = \{\alpha_t^{(p)}, \nu_t^{(p)}, \lambda_t^{(p)}, \beta_t^{(p)}, \alpha_t^{(i)}, \nu_t^{(i)}, \lambda_t^{(i)}, \beta_t^{(i)}\}$ in Theorem 3. The proof is provided in Appendix D.

Theorem 3. *The monotonicity of $V_t(\mathcal{S}_t, \mathcal{I}_t)$ over knowledge states can be summarized as follows:*

- (i) *it is non-increasing in $\alpha_t^{(i)}$ and non-decreasing in $\alpha_t^{(p)}$;*
- (ii) *it is non-increasing in $\beta_t^{(i)}$ and non-decreasing in $\beta_t^{(p)}$;*
- (iii) *it is non-increasing in $\nu_t^{(p)}$ and non-decreasing in $\nu_t^{(i)}$;*
- (iv) *for reasonably large $\lambda_t^{(p)}$ and $\lambda_t^{(i)}$ so that the predictive t -distribution in eq.(7) can be approximated by Gaussian, it is non-increasing in $\lambda_t^{(p)}$ and non-decreasing in $\lambda_t^{(i)}$.*

The hyperparameters included in the knowledge state are connected to the predictive means and variances; see Section 4.2. For the protein and impurity growth rates, the predictive means are $E[\tilde{\Phi}_{t'}|\mathcal{X}] = \alpha_t^{(p)}$ and $E[\tilde{\Psi}_{t'}|\mathcal{X}] = \alpha_t^{(i)}$, and the predictive variances are $\tilde{\sigma}_t^{(p)2} \equiv \text{Var}[\tilde{\Phi}_{t'}|\mathcal{X}_t] = \frac{\beta_t^{(p)}(1 + \nu_t^{(p)})}{(\lambda_t^{(p)} - 1)\nu_t^{(p)}}$ and $\tilde{\sigma}_t^{(i)2} \equiv \text{Var}[\tilde{\Psi}_{t'}|\mathcal{X}_t] = \frac{\beta_t^{(i)}(1 + \nu_t^{(i)})}{(\lambda_t^{(i)} - 1)\nu_t^{(i)}}$ respectively. Notice that the monotonicity of value function on our knowledge of expected protein and impurity growth, i.e., $\alpha_t^{(i)}$ and $\alpha_t^{(p)}$, is consistent with the monotonicity on protein and impurity levels in Theorem 1. It makes sense, since if the expected protein growth rate is larger, we will get more protein, the expected total reward is higher; and if the expected impurity growth rate is larger, we will get more impurities, the expected total reward is lower.

On the other hand, the scale parameters $\beta_t^{(i)}$ and $\beta_t^{(p)}$, as well as the shape parameters $\nu_t^{(i,n)}$, $\nu_t^{(p,n)}$ and $\lambda_t^{(p)}$, $\lambda_t^{(i)}$, directly relate to the predictive variances of impurity and protein growth rates accounting for process inherent stochastic uncertainty and model risk, i.e., $\tilde{\sigma}_t^{(p)2} = \frac{\beta_t^{(p)}}{(\lambda_t^{(p)} - 1)} \left(1 + \frac{1}{\nu_t^{(p)}}\right)$ and $\tilde{\sigma}_t^{(i)2} = \frac{\beta_t^{(i)}}{(\lambda_t^{(i)} - 1)} \left(1 + \frac{1}{\nu_t^{(i)}}\right)$. Notice that the predictive distribution of growth rates Φ_t and Ψ_t is symmetric on both side of the predictive mean. However, the exponential growth e^{Φ_t} and e^{Ψ_t} during each period fermentation (see eq. (2)) will be impacted more by right tail values than left tail, due to exponential transformation. Therefore, higher predictive variances imply higher expected protein and impurity levels in the next time period. Since the value function is non-increasing in impurity level and non-decreasing in protein level, the value function is also non-increasing in the predictive variance of impurity growth rate and non-decreasing in the predictive variance of protein growth rate. This intuition is consistent with the monotonicity results with respect to the (ii) $\beta_t^{(i)}$, $\beta_t^{(p)}$; (iii) $\nu_t^{(i,n)}$, $\nu_t^{(p,n)}$; and (iv) $\lambda_t^{(p)}$, $\lambda_t^{(i)}$ in Theorem 3.

The monotonicity with respect to $\lambda_t^{(p)}$ and $\lambda_t^{(i)}$ based on the exact predictive distribution given by eq.(7) is analytically intractable, the conclusion (iv) in Theorem 3 is derived based on Gaussian approximation assumption; see the proof in Appendix D.4. Since the predictive distribution is generalized t distribution; with reasonably large degrees of freedom (i.e., $\lambda_t^{(p)}$, $\lambda_t^{(i)}$), the predictive distribution can be accurately approximated by Gaussian,

$$\tilde{\Phi}_t \sim \mathcal{N}\left(\alpha_t^{(p)}, \tilde{\sigma}_t^{(p)2}\right), \quad \tilde{\Psi}_t \sim \mathcal{N}\left(\alpha_t^{(i)}, \tilde{\sigma}_t^{(i)2}\right). \quad (14)$$

6.4 Sensitivity Analysis Studying the Impact of Model Risk

In this section, we study the impact of model risk on the selection of optimal policy. *By comparing the optimal policy or harvest decision boundary under true θ^c with that under predictive distribution with different level of model risk,*

we can estimate the value of additional data. Under the perfect information situation, the underlying ‘‘correct’’ mean growth rate and stochastic uncertainty of protein and impurity accumulation in the exponential growth phase specified by $\mu_c^{(p)}, \sigma_c^{(p)2}, \mu_c^{(i)}, \sigma_c^{(i)2}$ are known, and the optimal policy can be given by Theorem 4.

Theorem 4. *Given the perfect information on the underlying process model F^c , the optimal harvest policy obtained by MDP is: at any time period t during the exponential growth phase, the optimal harvest region is determined by*

$$\left\{ (p_t, i_t) : \min_{m=1,2,\dots,\bar{T}-t} h(p_t, i_t; m) \geq 0; p_0 \leq p_t \leq \bar{P}; i_0 \leq i_t \leq \bar{I} \right\}, \text{ and}$$

$$\begin{aligned} h(p_t, i_t; m) \equiv & \frac{1-\gamma^m}{1-\gamma} c_u + c_0 \left[1 - \gamma^m \Phi \left(\frac{\ln \bar{I} - \ln i_t - m\mu_c^{(i)}}{\sqrt{m}\sigma_c^{(i)}} \right) \right] + \gamma^m r_f \left[1 - \Phi \left(\frac{\ln \bar{I} - \ln i_t - m\mu_c^{(i)}}{\sqrt{m}\sigma_c^{(i)}} \right) \right] \\ & + c_2 i_t \left[\gamma^m e^{m\mu_c^{(i)} + m\sigma_c^{(i)2}/2} \Phi \left(\frac{\ln \bar{I} - \ln i_t - m\mu_c^{(i)} - m\sigma_c^{(i)2}}{\sqrt{m}\sigma_c^{(i)}} \right) - 1 \right] \\ & - c_1 \left\{ \gamma^m \bar{P} \Phi \left(\frac{\ln \bar{I} - \ln i_t - m\mu_c^{(i)}}{\sqrt{m}\sigma_c^{(i)}} \right) \left[1 - \Phi \left(\frac{\ln \bar{P} - \ln p_t - m\mu_c^{(p)}}{\sqrt{m}\sigma_c^{(p)}} \right) \right] \right. \\ & \left. + \gamma^m p_t e^{m\mu_c^{(p)} + m\sigma_c^{(p)2}/2} \Phi \left(\frac{\ln \bar{I} - \ln i_t - m\mu_c^{(i)}}{\sqrt{m}\sigma_c^{(i)}} \right) \Phi \left(\frac{\ln \bar{P} - \ln p_t - m\mu_c^{(p)} - m\sigma_c^{(p)2}}{\sqrt{m}\sigma_c^{(p)}} \right) - p_t \right\}, \end{aligned} \quad (15)$$

where (p_0, i_0) are the starting conditions of the batch, $\Phi(\cdot)$ is the cumulative distribution function (CDF) of standard normal, and m is the number of possible future fermentation periods till harvest of this batch.

The intuition of Theorem 4 is that, at current time t , we can compare the reward of harvesting now with the expected discounted reward of harvesting in any future decision epoch of this batch. If we have the current reward is no less than the expected reward of harvesting at all possible future times, then our optimal decision should be harvest at current time t . The function $h(p_t, i_t; m)$ in (37) is computed by the current harvesting reward minus the expected discounted reward of harvesting m periods later (i.e., at future time $t + m$). Specifically, the first term of eq.(37) considers the additional fermentation operational cost for m periods; the second and third terms together consider the loss due to the potential batch failure; and the fourth and last terms consider the penalty and gain induced by additional impurity and protein accumulated during next m time periods. Therefore, if failure doesn’t happen at current time t , Theorem 4 defines the optimal harvest decision boundary for the underlying MDP by a series of inequalities that divides the physical states space $(p_t, i_t) \in [p_0, \bar{P}] \times [i_0, \bar{I}]$ into two regions corresponding to harvest and continue decisions. *More specific, given the current protein and impurity levels (p_t, i_t) , the optimal decision is to harvest if and only if $\min_{m=1,2,\dots,\bar{T}-t} h(p_t, i_t; m) \geq 0$.* The detailed proof is provided in Appendix E.

Then, we study the optimal policy under the impact of model risk. Suppose that the prior belief of underlying bioprocess model coefficients $\mathbf{p}(\theta)$ is given as in eq.(3) with hyper parameters $\alpha_0^{(p)}, \nu_0^{(p)}, \lambda_0^{(p)}, \beta_0^{(p)}, \alpha_0^{(i)}, \nu_0^{(i)}, \lambda_0^{(i)}, \beta_0^{(i)}$. Given the historical data \mathcal{X}_t collected so far, the posterior belief $\mathbf{p}(\theta|\mathcal{X}_t)$ is characterized by knowledge states $\mathcal{I}_t = (\alpha_t^{(p)}, \nu_t^{(p)}, \lambda_t^{(p)}, \beta_t^{(p)}, \alpha_t^{(i)}, \nu_t^{(i)}, \lambda_t^{(i)}, \beta_t^{(i)})$. Let J_t denotes the data size collected until t . With reasonably enough sample size J_t (implying reasonably large $\lambda_t^{(p)}, \lambda_t^{(i)}$), the posterior predictive distribution can be approximated by Gaussian $\tilde{\Phi} \sim \mathcal{N}(\alpha_t^{(p)}, \tilde{\sigma}_t^{(p)2})$ and $\tilde{\Psi} \sim \mathcal{N}(\alpha_t^{(i)}, \tilde{\sigma}_t^{(i)2})$ with predictive variances $\tilde{\sigma}_t^{(p)2}, \tilde{\sigma}_t^{(i)2}$. Therefore, at any decision time t , given the current belief on protein and impurity growth rates, the model based reinforcement learning has the optimal policy given by Theorem 5. Compared with Theorem 4, the key difference in Theorem 5 is the prediction risk accounting for both process inherent stochastic uncertainty and model risk.

Theorem 5. *Suppose the current knowledge state is $\mathcal{I}_t = (\alpha_t^{(p)}, \nu_t^{(p)}, \lambda_t^{(p)}, \beta_t^{(p)}, \alpha_t^{(i)}, \nu_t^{(i)}, \lambda_t^{(i)}, \beta_t^{(i)})$. The model based reinforcement learning has optimal policy: at any time period t , the optimal harvest region is determined by*

$$\left\{ (p_t, i_t) : \min_{m=1,2,\dots,\bar{T}-t} \tilde{h}(p_t, i_t; m) \geq 0; p_0 \leq p_t \leq \bar{P}; i_0 \leq i_t \leq \bar{I} \right\}, \text{ and}$$

$$\begin{aligned} \tilde{h}(p_t, i_t; m) \equiv & \frac{1-\gamma^m}{1-\gamma} c_u + c_0 \left[1 - \gamma^m \Phi \left(\frac{\ln \bar{I} - \ln i_t - m\alpha_t^{(i)}}{\sqrt{m}\tilde{\sigma}_t^{(i)}} \right) \right] + \gamma^m r_f \left[1 - \Phi \left(\frac{\ln \bar{I} - \ln i_t - m\alpha_t^{(i)}}{\sqrt{m}\tilde{\sigma}_t^{(i)}} \right) \right] \\ & + c_2 i_t \left[\gamma^m e^{m\alpha_t^{(i)} + m\tilde{\sigma}_t^{(i)2}/2} \Phi \left(\frac{\ln \bar{I} - \ln i_t - m\alpha_t^{(i)} - m\tilde{\sigma}_t^{(i)2}}{\sqrt{m}\tilde{\sigma}_t^{(i)}} \right) - 1 \right] \end{aligned}$$

$$\begin{aligned}
& -c_1 \left\{ \gamma^m \bar{P} \Phi \left(\frac{\ln \bar{I} - \ln i_t - m\alpha_t^{(i)}}{\sqrt{m\tilde{\sigma}_t^{(i)}}} \right) \left[1 - \Phi \left(\frac{\ln \bar{P} - \ln p_t - m\alpha_t^{(p)}}{\sqrt{m\tilde{\sigma}_t^{(p)}}} \right) \right] \right. \\
& \quad \left. + \gamma^m p_t e^{m\alpha_t^{(p)} + m\tilde{\sigma}_t^{(p)2}/2} \Phi \left(\frac{\ln \bar{I} - \ln i_t - m\alpha_t^{(i)}}{\sqrt{m\tilde{\sigma}_t^{(i)}}} \right) \Phi \left(\frac{\ln \bar{P} - \ln p_t - m\alpha_t^{(p)} - m\tilde{\sigma}_t^{(p)2}}{\sqrt{m\tilde{\sigma}_t^{(p)}}} \right) - p_t \right\}. \quad (16)
\end{aligned}$$

Similarly, Theorem 5 gives the harvest decision boundary with respect to the protein and impurity levels based on the current knowledge state \mathcal{I}_t , which is given by $\tilde{h}(p_t, i_t; m) \geq 0$, incorporating our current beliefs of the protein and impurity accumulation through predictive distribution. For simplification, we assume the improper prior that $\alpha_0^{(p)} = \nu_0^{(p)} = \lambda_0^{(p)} = \beta_0^{(p)} = \alpha_0^{(i)} = \nu_0^{(i)} = \lambda_0^{(i)} = \beta_0^{(i)} = 0$. Then given the process data \mathcal{X}_t with sample size J_t , based on the posterior updates, we have the knowledge state \mathcal{I}_t specified by,

$$\begin{cases} \alpha_t^{(p)} = \bar{\phi}, \nu_t^{(p)} = J_t, \lambda_t^{(p)} = \frac{J_t}{2}, \beta_t^{(p)} = \frac{1}{2} \sum_{j=1}^{J_t} (\phi^{(j)} - \bar{\phi})^2, \\ \alpha_t^{(i)} = \bar{\psi}, \nu_t^{(i)} = J_t, \lambda_t^{(i)} = \frac{J_t}{2}, \beta_t^{(i)} = \frac{1}{2} \sum_{j=1}^{J_t} (\psi^{(j)} - \bar{\psi})^2, \end{cases}$$

where $\bar{\phi} = \sum_{j=1}^{J_t} \phi^{(j)} / J_t$ and $\bar{\psi} = \sum_{j=1}^{J_t} \psi^{(j)} / J_t$, and obtain the posterior predictive variances,

$$\tilde{\sigma}_t^{(p)2} = \frac{J_t + 1}{(J_t - 2)J} \sum_{j=1}^{J_t} (\phi^{(j)} - \bar{\phi})^2, \quad \tilde{\sigma}_t^{(i)2} = \frac{J_t + 1}{(J_t - 2)J} \sum_{j=1}^{J_t} (\psi^{(j)} - \bar{\psi})^2. \quad (17)$$

We can show the asymptotic consistency of the posterior predictive means and variances, as well as the the harvest decision boundary in the Theorem 6.

Theorem 6. *As the amount of bioprocess historical data $J_t \rightarrow \infty$, we have $\alpha_t^{(p)} \xrightarrow{p} \mu_c^{(p)}$, $\alpha_t^{(i)} \xrightarrow{p} \mu_c^{(i)}$, and $\tilde{\sigma}_t^{(p)2} \xrightarrow{p} \sigma_c^{(p)2}$, $\tilde{\sigma}_t^{(i)2} \xrightarrow{p} \sigma_c^{(i)2}$, i.e., the asymptotic convergence to underlying true model coefficients in probability, so that for any $(p_t, i_t) \in [p_0, \bar{P}] \times [i_0, \bar{I}]$ and $m = 1, 2, \dots, \bar{T} - t$, $\tilde{h}(p_t, i_t; m) \xrightarrow{p} h(p_t, i_t; m)$. Thus, as the amount of process historical data goes to infinity, the harvest decision boundary under model risk will converge to the optimal boundary with the perfect information on the underlying process model F^c .*

Based on Theorem 6, the posterior predictive means and variances of protein and impurity growth rates will converge to the underlying true coefficients, as the amount of historical bioprocess data increases. In addition, based on the proof in Appendix G, for predictive variance, we have $E[\tilde{\sigma}_t^{(p)2}] = \sigma_c^{(p)2} + \frac{(2J_t - 1)\sigma_c^{(p)2}}{(J_t^2 - 2J_t)}$ and $\text{Var}[\tilde{\sigma}_t^{(p)2}] = \frac{2(J_t^3 + J_t^2 - J_t - 1)\sigma_c^{(p)4}}{J_t^4 - 4J_t^3 + 4J_t^2}$. For $J_t > 2$, notice that the bias $E[\tilde{\sigma}_t^{(p)2} - \sigma_c^{(p)2}] = \frac{(2J_t - 1)\sigma_c^{(p)2}}{(J_t^2 - 2J_t)} > 0$. Therefore, under model risk, on average the predictive variance $\tilde{\sigma}_t^{(p)2}$ will be greater than true variance $\sigma_c^{(p)2}$. As the amount of historical data J_t increases, the predictive variance will gradually converge in probability to the variance with perfect information of underlying stochastic process F^c . Similar results also apply for impurity growth rate.

For the harvest regions given by Theorems 4 and 5, it's challenging to obtain the closed-form analytical decision boundary. To understand how model risk impacts on the optimal harvest decision region or boundary through predictive means and standard deviations (SDs) $\alpha_t^{(p)}$, $\alpha_t^{(i)}$, $\tilde{\sigma}_t^{(p)}$, $\tilde{\sigma}_t^{(i)}$, we obtain the optimal harvest decision boundary numerically and show how it moves with changing in $\alpha_t^{(p)}$, $\alpha_t^{(i)}$, $\tilde{\sigma}_t^{(p)}$, $\tilde{\sigma}_t^{(i)}$. The results are given in Figure 2, where different curves represents the optimal decision boundaries under different parameter values, and the region above each curve denotes the harvest region. According to the results, we can see that as the predictive mean of protein $\alpha_t^{(p)}$ increases, the harvest boundary will move up. The difference on left part (with small amount of protein p_t) is larger than on the right (with large amount of protein p_t), since as protein approaching to the limit, increasing in $\alpha_t^{(p)}$ provides less marginal benefit in potential protein increasement during the next period. As the predictive mean of impurity $\alpha_t^{(i)}$ increases, the harvest boundary will move down. Based on our current beliefs with larger $\alpha_t^{(i)}$, the probability reaching batch failure is greater so that we need to harvest with smaller amount of impurity. Further, as the predictive standard deviation (SD) of protein $\tilde{\sigma}_t^{(p)}$ increases, the decision boundary will shift to the left. With larger $\tilde{\sigma}_t^{(p)}$, i.e., higher uncertainty of protein growth, we tend to harvest with smaller amount of protein especially when it's close to the maximum protein level. On the other hand, as predictive SD of impurity $\tilde{\sigma}_t^{(i)}$ increases, the boundary will move down. With larger $\tilde{\sigma}_t^{(i)}$, i.e., higher uncertainty of impurity growth, we tend to harvest with smaller amount of impurity to avoid batch failure.

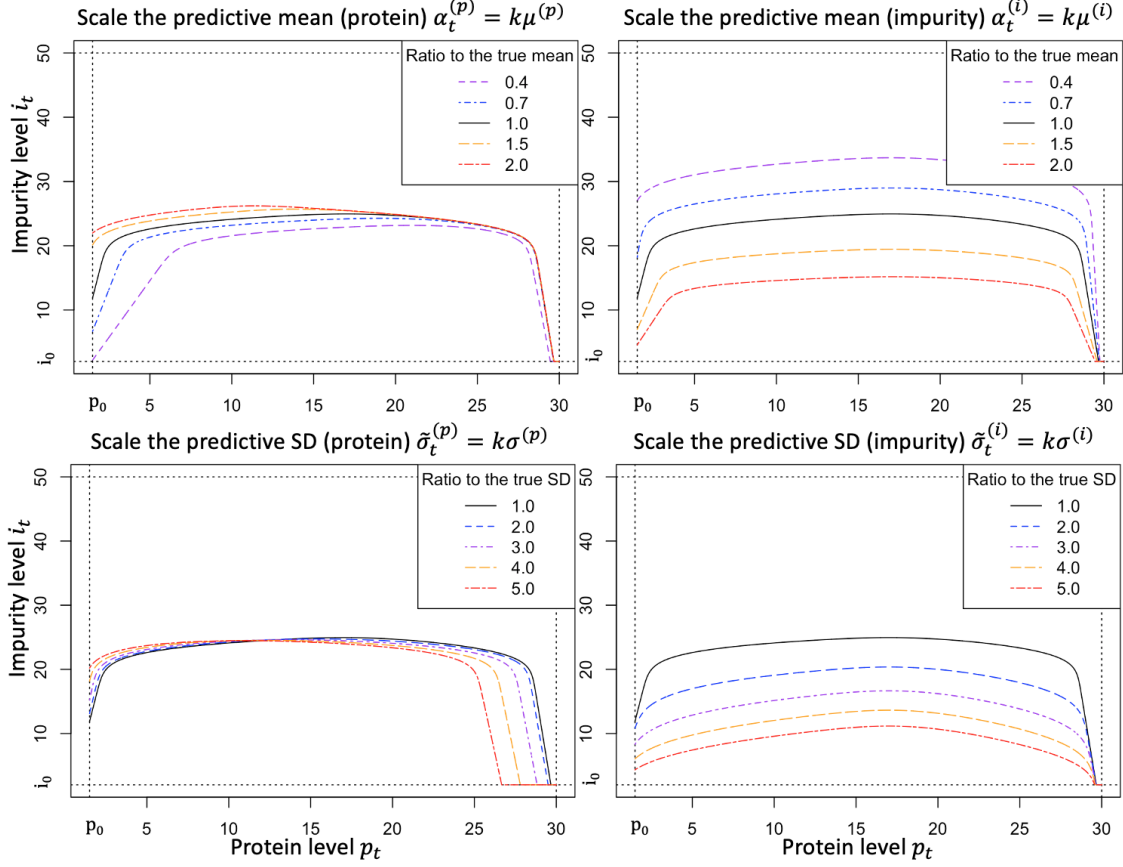


Figure 2: Illustration of how the harvest decision boundary curve is impacted by model risk through difference in predictive means $\alpha_t^{(p)}$, $\alpha_t^{(i)}$, and predictive SDs $\tilde{\sigma}_t^{(p)}$, $\tilde{\sigma}_t^{(i)}$.

In addition, under different amounts of bioprocess historical data J_t , we compute the expected knowledge states with respect to the uncertainty of real process trajectory realizations, and plot the corresponding boundaries. Then we compare the expected boundaries under different amounts of data with the true boundary to illustrate how different levels of model risk impact on the optimal policy; see Figure 3. Under higher level of model risk (smaller amount of historical data), our optimal harvest decisions tend to be *more conservative*: given the current protein level p_t , we will harvest with smaller amount of impurity i_t to hedge against the additional prediction risk induced by higher model risk. As the amount of historical data J_t increases, the boundary will converge to the true optimal harvest boundary.

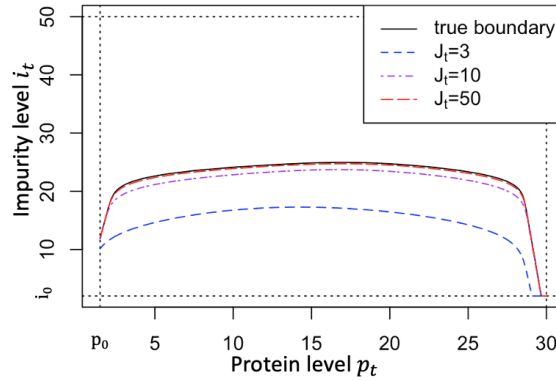


Figure 3: Expected optimal harvest boundaries under different amount of historical bioprocess data J_t .

7 Algorithm Procedure for Proposed Reinforcement Learning Framework

In this section, we will provide the algorithm procedure for the optimization solution methodology. To solve the model-based reinforcement learning accounting for model risk, we apply the Bayesian sparse sampling approach, [36, 37], which can produce a near optimal action for any (hyper) state encountered [38]. Further, the Q-function is a deterministic function of harvest decision $a_t = H$ and we only need to estimate value of the continue action $a_t = C$, which helps to control the computational complexity.

Here we consider the process learning and decision making procedure for each batch fermentation, which can be easily generalized for multiple batches. Given the hyper state $\mathcal{H}_t \equiv (\mathcal{S}_t, \mathcal{I}_t)$, to evaluate the performance by taking action $a_t \in \{C, H\}$, the Q-function is provided as follows,

$$Q_T(p_T, i_T, \mathcal{I}_T, a_T = H) = \begin{cases} r_h(p_T, i_T), & \text{if } i_T \neq I_f \\ -r_f, & \text{if } i_T = I_f \end{cases}$$

and

$$Q_t(p_t, i_t, \mathcal{I}_t, a_t = C) = -c_u + \gamma E \left[\max_{a_{t+1}} Q_{t+1}(p_{t+1}, i_{t+1}, \mathcal{I}_{t+1}, a_{t+1}) \right].$$

Notice that we have $V_t(\mathcal{S}_t, \mathcal{I}_t) = \max_{a_t} Q_t(\mathcal{S}_t, \mathcal{I}_t, a_t)$, so that the optimal policy can be specified as $\pi^*(\mathcal{S}_t, \mathcal{I}_t) = a_t^* = \arg \max_{a_t} Q_t(\mathcal{S}_t, \mathcal{I}_t, a_t)$.

Typically, the Bayesian reinforcement learning can be solved in two phases: offline planning and online execution. Since the Bayesian reinforcement learning directly incorporates the knowledge states \mathcal{I}_t , the hyper state transitioning $\Pr(\mathcal{S}_{t+1}, \mathcal{I}_{t+1} | \mathcal{S}_t, \mathcal{I}_t, a_t)$ in eq.(9) is known. Theoretically we are able to solve $Q_t(\mathcal{S}_t, \mathcal{I}_t, a_t)$ and $\pi^*(\mathcal{S}_t, \mathcal{I}_t)$ without interacting with the environment. In other words, we try to find the optimal policy $\pi^* : (\mathcal{S}_t, \mathcal{I}_t) \rightarrow a_t$ that maps any feasible hyper state to an action. Then, in the online execution phase or during the real biomanufacturing fermentation process, at each decision epoch t with hyper state $(\mathcal{S}_t, \mathcal{I}_t)$, we just follow π^* to execute the optimal action $a_t^* = \pi^*(\mathcal{S}_t, \mathcal{I}_t)$. However, offline planning needs to implicitly account for all possible scenarios, which could be notoriously difficult for the entire hyper state space [19]. Therefore, we consider the online partial planning through Bayesian sparse sampling which generates future trajectories, modeling the hyper state evolution uncertainty, to estimate the Q-function at current hyper states, and then guide the optimal action.

Specifically, through the Bellman's equation, $Q_t(\mathcal{S}_t, \mathcal{I}_t, a_t = C)$ can be computed through dynamic programming. At the stopping time T , i.e., $a_T = H$, we have

$$Q_T(p_T, i_T, \mathcal{I}_T, a_T = H) = \begin{cases} r_h(p_T, i_T), & \text{if } i_T \neq I_f \\ -r_f, & \text{if } i_T = I_f \end{cases}, \quad (18)$$

and for any $0 \leq t < T$, we can solve Q-function backward for $a_t = C$,

$$Q_t(p_t, i_t, \mathcal{I}_t, a_t = C) = -c_u + \gamma E \left[\max_{a_{t+1}} Q_{t+1}(p_{t+1}, i_{t+1}, \mathcal{I}_{t+1}, a_{t+1}) \right],$$

where the expectation is taken with respect to the hyper state transitioning $\Pr(\mathcal{S}_{t+1}, \mathcal{I}_{t+1} | \mathcal{S}_t, \mathcal{I}_t, a_t)$. Since there's no closed-form solution, we estimate the expectation by using the sample average approximation (SAA).

Given the current hyper state $\mathcal{H}_t \equiv (\mathcal{S}_t, \mathcal{I}_t) = (p_t, i_t, \mathcal{I}_t)$, we can generate the samples or scenarios of next hyper state through transitioning $\Pr(\mathcal{S}_{t+1}, \mathcal{I}_{t+1} | \mathcal{S}_t, \mathcal{I}_t, a_t) = \Pr(\mathcal{S}_{t+1} | \mathcal{S}_t, \mathcal{I}_t, a_t) \Pr(\mathcal{I}_{t+1} | \mathcal{S}_{t+1}, \mathcal{S}_t, \mathcal{I}_t, a_t)$ in two steps. First, we sample the K scenarios of physical states (p_{t+1}, i_{t+1}) from predictive distribution $\Pr(\mathcal{S}_{t+1} | \mathcal{S}_t, \mathcal{I}_t, a_t)$. We can sample the protein growth model coefficients from the posterior distribution, $(\tilde{\mu}^{(p,k)}, \tilde{\sigma}^{(p,k)2}) \sim \mathcal{N}(\alpha_t^{(p)}, \sigma_n^{(p)2} / \nu_t^{(p)}) \cdot \text{Inv}\Gamma(\lambda_t^{(p)}, \beta_t^{(p)})$, generate the realizations of protein growth rate $\tilde{\phi}_t^{(k)} \sim \mathcal{N}(\tilde{\mu}^{(p,k)}, \tilde{\sigma}^{(p,k)2})$ and obtain the samples of next protein level $p_{t+1}^{(k)} = p_t \cdot e^{\tilde{\phi}_t^{(k)}}$ with $k = 1, 2, \dots, K$. Equivalently, we can directly sample the protein growth rate from the posterior predictive distribution, i.e., $\tilde{\phi}_t^{(k)} \sim f_t^{(p)}(\phi_t | \mathcal{I}_t) \equiv f_t^{(p)}(\phi_t | \mathcal{X}_t)$ given by eq.(8). Similar procedure also applies to generate the sample of impurity growth rate samples $\tilde{\psi}_t^{(k)}$ and $i_{t+1}^{(k)} = i_t \cdot e^{\tilde{\psi}_t^{(k)}}$ with $k = 1, 2, \dots, K$. Second, based on the collected samples of protein and impurity growth rates $\tilde{\phi}_t^{(k)}$ and $\tilde{\psi}_t^{(k)}$, the knowledge state can be updated $\mathcal{I}_t \rightarrow \mathcal{I}_{t+1}^{(k)}$ based on eq.(6). Therefore, the Q-function value at current hyper state with $a_t = C$ can be estimated by using SAA,

$$\hat{Q}_t(p_t, i_t, \mathcal{I}_t, a_t = C) = -c_u + \frac{\gamma}{K} \sum_{k=1}^K \max_{a_{t+1}} Q_{t+1}(p_{t+1}^{(k)}, i_{t+1}^{(k)}, \mathcal{I}_{t+1}^{(k)}, a_{t+1}). \quad (19)$$

Built on this idea, the Bayesian sparse sampling considers a look-ahead tree starting with the root at the current hyper state \mathcal{H}_t , and it is followed by two potential actions: harvest or continue fermentation. The Q-function value of harvest decision is provided by known reward $R(\mathcal{S}_t, a_t = H)$. For $a_t = C$, the expected value function in the next time period $E[\max_{a_{t+1}} Q_{t+1}(\mathcal{H}_{t+1}, a_{t+1})]$ will be estimated by using SAA, which grows the tree into K following nodes that each representing a sample of the next hyper state $\mathcal{H}_{t+1}^{(k)} = (p_{t+1}^{(k)}, i_{t+1}^{(k)}, \mathcal{I}_{t+1}^{(k)})$ with $k = 1, 2, \dots, K$. The same procedure repeats for each node until all the leaf nodes reach to the end of the current batch, i.e., the harvest decision or stopping time T ; see the illustration of the lookahead tree in Figure 4. The optimal value and action estimates are computed from leaf nodes rolling-backing up to the root. The sparse sampling procedure for estimating Q-function as well as the value function at given hyper state \mathcal{H}_t can be summarized in Algorithm 1. Further, we can provide the Bayesian Sparse Sampling based online learning and decision support for bioprocess fermentation procedure in Algorithm 2. In literature, the computation time/complexity is limited by controlling the number of next states samples (or branching factor) K , usually set $K = 4, 5$ [37]; and the depth of lookahead search tree, especially for long or infinite horizon problems, at the expense of lesser accuracy. Theoretical results of how the sampling settings related to the efficiency and near optimality have been studied in [38]. In our empirical study, we use $K = 10$, and the depth of search tree equal to the number of periods until the stationary phase, \bar{T} .

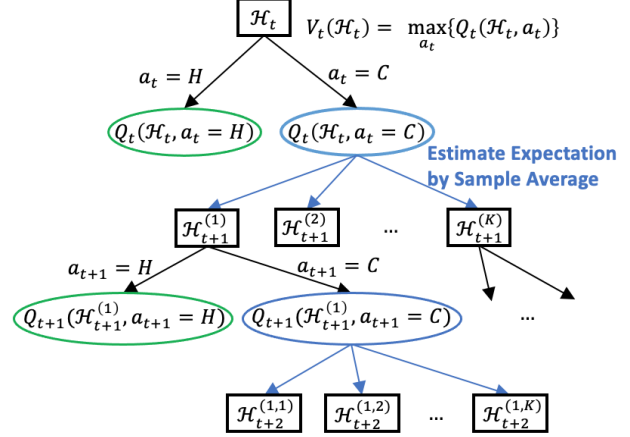


Figure 4: Illustration of the lookahead tree for Bayesian sparse sampling.

ALGORITHM 1: Bayesian Sparse Sampling for Estimating Q-Function and Value Function

Input: The current hyper state $\mathcal{H}_t \equiv (\mathcal{S}_t, \mathcal{I}_t) = (p_t, i_t, \mathcal{I}_t)$, number of samples K .

Output: Estimated Q-function $\hat{Q}_t(p_t, i_t, \mathcal{I}_t, a_t)$ and value function $\hat{V}_t(p_t, i_t, \mathcal{I}_t)$.

Function Valuefunction $(p_t, i_t, \mathcal{I}_t)$:

```

if  $p_t == \bar{P}$  or  $i_t \geq \bar{I}$  or  $t == \bar{T}$  then
  (A1) return harvest reward  $R(p_t, i_t, a_t = H)$  as in eq.(11);
else
  (A2) Generate  $K$  samples of next hyper state  $\mathcal{H}_{t+1}^{(k)} = (p_{t+1}^{(k)}, i_{t+1}^{(k)}, \mathcal{I}_{t+1}^{(k)})$ ,  $k = 1, 2, \dots, K$  from
     $\Pr(\mathcal{S}_{t+1}, \mathcal{I}_{t+1} | \mathcal{S}_t, \mathcal{I}_t, a_t)$  as discussed in Section 7;
  (A3) For each  $k$ , call  $\hat{V}_{t+1}^{(k)}(\mathcal{H}_{t+1}^{(k)}) = \text{valuefunction}(p_{t+1}^{(k)}, i_{t+1}^{(k)}, \mathcal{I}_{t+1}^{(k)})$  to estimate the value function of hyper state
     $\mathcal{H}_{t+1}^{(k)}$  at the next decision epoch  $t + 1$ ;
  (A4) Use the Bellman's Equation and estimate the expectation by sample average
     $\hat{V}_t(\mathcal{H}_t) = \max \left\{ R(p_t, i_t, a_t = H), -c_u + \frac{\gamma}{K} \sum_{k=1}^K \hat{V}_{t+1}^{(k)}(\mathcal{H}_{t+1}^{(k)}) \right\}$ , return  $\hat{V}_t(\mathcal{H}_t)$ ;

```

Function Qfunction $(p_t, i_t, \mathcal{I}_t, a_t)$:

```

if  $a_t == H$  then
  (B1) return harvest reward  $R(p_t, i_t, a_t = H)$  as in eq.(11);
else
  (B2) Generate  $K$  samples of next hyper state  $\mathcal{H}_{t+1}^{(k)} = (p_{t+1}^{(k)}, i_{t+1}^{(k)}, \mathcal{I}_{t+1}^{(k)})$  with  $k = 1, 2, \dots, K$  from
     $\Pr(\mathcal{S}_{t+1}, \mathcal{I}_{t+1} | \mathcal{S}_t, \mathcal{I}_t, a_t)$  as discussed in Section 7;
  (B3) For each  $k$ , call  $\hat{V}_{t+1}^{(k)}(\mathcal{H}_{t+1}^{(k)}) = \text{valuefunction}(p_{t+1}^{(k)}, i_{t+1}^{(k)}, \mathcal{I}_{t+1}^{(k)})$  to estimate the value function of hyper state
     $\mathcal{H}_{t+1}^{(k)}$  at the next decision epoch  $t + 1$ ;
  (B4) Use the Bellman's Equation on Q-function and estimate the expectation by sample average approximation,
     $\hat{Q}_t(\mathcal{H}_t, a_t = C) = -c_u + \frac{\gamma}{K} \sum_{k=1}^K \hat{V}_{t+1}^{(k)}(\mathcal{H}_{t+1}^{(k)})$ , return  $\hat{Q}_t(\mathcal{H}_t, a_t = C)$ ;

```

8 Case Study

In this section, we conduct the empirical study to: (1) analyze how different levels of model risk impact on the optimal policy and the value function, and (2) compare the performance of proposed model based reinforcement learning accounting for model risk with current industry practice and demonstrate its efficacy.

ALGORITHM 2: Online Learning and Control for Bioprocess Fermentation

Input: The prior $\mathcal{I}_0 = \{\alpha_0^{(p)}, \nu_0^{(p)}, \lambda_0^{(p)}, \beta_0^{(p)}, \alpha_0^{(i)}, \nu_0^{(i)}, \lambda_0^{(i)}, \beta_0^{(i)}\}$, the reward $R(\mathcal{S}_t, a_t)$.

Output: The stopping time T and total reward $Total.R$.

(1) Set the initial physical states $\mathcal{S}_0 = (p_0, i_0)$, the total reward $Total.R = 0$. Start the fermentation process for the current batch;

for $t = 0, 1, \dots, \bar{T}$ **do**

if $p_t < \bar{P}$ and $i_t < \bar{I}$ and $t < \bar{T}$ **then**

 (3) Estimate Q-function by calling $\hat{Q}_t(p_t, i_t, \mathcal{I}_t, a_t) = \text{Qfunction}(p_t, i_t, \mathcal{I}_t, a_t)$;

 (4) Guide the next action by $\hat{a}_t^* = H$ if $\hat{Q}_t(p_t, i_t, \mathcal{I}_t, a_t = H) \geq \hat{Q}_t(p_t, i_t, \mathcal{I}_t, a_t = C)$, and $\hat{a}_t^* = C$ otherwise;

else

 (5) The next action $\hat{a}_t^* = H$;

if $\hat{a}_t^* == C$ **then**

 (6) Continue the fermentation process for one period, $Total.R = Total.R - \gamma^t c_u$, and observe the new physical states (p_{t+1}, i_{t+1}) ;

 (9) Update the knowledge states $\mathcal{I}_t \rightarrow \mathcal{I}_{t+1}$ based on eq.(6) ;

else

 (10) Harvest the current batch, set the stopping time $T = t$ and $Total.R = Total.R + \gamma^t R(\mathcal{S}_t, a_t = H)$, break the for loop;

end

(11) Output the total reward $Total.R$;

8.1 Empirical Study for Sensitivity on Model Uncertainty

During the exponential growth in the fermentation process, we consider cases with: (1) low stochastic uncertainty, i.e., underlying protein and impurity growth parameters $\mu_c^{(p)} = 0.488, \sigma_c^{(p)} = 0.144, \mu_c^{(i)} = 0.488, \sigma_c^{(i)} = 0.144$, which can represent a well established production process for existing product; and (2) high stochastic uncertainty, i.e., underlying protein and impurity growth parameters $\mu_c^{(p)} = 0.488, \sigma_c^{(p)} = 0.488, \mu_c^{(i)} = 0.488, \sigma_c^{(i)} = 0.488$, which can represent a process for a new drug under development. This setting is constructed based on 21 batches of real-world biopharmaceutical manufacturing data. Here, we set the maximum achievable protein amount $\bar{P} = 30$, the batch failure impurity threshold $\bar{I} = 50$, and the time for a batch to reach stationary phase $\bar{T} = 8$. The starting protein and impurity for each batch are $p_0 = 1.5, i_0 = 2.0$. Following the study in [3], we consider the linear form reward function, and apply the similar reward and cost settings, including linear harvest reward $r_h(p, i) = 10p - i$, the one-step operation cost $c_u = 2$, and the batch failure penalty $r_f = 880$.

For comparison, we first solve the MDP with the perfect information on the underlying true bioprocess models as the benchmark, which leads to the best potential performance we can achieve. Given the transition models of fermentation process, we can solve the MDP by using the dynamic programming, and the Q-function can be computed backward from $t = T$ to 0 based on the Bellman's equation. At decision time t , by comparing the Q-value with different actions (i.e., continue fermentation or harvest) for any given protein and impurity levels, we could obtain the optimal policy for fermentation harvest decision. The results at a typical decision time are shown in Figure 5, presenting the optimal harvest decision boundary (left panel) and the Q-function (right panel) over the non-failure part of physical state space, i.e., $p_t \in [1.5, 30]$ and $i_t \in [2.0, 50]$, for both low and high stochastic uncertainty process. Here we consider a representative time period $t = 6$ for illustration. *Based on harvest decision boundaries in Figure 5, we can see that under higher stochastic uncertainty, we will harvest earlier with smaller protein and impurity levels to proactively hedge against the higher prediction risk.*

To study the impact of different levels of model risk on the optimal policy and value function, we further solve the bioprocess model-based reinforcement learning under model risk by using the Bayesian sparse sampling described in Section 7. We start with the noninformative prior $\alpha_0^{(p)} = \nu_0^{(p)} = \lambda_0^{(p)} = \beta_0^{(p)} = \alpha_0^{(i)} = \nu_0^{(i)} = \lambda_0^{(i)} = \beta_0^{(i)} = 0$. Since we focus on process development and early stage of production in this paper, the amount of historical data is very limited. Here, we consider different amounts of historical fermentation process data till time t , $J_t = 3, 10, 20$, which leads to different levels of model risk. For each case (i.e., $J_t = 3, 10, 20$), we perform 100 macro-replications to assess the performance of proposed reinforcement learning framework. In each macro-replication, we generate J_t number of real process data from the underlying true distribution F^c for protein and impurity growth, and then update the knowledge state $\mathcal{I}_t = \{\alpha_t^{(p)}, \nu_t^{(p)}, \lambda_t^{(p)}, \beta_t^{(p)}, \alpha_t^{(i)}, \nu_t^{(i)}, \lambda_t^{(i)}, \beta_t^{(i)}\}$ as in eq.(4). After that, with knowledge state \mathcal{I}_t we estimate the Q-function for continue decision over the physical state space $(p_t, i_t) \in [1.5, 30] \times [2.0, 50]$ based on Bayesian sparse sampling in Algorithm 1. The optimal policy can be computed by comparing the Q-function value with

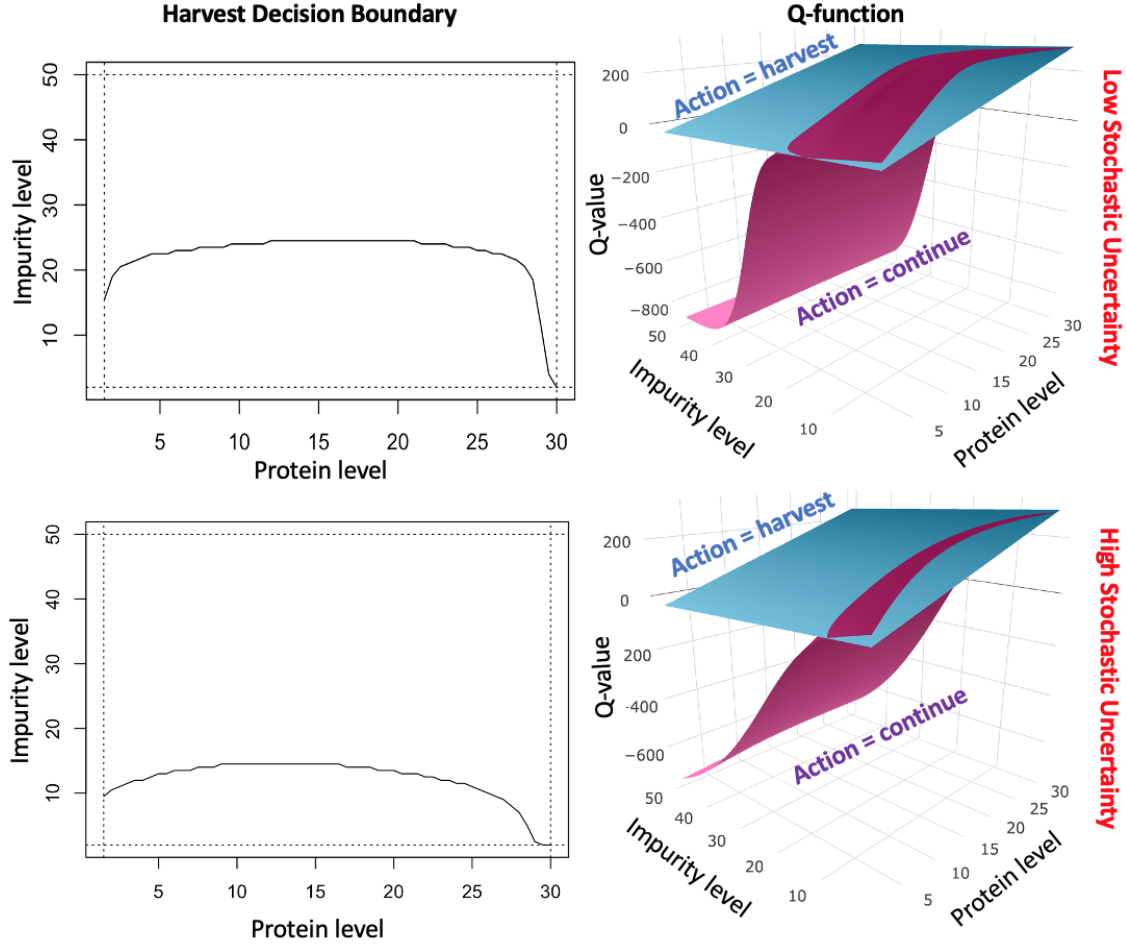


Figure 5: The results of the true MDP for fermentation over physical states space at $t = 6$: (1) Left panel: the optimal policy (above curve denotes harvest region); (2) Right panel: the Q-function value with different actions.

different decisions. We can obtain the mean decision boundary, as well as the 95% confidence bands of the optimal decision boundaries based on the results from macro-replications at each level of model risk. The representative results of decision boundary for cases with low and high stochastic uncertainty are shown in left panels of Figures 6 and 7. Further, in the right panels of Figures 6 and 7, we provide the 95% confidence bands of the estimated Q-function for continue decision, under different levels of model risk and stochastic uncertainty.

Based on the results in Figures 6 and 7 for both low and high stochastic uncertainty cases, we observe similar trend showing how the optimal harvest boundary moves as the number of historical data increases from $J_t = 3$ to $J_t = 20$. If we only have three historical observations, the model risk is large, so that the 95% confidence region of potential boundaries is also wide. The expected boundary lies below the true optimal boundary. It implies that for the cases with high model risk, we will tend to harvest with smaller amount of protein and impurity (i.e., be more “conservative”). This observation is consistent with the conclusion of sensitivity analysis in Section 6.4. As the amount of historical data increase, the 95% confidence region of decision boundaries shrinks surrounding around the optimal harvest boundary obtained under the situation with perfect information on the underlying process model. Further, comparing the results in Figures 6 and 7, we can see that if the inherent variability of underlying bioprocess is high, the impact of model risk on optimal policy would be more severe.

8.2 Comparison with the Current Practice

In this section, we will compare the performance of the proposed bioprocess model-based reinforcement learning accounting for model risk, with the model-based reinforcement learning ignoring model risk, and the current industry practice with certain fixed threshold for fermentation stopping decisions. Here, we assume the current industry practice or “Fix Threshold” method following a 60% threshold on impurity limit \bar{I} for harvest decisions, trying to avoid failure,

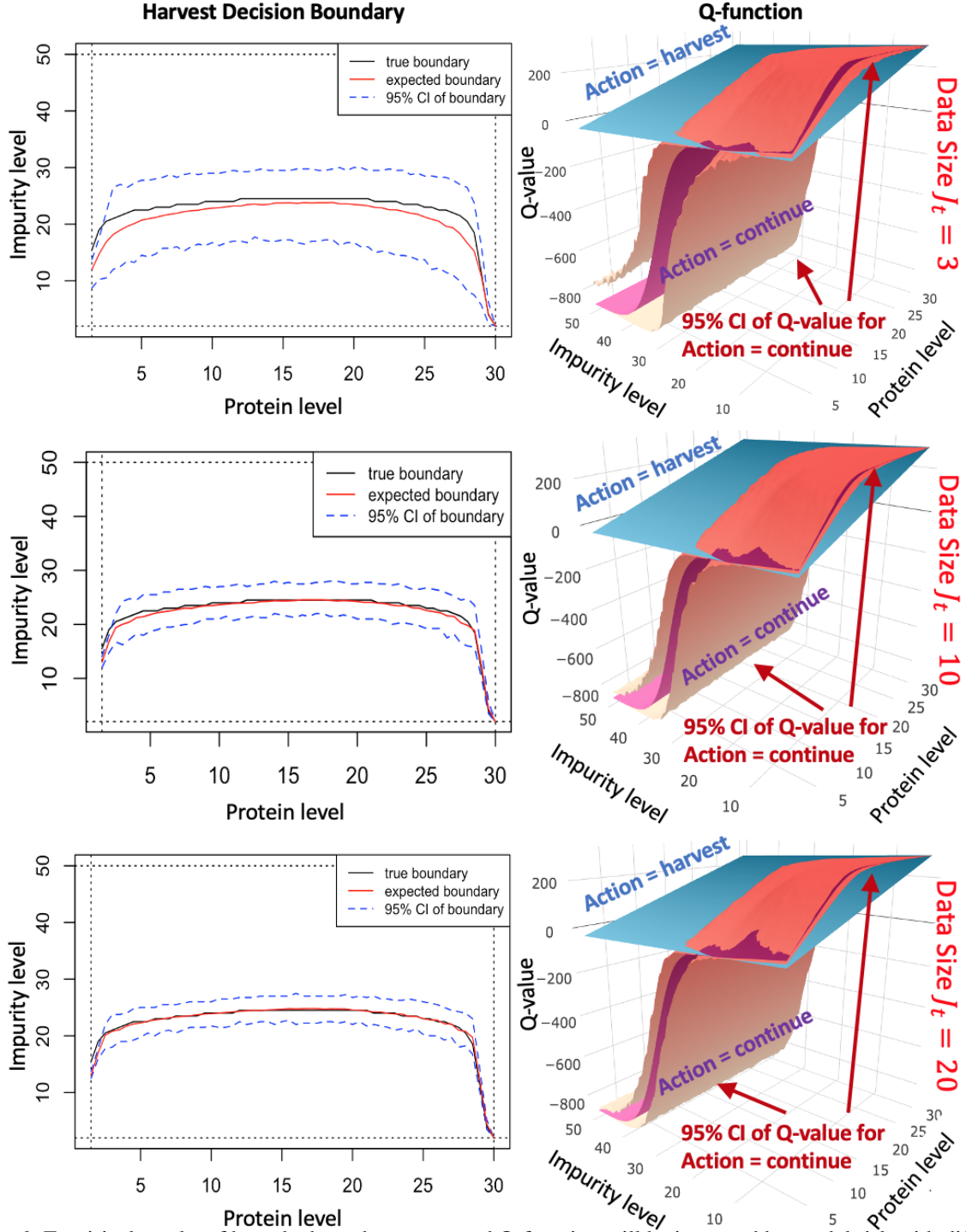


Figure 6: Empirical results of how the boundary curve and Q-function will be impacted by model risk with different amount of bioprocess data for low stochastic uncertainty case.

i.e., it will harvest once impurity level passes the threshold $i_t \geq 60\% \bar{I}$, or protein level reaches to the limit $p_t = \bar{P}$, or we move to stationary phase $t = \bar{T}$. On the other hand, for model-based reinforcement learning ignoring model risk, given the historical data, it estimates the state transition model parameters and takes the point estimate as the true parameters θ^c . Then, using the estimated model as the transition model, it solves a MDP to guide the fermentation harvest decisions. In addition, we consider the ideal case with the perfect information on underlying process model, defined as “Perfect Info MDP”. We execute those different methodologies as well as our proposed model-based

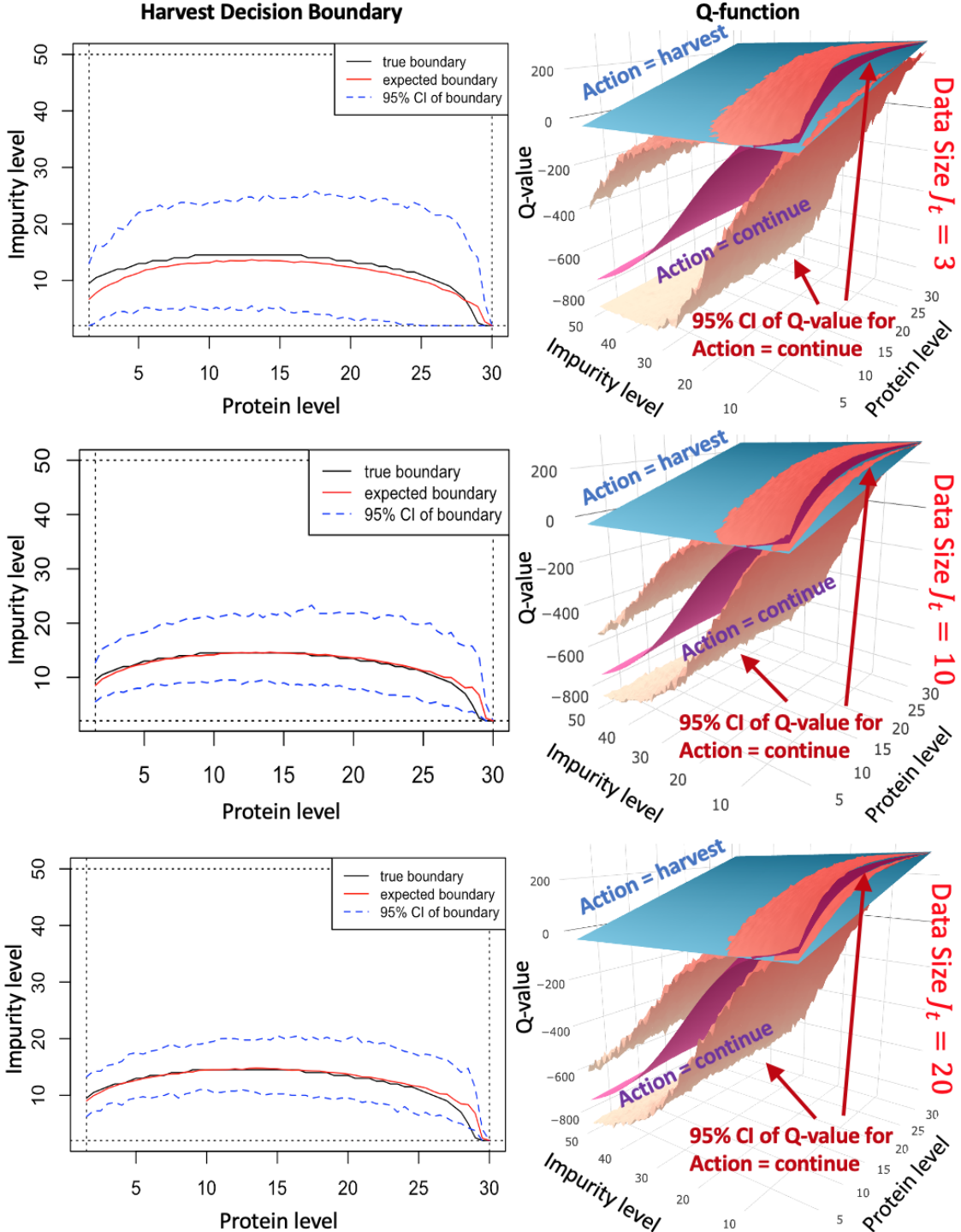


Figure 7: Empirical results of how the boundary curve and Q-function will be impacted by model risk with different amount of bioprocess data for high stochastic uncertainty case.

reinforcement learning accounting for model risk, to guide the harvest decision for each batch of fermentation process and record the total reward achieved. Specifically, for any policy π obtained by these approaches, we *evaluate* the performance of policy through the total expected reward achieved under true process model, as defined in Section 3.2 and discount factor $\gamma = 1$,

$$\rho^c(\pi) = \mathbb{E}_{\tau^c} \left[\sum_{t=0}^T R(S_t, a_t) \middle| S_0, \pi \right],$$

the expectation takes with respect to the stochastic decision process trajectory $\tau^c \equiv (\mathcal{S}_0, a_0, \mathcal{S}_1, a_1, \dots, \mathcal{S}_{T-1}, a_{T-1}, \mathcal{S}_T)$, following underlying physical state transition $\Pr(\mathcal{S}_{t+1}|\mathcal{S}_t, a_t; \theta^c)$ and decision policy $a_t = \pi_t(\mathcal{S}_t)$. It can be estimated from N replications of simulation experiments of single batch fermentation process. Based on the given policy π , we can generate trajectory realizations $\tau_n^c \equiv (\mathcal{S}_0^{(n)}, a_0^{(n)}, \mathcal{S}_1^{(n)}, a_1^{(n)}, \dots, \mathcal{S}_{T-1}^{(n)}, a_{T-1}^{(n)}, \mathcal{S}_T^{(n)})$ with $n = 1, 2, \dots, N$ from the underlying model, and the total expected reward can be estimated by,

$$\widehat{\rho}^c(\pi) = \frac{1}{N} \sum_{n=1}^N \sum_{t=0}^T R(\mathcal{S}_t^{(n)}, \pi_t(\mathcal{S}_t^{(n)})).$$

Further, to assess the process stability, we measure the batch-to-batch variation through the standard deviation (SD) of the total reward,

$$\text{SD}^c(\pi) = \text{SD}_{\tau^c} \left[\sum_{t=0}^T R(\mathcal{S}_t, a_t) \middle| \mathcal{S}_0, \pi \right],$$

which is estimated by sample SD from N replications of simulation experiments, i.e.,

$$\widehat{\text{SD}}^c(\pi) = \sqrt{\frac{1}{N-1} \sum_{n=1}^N \left[\sum_{t=0}^T R(\mathcal{S}_t^{(n)}, \pi_t(\mathcal{S}_t^{(n)})) - \widehat{\rho}^c(\pi) \right]^2}.$$

For each method or policy, we run $N = 100$ replications to compare the average reward and the variations measured by standard deviation (SD). For the reinforcement learning methodologies, we will first compare the performance under different size of historical data before this batch fermentation, $J_t = 3, 10, 20$. Similarly as in Section 8.1, we consider both low and high stochastic uncertainty cases. The results are shown in Tables 1 and 2.

Table 1: The mean and SD of reward obtained by using fixed threshold or perfect information MDP.

	Small Stochastic Uncertainty		Large Stochastic Uncertainty	
	$\widehat{\rho}^c(\pi)$	$\widehat{\text{SD}}^c(\pi)$	$\widehat{\rho}^c(\pi)$	$\widehat{\text{SD}}^c(\pi)$
Fixed Threshold	120.40	305.30	7.10	405.80
Perfect Info MDP	177.23	125.86	122.86	152.26

Table 2: The mean and SD of reward obtained by using the reinforcement learning ignoring and accounting for model risk under the situations with different amounts of historical data J_t .

Small Stochastic Uncertainty						
	$J_t = 3$		$J_t = 10$		$J_t = 20$	
	$\widehat{\rho}^c(\pi)$	$\widehat{\text{SD}}^c(\pi)$	$\widehat{\rho}^c(\pi)$	$\widehat{\text{SD}}^c(\pi)$	$\widehat{\rho}^c(\pi)$	$\widehat{\text{SD}}^c(\pi)$
RL ignoring MR	132.00	221.68	143.47	196.39	153.98	165.79
RL with MR	159.16	128.76	171.63	126.68	176.30	126.26
Large Stochastic Uncertainty						
	$J_t = 3$		$J_t = 10$		$J_t = 20$	
	$\widehat{\rho}^c(\pi)$	$\widehat{\text{SD}}^c(\pi)$	$\widehat{\rho}^c(\pi)$	$\widehat{\text{SD}}^c(\pi)$	$\widehat{\rho}^c(\pi)$	$\widehat{\text{SD}}^c(\pi)$
RL ignoring MR	69.11	266.97	84.52	249.96	98.60	205.13
RL with MR	85.80	228.61	98.40	204.27	117.30	182.09

Based on the results in Tables 1 and 2, we can observe that for both low and high stochastic uncertainty cases, under different amount of historical process data (i.e., different level of model risk), the proposed model-based reinforcement learning accounting for model risk can outperform the reinforcement learning ignoring model risk and the fix threshold method, in terms of achieving more profit (larger mean reward) and more reliable system (smaller SD). Basically, the proposed methodology and the reinforcement learning ignoring model risk both have better performance than the fix threshold method, but worse than the MDP under perfect information, because of the impact of model risk. As the number of historical data J_t increases, the average reward will increase while variability will decrease, the performance of both reinforcement learning methodologies accounting for and ignoring model risk converges to that of MDP under perfect information. Comparing the performance under different level of stochastic uncertainty, all the methodologies performs better when the underlying bioprocess is more stable or inherent process stochastic uncertainty is smaller.

After that, we further provide the sensitivity study on the different protein value and failure penalty cost of the reward settings, which could be caused by difference in (1) scale of the bioreactor/project (e.g., lab-scale or production-scale); (2) type of cells (e.g., bacteria cell or virus) requiring different levels of monitoring, labor, equipment cleaning cost; and (3) cost of raw materials and media. More specific, we consider three levels of protein value, i.e., $r_h(p, i) = 5p - i$, $r_h(p, i) = 10p - i$ and $r_h(p, i) = 15p - i$; and three levels of failure cost, $r_f = 400, 880, 1000$. Similarly we compute the mean and SD of reward realized by 100 batch fermentation, using fix threshold method, the proposed model-based reinforcement learning accounting for and ignoring model risk, and the MDP under perfect information of F^c . For both reinforcement learning methodologies, we fix the size of historical data $J_t = 10$. We consider the process at low stochastic uncertainty, the corresponding results are shown in Table 3. Comparing the different methodologies at each value/cost setting, we can see that the proposed model-based reinforcement learning accounting for model risk outperforms the reinforcement learning ignoring model risk, while both reinforcement learning approaches perform better than fixed threshold but worse than MDP with perfect information. For each approach, as the value of protein increase, the average reward and the variation (i.e., SD) will increase; and as the failure cost increase, the average reward will decrease but the variation will increase. This matches with our intuition, since higher value of protein will increase the value for non-failure batches; higher failure cost will increase the penalty for failure batches; while both increases the range of potential reward of a batch fermentation. For lower protein value or/and lower failure cost cases, which induce smaller variations, the proposed reinforcement learning accounting for model risk (with $J_t = 10$) can achieve performance closer to MDP with perfect information. In other words, *the impact of model risk for bio-drugs with low value and penalty cost is less than those with high value and high penalty cost.*

Table 3: The mean and standard deviation (SD) of reward achieved for 100 batch fermentation by different methodologies, with different protein value and failure cost.

		Fixed Threshold		RL ignoring MR		RL with MR		Perfect Info MDP	
Protein Value	Failure Cost	$\hat{\rho}^c(\pi)$	$\widehat{SD}^c(\pi)$	$\hat{\rho}^c(\pi)$	$\widehat{SD}^c(\pi)$	$\hat{\rho}^c(\pi)$	$\widehat{SD}^c(\pi)$	$\hat{\rho}^c(\pi)$	$\widehat{SD}^c(\pi)$
5	400	29.68	142.86	66.22	58.89	71.28	33.90	72.20	34.01
10	400	140.60	184.12	155.00	135.88	181.34	110.70	185.71	87.15
15	400	251.51	226.89	298.34	140.28	299.47	123.00	314.25	105.63
5	880	-13.52	279.42	61.42	102.12	71.28	33.90	71.80	33.87
10	880	97.40	318.19	143.47	196.39	171.63	126.68	177.23	125.86
15	880	208.31	358.48	268.61	227.41	281.01	194.74	295.97	152.93
5	1000	-24.32	313.76	60.22	113.53	71.28	33.90	71.33	34.23
10	1000	86.60	352.19	139.87	215.71	170.43	137.03	176.03	136.27
15	1000	197.51	392.07	246.12	246.75	271.32	209.92	294.77	162.50

Conclusions

To guide the optimal, robust and customized harvest decision making for biopharmaceutical manufacturing fermentation process, we propose bioprocess model-based reinforcement learning framework accounting for model risk. The proposed framework can be applicable to various situations with limited real-world data, such as process development. We consider a hybrid model, characterizing the fermentation process inherent stochastic uncertainty, which can leverage on the information from ODE-based cell growth kinetics mechanism. The posterior distribution and Bayesian update are derived to quantify the estimation uncertainty and facilitate the online learning of interpretable model parameters. The developed reinforcement learning approach rigorously considers the impact of model risk through: (1) explicitly incorporating and updating the estimation uncertainty of underlying bioprocess model; and (2) correctly quantifying the prediction risk induced by both process inherent stochastic uncertainty and model risk. Then, we provide structural and sensitivity analyses to study the monotonicity properties of value function and optimal policy, and provide the insights on how model risk impacts on the optimal harvest policy. To solve the proposed model-based reinforcement learning, we apply the Bayesian sparse sampling, which can balance exploration and exploitation, and simultaneously facilitate the online learning and guide the search of reliable optimal fermentation harvest decision. The empirical study demonstrates that the proposed model-based reinforcement learning framework can outperform the existing industry practice (i.e., fixed threshold policy and reinforcement learning ignoring model risk) under various situations.

A Proof of Proposition 1

Proposition 1: Given the knowledge state \mathcal{I}_t , we can decompose the predictive variances $\tilde{\sigma}_t^{(p)2}$ and $\tilde{\sigma}_t^{(i)2}$ for protein and impurity,

$$\tilde{\sigma}_t^{(p)2} = \hat{\sigma}_t^{(p)2} + \check{\sigma}_t^{(p)2}; \quad \tilde{\sigma}_t^{(i)2} = \hat{\sigma}_t^{(i)2} + \check{\sigma}_t^{(i)2};$$

where $\hat{\sigma}_t^{(p)2} = \frac{\beta_t^{(p)}}{\lambda_t^{(p)} - 1}$, $\hat{\sigma}_t^{(i)2} = \frac{\beta_t^{(i)}}{\lambda_t^{(i)} - 1}$ measure the prediction risk contribution from bioprocess inherent stochastic uncertainty; and $\check{\sigma}_t^{(p)2} = \frac{\beta_t^{(p)}}{(\lambda_t^{(p)} - 1)\nu_t^{(p)}}$, $\check{\sigma}_t^{(i)2} = \frac{\beta_t^{(i)}}{(\lambda_t^{(i)} - 1)\nu_t^{(i)}}$ measure the contribution from model risk, for protein and impurity growth rates respectively.

Proof. Let $\Theta = \{\tilde{\mu}^{(p)}, \tilde{\sigma}^{(p)2}, \tilde{\mu}^{(i)}, \tilde{\sigma}^{(i)2}\} \sim p(\theta|\mathcal{X}_t)$ denote the random samples of protein and impurity growth coefficients generated from the posterior distribution. More specific, we have $\tilde{\mu}^{(p)}, \tilde{\sigma}^{(p)2}|\mathcal{X}_t \sim \mathcal{N}(\alpha_t^{(p)}, \sigma^{(p)2}/\nu_t^{(p)}) \cdot \text{Inv}\Gamma(\lambda_t^{(p)}, \beta_t^{(p)})$ and $\tilde{\mu}^{(i)}, \tilde{\sigma}^{(i)2}|\mathcal{X}_t \sim \mathcal{N}(\alpha_t^{(i)}, \sigma^{(i)2}/\nu_t^{(i)}) \cdot \text{Inv}\Gamma(\lambda_t^{(i)}, \beta_t^{(i)})$. Then, the variance of the compound variable $\tilde{\Phi}_{t'} \sim \mathcal{N}(\tilde{\mu}^{(p)}, \tilde{\sigma}^{(p)2})$, characterized by predictive variance $\tilde{\sigma}_t^{(p)2}$, can be decomposed as the following,

$$\begin{aligned} \tilde{\sigma}_t^{(p)2} &= \text{Var} \left[\tilde{\Phi}_{t'} | \mathcal{X}_t \right] = \mathbf{E}_{\Theta} \left[\text{Var} \left(\tilde{\Phi}_{t'} | \Theta \right) | \mathcal{X}_t \right] + \text{Var}_{\Theta} \left[\mathbf{E} \left(\tilde{\Phi}_{t'} | \Theta \right) | \mathcal{X}_t \right] \\ &= \mathbf{E}_{\Theta} \left[\tilde{\sigma}^{(p)2} | \mathcal{X}_t \right] + \text{Var}_{\Theta} \left[\tilde{\mu}^{(p)} | \mathcal{X}_t \right] \\ &= \mathbf{E}_{\Theta} \left[\tilde{\sigma}^{(p)2} | \mathcal{X}_t \right] + \mathbf{E}_{\Theta} \left[\text{Var} \left(\tilde{\mu}^{(p)} | \tilde{\sigma}^{(p)2} \right) | \mathcal{X}_t \right] + \text{Var}_{\Theta} \left[\mathbf{E} \left(\tilde{\mu}^{(p)2} | \tilde{\sigma}^{(p)2} \right) | \mathcal{X}_t \right] \\ &= \mathbf{E}_{\Theta} \left[\tilde{\sigma}^{(p)2} | \mathcal{X}_t \right] + \mathbf{E}_{\Theta} \left[\tilde{\sigma}^{(p)2} / \nu_t^{(p)} | \mathcal{X}_t \right] + \text{Var}_{\Theta} \left[\alpha_t^{(p)} | \mathcal{X}_t \right] \\ &= \frac{\beta_t^{(p)}}{\lambda_t^{(p)} - 1} + \frac{\beta_t^{(p)}}{(\lambda_t^{(p)} - 1)\nu_t^{(p)}}, \end{aligned} \quad (20)$$

where the first and third equations hold by law of total variance, and the last term in the fourth equation is zero with given knowledge states \mathcal{I}_t . Therefore, the first term on the right side of eq.(20), denoted by $\hat{\sigma}_t^{(p)2} = \mathbf{E}_{\Theta} \left[\tilde{\sigma}^{(p)2} | \mathcal{X}_t \right] = \frac{\beta_t^{(p)}}{\lambda_t^{(p)} - 1}$, measures the prediction variance contributed from bioprocess inherent stochastic uncertainty for protein growth. And the second term, denoted by $\check{\sigma}_t^{(p)2} = \mathbf{E}_{\Theta} \left[\text{Var} \left(\tilde{\mu}^{(p)} | \tilde{\sigma}^{(p)2} \right) | \mathcal{X}_t \right] = \frac{\beta_t^{(p)}}{(\lambda_t^{(p)} - 1)\nu_t^{(p)}}$, measures the contribution from model risk. Similar decomposition also applies for the variance of the compound variable $\tilde{\Psi}_{t'} \sim \mathcal{N}(\tilde{\mu}^{(i)}, \tilde{\sigma}^{(i)2})$,

$$\begin{aligned} \tilde{\sigma}_t^{(i)2} &= \text{Var} \left[\tilde{\Psi}_{t'} | \mathcal{X}_t \right] = \mathbf{E}_{\Theta} \left[\text{Var} \left(\tilde{\Psi}_{t'} | \Theta \right) | \mathcal{X}_t \right] + \text{Var}_{\Theta} \left[\mathbf{E} \left(\tilde{\Psi}_{t'} | \Theta \right) | \mathcal{X}_t \right] \\ &= \mathbf{E}_{\Theta} \left[\tilde{\sigma}^{(i)2} | \mathcal{X}_t \right] + \text{Var}_{\Theta} \left[\mu^{(i)} | \mathcal{X}_t \right] = \frac{\beta_t^{(i)}}{\lambda_t^{(i)} - 1} + \frac{\beta_t^{(i)}}{(\lambda_t^{(i)} - 1)\nu_t^{(i)}}, \end{aligned} \quad (21)$$

□

B Proof of Theorem 1

Theorem 1: Given the knowledge state \mathcal{I}_t , the value function $V_t(\mathcal{S}_t, \mathcal{I}_t)$ with $\mathcal{S}_t = (p_t, i_t)$ is a non-increasing function in the impurity level i_t and a non-decreasing function in the protein level p_t .

Proof. At the fermentation stopping time T , we have that

$$V_T(p_T, i_T, \mathcal{I}_T) = \begin{cases} r_h(p_T, i_T), & i_T \neq I_f \\ -r_f, & i_T = I_f \end{cases}$$

which is non-increasing in impurity i_T and non-decreasing in protein p_T . Based on the value function given in Section 5, we can prove Theorem 1 through backward induction.

Assume that $V_{t+1}(p_{t+1}, i_{t+1}, \mathcal{I}_{t+1})$ is non-increasing in i_{t+1} , and non-decreasing in p_{t+1} . Then, we can consider at time t ,

$$V_t(p_t, i_t, \mathcal{I}_t) = \begin{cases} \max\{r_h(p_t, i_t), -c_u + \gamma E[V_{t+1}(p_t e^{\phi_t}, i_t e^{\psi_t}, \mathcal{I}_{t+1})]\}, & i_t \neq I_f \\ -r_f, & i_t = I_f \end{cases} \quad (22)$$

For $i_t^+ \geq i_t$,

$$\begin{aligned} E[V_{t+1}(p_t e^{\phi_t}, i_t e^{\psi_t}, \mathcal{I}_{t+1})] &= -r_f \int_{\ln \bar{I} - \ln i_t}^{\infty} f_t^{(i)}(\psi_t) d\psi_t \\ &+ \int_0^{\ln \bar{I} - \ln i_t} \int_0^{\ln \bar{P}} V_{t+1}(p_t e^{\phi_t}, i_t e^{\psi_t}, \mathcal{I}_{t+1}) f_t^{(p)}(\phi_t) f_t^{(i)}(\psi_t) d\phi_t d\psi_t \\ &= -r_f \int_{\ln \bar{I} - \ln i_t}^{\infty} f_t^{(i)}(\psi_t) d\psi_t \\ &+ \int_{\ln \bar{I} - \ln i_t^+}^{\ln \bar{I} - \ln i_t} \int_0^{\ln \bar{P}} V_{t+1}(p_t e^{\phi_t}, i_t e^{\psi_t}, \mathcal{I}_{t+1}) f_t^{(p)}(\phi_t) f_t^{(i)}(\psi_t) d\phi_t d\psi_t \\ &+ \int_0^{\ln \bar{I} - \ln i_t^+} \int_0^{\ln \bar{P}} V_{t+1}(p_t e^{\phi_t}, i_t e^{\psi_t}, \mathcal{I}_{t+1}) f_t^{(p)}(\phi_t) f_t^{(i)}(\psi_t) d\phi_t d\psi_t \\ &\geq -r_f \int_{\ln \bar{I} - \ln i_t}^{\infty} f_t^{(i)}(\psi_t) d\psi_t - r_f \int_{\ln \bar{I} - \ln i_t^+}^{\ln \bar{I} - \ln i_t} f_t^{(i)}(\psi_t) d\psi_t \\ &+ \int_0^{\ln \bar{I} - \ln i_t^+} \int_0^{\ln \bar{P}} V_{t+1}(p_t e^{\phi_t}, i_t^+ e^{\psi_t}, \mathcal{I}_{t+1}) f_t^{(p)}(\phi_t) f_t^{(i)}(\psi_t) d\phi_t d\psi_t \\ &= E[V_{t+1}(p_t e^{\phi_t}, i_t^+ e^{\psi_t}, \mathcal{I}_{t+1})] \end{aligned} \quad (23)$$

where the inequality hold because that $V_{t+1}(p_t e^{\phi_t}, i_t e^{\psi_t}, \mathcal{I}_{t+1}) \geq -r_f$, $i_t e^{\psi_t} \leq i_t^+ e^{\psi_t}$ and induction assumption. Therefore, we have $V_t(p_t, i_t, \mathcal{I}_t)$ is also non-increasing in i_t . On the other hand, for $p_t^+ \geq p_t$,

$$\begin{aligned} E[V_{t+1}(p_t e^{\phi_t}, i_t e^{\psi_t}, \mathcal{I}_{t+1})] &= -r_f \int_{\ln \bar{I} - \ln i_t}^{\infty} f_t^{(i)}(\psi_t) d\psi_t \\ &+ \int_0^{\ln \bar{I} - \ln i_t} \int_0^{\ln \bar{P}} V_{t+1}(p_t e^{\phi_t}, i_t e^{\psi_t}, \mathcal{I}_{t+1}) f_t^{(p)}(\phi_t) f_t^{(i)}(\psi_t) d\phi_t d\psi_t \\ &\leq -r_f \int_{\ln \bar{I} - \ln i_t}^{\infty} f_t^{(i)}(\psi_t) d\psi_t \\ &+ \int_0^{\ln \bar{I} - \ln i_t} \int_0^{\ln \bar{P}} V_{t+1}(p_t^+ e^{\phi_t}, i_t e^{\psi_t}, \mathcal{I}_{t+1}) f_t^{(p)}(\phi_t) f_t^{(i)}(\psi_t) d\phi_t d\psi_t \\ &= E[V_{t+1}(p_t^+ e^{\phi_t}, i_t e^{\psi_t}, \mathcal{I}_{t+1})] \end{aligned} \quad (24)$$

where the inequality hold because that $p_t e^{\phi_t} \leq p_t^+ e^{\phi_t}$ and induction assumption. Therefore, we have $V_t(p_t, i_t, \mathcal{I}_t)$ is also non-decreasing in p_t . □

C Proof of Theorem 2

Theorem 2: At any time period t , given any feasible protein level p_t , there exists a threshold i_t^* such that the optimal decision is to harvest if the impurity level $i_t \geq i_t^*$ and following condition holds for all $i_t^+ > i_t^- \geq 0$:

$$\begin{aligned} r_h(p_t, i_t^-) - r_h(p_t, i_t^+) &\leq \gamma r_f [\Pr(i_{t+1} \leq \bar{I} | i_t^-) - \Pr(i_{t+1} \leq \bar{I} | i_t^+)] \\ &+ \gamma \int_0^{\ln \bar{I} - \ln i_t^-} [r_h(p_t, i_t^- e^{\psi_t}) - r_h(\bar{P}, i_t^- e^{\psi_t})] f_t^{(i,n)}(\psi_t) d\psi_t, \end{aligned} \quad (25)$$

where $\Pr(i_{t+1} \leq \bar{I} | i_t) = \Pr(i_t e^{\psi_t} \leq \bar{I}) = \int_0^{\ln \bar{I} - \ln i_t} f_t^{(i,n)}(\psi_t) d\psi_t$ is the probability that the batch failure doesn't happen in next period given the current impurity level i_t .

Proof. Notice Theorem 2 indicates that if $\pi^*(p_t, i_t^-, \mathcal{I}_t) = H$, then $\pi^*(p_t, i_t^+, \mathcal{I}_t) = H$. This directly holds if $i_t^+ > \bar{I}$. On the other hand if $i_t^+ \leq \bar{I}$, assume that the contradiction hypothesis $\pi^*(p_t, i_t^+, \mathcal{I}_t) = C$ holds,

$$\begin{aligned} r_h(p_t, i_t^-) &\geq -c_u + \gamma \mathbb{E} [V_{t+1}(p_t e^{\phi_t}, i_t^- e^{\psi_t}, \mathcal{I}_{t+1})] \\ r_h(p_t, i_t^+) &\leq -c_u + \gamma \mathbb{E} [V_{t+1}(p_t e^{\phi_t}, i_t^+ e^{\psi_t}, \mathcal{I}_{t+1})]. \end{aligned}$$

Then, we have,

$$\begin{aligned} r_h(p_t, i_t^-) - r_h(p_t, i_t^+) &\geq \gamma \mathbb{E} [V_{t+1}(p_t e^{\phi_t}, i_t^- e^{\psi_t}, \mathcal{I}_{t+1})] - \gamma \mathbb{E} [V_{t+1}(p_t e^{\phi_t}, i_t^+ e^{\psi_t}, \mathcal{I}_{t+1})] \\ &= -\gamma r_f \int_{\ln \bar{I} - \ln i_t^-}^{\infty} f_t^{(i)}(\psi_t) d\psi_t + \gamma r_f \int_{\ln \bar{I} - \ln i_t^+}^{\infty} f_t^{(i)}(\psi_t) d\psi_t \\ &\quad + \gamma \int_0^{\ln \bar{I} - \ln i_t^-} \int_0^{\ln \bar{P}} V_{t+1}(p_t e^{\phi_t}, i_t^- e^{\psi_t}, \mathcal{I}_{t+1}) f_t^{(p)}(\phi_t) f_t^{(i)}(\psi_t) d\phi_t d\psi_t \\ &\quad - \gamma \int_0^{\ln \bar{I} - \ln i_t^+} \int_0^{\ln \bar{P}} V_{t+1}(p_t e^{\phi_t}, i_t^+ e^{\psi_t}, \mathcal{I}_{t+1}) f_t^{(p)}(\phi_t) f_t^{(i)}(\psi_t) d\phi_t d\psi_t \\ &\geq \gamma r_f \left[\int_0^{\ln \bar{I} - \ln i_t^-} f_t^{(i)}(\psi_t) d\psi_t - \int_0^{\ln \bar{I} - \ln i_t^+} f_t^{(i)}(\psi_t) d\psi_t \right] \\ &\quad + \gamma \int_0^{\ln \bar{I} - \ln i_t^-} \int_0^{\ln \bar{P}} r_h(p_t, i_t^- e^{\psi_t}) f_t^{(p)}(\phi_t) f_t^{(i)}(\psi_t) d\phi_t d\psi_t \\ &\quad - \gamma \int_0^{\ln \bar{I} - \ln i_t^+} \int_0^{\ln \bar{P}} V_{t+1}(\bar{P}, i_t^- e^{\psi_t}, \mathcal{I}_{t+1}) f_t^{(p)}(\phi_t) f_t^{(i)}(\psi_t) d\phi_t d\psi_t \end{aligned} \quad (26)$$

$$\begin{aligned} &\geq \gamma r_f \left[\int_0^{\ln \bar{I} - \ln i_t^-} f_t^{(i)}(\psi_t) d\psi_t - \int_0^{\ln \bar{I} - \ln i_t^+} f_t^{(i)}(\psi_t) d\psi_t \right] \\ &\quad + \gamma \int_0^{\ln \bar{I} - \ln i_t^-} r_h(p_t, i_t^- e^{\psi_t}) f_t^{(i)}(\psi_t) d\psi_t - \gamma \int_0^{\ln \bar{I} - \ln i_t^-} r_h(\bar{P}, i_t^- e^{\psi_t}) f_t^{(i)}(\psi_t) d\psi_t \end{aligned} \quad (27)$$

$$\begin{aligned} &\geq \gamma r_f \left[\int_0^{\ln \bar{I} - \ln i_t^-} f_t^{(i)}(\psi_t) d\psi_t - \int_0^{\ln \bar{I} - \ln i_t^+} f_t^{(i)}(\psi_t) d\psi_t \right] \\ &\quad + \gamma \int_0^{\ln \bar{I} - \ln i_t^-} [r_h(p_t, i_t^- e^{\psi_t}) - r_h(\bar{P}, i_t^- e^{\psi_t})] f_t^{(i)}(\psi_t) d\psi_t \end{aligned}$$

which contradict the condition, so that we have $\pi^*(p_t, i_t^+) = H$. Notice that, inequality (26) holds because that $V_{t+1}(p_t e^{\phi_t}, i_t^- e^{\psi_t}, \mathcal{I}_{t+1}) \geq V_{t+1}(p_t, i_t^- e^{\psi_t}, \mathcal{I}_{t+1}) \geq r_h(p_t, i_t^- e^{\psi_t})$ by definition of value function and it is non-decreasing in p_t ($p_t \leq p_t e^{\phi_t} \leq \bar{P}$); and $V_{t+1}(p_t e^{\phi_t}, i_t^+ e^{\psi_t}, \mathcal{I}_{t+1}) \leq V_{t+1}(\bar{P}, i_t^- e^{\psi_t}, \mathcal{I}_{t+1})$ as value function is non-decreasing in p_t and non-increasing in i_t . inequality (27) holds because that $\ln \bar{I} - \ln i_t^+ \leq \ln \bar{I} - \ln i_t^-$ and $V_{t+1}(\bar{P}, i_t^- e^{\psi_t}, \mathcal{I}_{t+1}) = r_h(\bar{P}, i_t^- e^{\psi_t})$ by boundary harvest condition, and then integrate out ϕ_t . \square

D Proof of Theorem 3

Theorem 3: The monotonicity of $V_t(\mathcal{S}_t, \mathcal{I}_t)$ over knowledge states can be summarized as follows:

- (i) it is non-increasing in $\alpha_t^{(i)}$ and non-decreasing in $\alpha_t^{(p)}$;
- (ii) it is non-increasing in $\beta_t^{(i)}$ and non-decreasing in $\beta_t^{(p)}$;
- (iii) it is non-increasing in $\nu_t^{(p)}$ and non-decreasing in $\nu_t^{(i)}$;
- (iv) for reasonably large $\lambda_t^{(p)}$ and $\lambda_t^{(i)}$ so that the predictive t-distribution in eq.(7) can be approximated by Gaussian, it is non-increasing in $\lambda_t^{(p)}$ and non-decreasing in $\lambda_t^{(i)}$.

D.1 Proof of Part (i)

Proof. Here we first consider the non-decreasing in $\alpha_t^{(p)}$ part, and the proof of the non-increasing in $\alpha_t^{(i)}$ part can follow the similar procedure. Given the other hyper-parameters $(\nu_t^{(p)}, \lambda_t^{(p)}, \beta_t^{(p)}, \alpha_t^{(i)}, \nu_t^{(i)}, \lambda_t^{(i)}, \beta_t^{(i)})$ to be the same at t , suppose $\alpha_t^{(p)+} - \alpha_t^{(p)} = \delta \geq 0$.

Notice at the stopping time T ,

$$V_T(p_T, i_T, \mathcal{I}_T) = \begin{cases} r_h(p_T, i_T), & i_T \neq I_f \\ -r_f, & i_T = I_f \end{cases}$$

which is non-decreasing in $\alpha_T^{(p)}$. Based on the Bellman's equation for value function, we can prove it through backward induction. Assume that $V_{t+1}(p_{t+1}, i_{t+1}, \mathcal{I}_{t+1})$ is non-decreasing in $\alpha_{t+1}^{(p)}$. Then at time t ,

$$V_t(p_t, i_t, \mathcal{I}_t) = \begin{cases} \max\{r_h(p_t, i_t), -c_u + \gamma E[V_{t+1}(p_t e^{\phi_t}, i_t e^{\psi_t}, \mathcal{I}_{t+1})]\}, & i_t \neq I_f \\ -r_f, & i_t = I_f \end{cases}$$

The difference in $\alpha_t^{(p)}$ will impact the expectation through the predictive distribution $f_t^{(p)}(\phi_t | \alpha_t^{(p)})$; and also the knowledge hyper parameters $\alpha_{t+1}^{(p)}, \beta_{t+1}^{(p)}$ through the knowledge states update, see eq.(6). Then,

$$\begin{aligned} E[V_{t+1}(p_t e^{\phi_t}, i_t e^{\psi_t}, \mathcal{I}_{t+1}(\alpha_{t+1}^{(p)}, \beta_{t+1}^{(p)})) | \alpha_t^{(p)}] &= -r_f \int_{\ln \bar{T} - \ln i_t}^{\infty} f_t^{(i)}(\psi_t) d\psi_t \\ &+ \int_0^{\ln \bar{T} - \ln i_t} \int_0^{\ln \bar{P}} V_{t+1}(p_t e^{\phi_t}, i_t e^{\psi_t}, \mathcal{I}_{t+1}(\alpha_{t+1}^{(p)}, \beta_{t+1}^{(p)})) f_t^{(p)}(\phi_t | \alpha_t^{(p)}) f_t^{(i)}(\psi_t) d\phi_t d\psi_t \\ &\leq -r_f \int_{\ln \bar{T} - \ln i_t}^{\infty} f_t^{(i)}(\psi_t) d\psi_t \\ &+ \int_0^{\ln \bar{T} - \ln i_t} \int_{-\delta}^{\ln \bar{P} - \delta} V_{t+1}(p_t e^{\phi_t + \delta}, i_t e^{\psi_t}, \mathcal{I}_{t+1}(\alpha_{t+1}^{(p)+}, \beta_{t+1}^{(p)})) f_t^{(p)}(\phi_t | \alpha_t^{(p)}) f_t^{(i)}(\psi_t) d\phi_t d\psi_t \end{aligned} \quad (28)$$

$$\begin{aligned} &\leq -r_f \int_{\ln \bar{T} - \ln i_t}^{\infty} f_t^{(i)}(\psi_t) d\psi_t \\ &+ \int_0^{\ln \bar{T} - \ln i_t} \int_0^{\ln \bar{P}} V_{t+1}(p_t e^{\phi'_t}, i_t e^{\psi_t}, \mathcal{I}_{t+1}(\alpha_{t+1}^{(p)+}, \beta_{t+1}^{(p)+})) f_t^{(p)}(\phi'_t | \alpha_t^{(p)+}) f_t^{(i)}(\psi_t) d\phi'_t d\psi_t \end{aligned} \quad (29)$$

$$= E[V_{t+1}(p_t e^{\phi_t}, i_t e^{\psi_t}, \mathcal{I}_{t+1}) | \alpha_t^{(p)+}], \quad (30)$$

where $\phi'_t = \phi_t + \delta$, $\alpha_{t+1}^{(p)+} = \alpha_t^{(p)+} + \frac{\phi'_t - \alpha_t^{(p)+}}{\nu_{t+1}^{(p)}} = \alpha_t^{(p)+} + \frac{\phi_t - \alpha_t^{(p)}}{\nu_{t+1}^{(p)}} = \alpha_t^{(p)} + \delta$, and $\beta_{t+1}^{(p)+} = \beta_t^{(p)} + \frac{\nu_t^{(p)}(\phi'_t - \alpha_t^{(p)+})^2}{2\nu_{t+1}^{(p)}} = \beta_t^{(p)} + \frac{\nu_t^{(p)}(\phi_t - \alpha_t^{(p)})^2}{2\nu_{t+1}^{(p)}} = \beta_{t+1}^{(p)}$. The inequality (28) holds because the value function is non-decreasing in p_t (since $p_t e^{\phi_t + \delta} \geq p_t e^{\phi_t}$), and induction assumption (since $\alpha_{t+1}^{(p)+} \geq \alpha_{t+1}^{(p)}$). And eq.(29) holds by performing variable replacement $\phi'_t = \phi_t + \delta$. Thus, we have $V_t(p_t, i_t, \mathcal{I}_t(\alpha_t^{(p)})) \leq V_t(p_t, i_t, \mathcal{I}_t(\alpha_t^{(p)+}))$.

On the other hand, considering $\alpha_t^{(i)+} - \alpha_t^{(i)} = \delta \geq 0$, we have

$$\begin{aligned} E[V_{t+1}(p_t e^{\phi_t}, i_t e^{\psi_t}, \mathcal{I}_{t+1}(\alpha_{t+1}^{(i)}, \beta_{t+1}^{(i)})) | \alpha_t^{(i)}] &= -r_f \int_{\ln \bar{T} - \ln i_t}^{\infty} f_t^{(i)}(\psi_t | \alpha_t^{(i)}) d\psi_t \\ &+ \int_0^{\ln \bar{T} - \ln i_t} \int_0^{\ln \bar{P}} V_{t+1}(p_t e^{\phi_t}, i_t e^{\psi_t}, \mathcal{I}_{t+1}(\alpha_{t+1}^{(i)}, \beta_{t+1}^{(i)})) f_t^{(p)}(\phi_t) f_t^{(i)}(\psi_t | \alpha_t^{(i)}) d\phi_t d\psi_t \\ &\geq -r_f \int_{\ln \bar{T} - \ln i_t - \delta}^{\infty} f_t^{(i)}(\psi_t) d\psi_t \\ &+ \int_{-\delta}^{\ln \bar{T} - \ln i_t - \delta} \int_0^{\ln \bar{P}} V_{t+1}(p_t e^{\phi_t}, i_t e^{\psi_t + \delta}, \mathcal{I}_{t+1}(\alpha_{t+1}^{(i)+}, \beta_{t+1}^{(i)})) f_t^{(p)}(\phi_t) f_t^{(i)}(\psi_t | \alpha_t^{(i)}) d\phi_t d\psi_t \end{aligned}$$

$$\begin{aligned}
&\geq -r_f \int_{\ln \bar{I} - \ln i_t}^{\infty} f_t^{(i)}(\psi'_t | \alpha_t^{(i)+}) d\psi'_t \\
&\quad + \int_0^{\ln \bar{I} - \ln i_t} \int_0^{\ln \bar{P}} V_{t+1}(p_t e^{\phi_t}, i_t e^{\psi'_t}, \mathcal{I}_{t+1}(\alpha_{t+1}^{(i)+}, \beta_{t+1}^{(i)+})) f_t^{(p)}(\phi_t) f_t^{(i)}(\psi'_t | \alpha_t^{(i)+}) d\phi_t d\psi'_t \\
&= \mathbb{E}[V_{t+1}(p_t e^{\phi_t}, i_t e^{\psi_t}, \mathcal{I}_{t+1}) | \alpha_t^{(i)+}], \tag{31}
\end{aligned}$$

with $\psi'_t = \psi_t + \delta$, $\alpha_{t+1}^{(i)+} = \alpha_t^{(i)+} + \frac{\psi'_t - \alpha_t^{(i)+}}{\nu_{t+1}^{(i)}} = \alpha_t^{(i)+} + \frac{\phi_t - \alpha_t^{(i)}}{\nu_{t+1}^{(i)}} = \alpha_t^{(i)} + \delta$, and $\beta_{t+1}^{(i)+} = \beta_t^{(i)} + \frac{\nu_t^{(i)}(\psi'_t - \alpha_t^{(i)+})^2}{2\nu_{t+1}^{(i)}} = \beta_t^{(i)} + \frac{\nu_t^{(i)}(\psi_t - \alpha_t^{(i)})^2}{2\nu_{t+1}^{(i)}} = \beta_{t+1}^{(i)}$. Similarly, the inequalities hold because the value function is non-increasing in i_t and non-increasing in $\alpha_{t+1}^{(i)}$ by induction assumption, as well as performing variable replacement $\psi'_t = \psi_t + \delta$. Thus, we have $V_t(p_t, i_t, \mathcal{I}_t(\alpha_t^{(i)})) \geq V_t(p_t, i_t, \mathcal{I}_t(\alpha_t^{(i)+}))$. \square

D.2 Proof of Part (ii)

Proof. Here we consider the non-decreasing in $\beta_t^{(p)}$, as the proof of the non-increasing in $\beta_t^{(i)}$ can follow the similar procedure. Given the other hyper-parameters $(\alpha_t^{(p)}, \nu_t^{(p)}, \lambda_t^{(p)}, \alpha_t^{(i)}, \nu_t^{(i)}, \lambda_t^{(i)}, \beta_t^{(i)})$ to be the same at t , suppose $\beta_t^{(p)+} \geq \beta_t^{(p)} > 0$.

Notice at the stopping time T ,

$$V_T(p_T, i_T, \mathcal{I}_T) = \begin{cases} r_h(p_T, i_T), & i_T \neq I_f \\ -r_f, & i_T = I_f \end{cases}$$

which is non-decreasing in $\beta_T^{(p)}$. Based on the Bellman's equation for value function, we can prove it through Dynamic programming or backward induction. Assume that $V_{t+1}(p_{t+1}, i_{t+1}, \mathcal{I}_{t+1})$ is non-decreasing in $\beta_{t+1}^{(p)}$. Then at any time t ,

$$V_t(p_t, i_t, \mathcal{I}_t) = \begin{cases} \max\{r_h(p_t, i_t), -c_u + \gamma \mathbb{E}[V_{t+1}(p_t e^{\phi_t}, i_t e^{\psi_t}, \mathcal{I}_{t+1})]\}, & i_t \neq I_f \\ -r_f, & i_t = I_f \end{cases}$$

The difference in $\beta_t^{(p)}$ will impact the expectation through the predictive distribution $f_t^{(p)}(\phi_t | \beta_t^{(p)})$; and also the knowledge hyper parameters $\alpha_{t+1}^{(p)}, \beta_{t+1}^{(p)}$ through the knowledge states update, see eq.(6). Then,

$$\begin{aligned}
\mathbb{E}[V_{t+1}(p_t e^{\phi_t}, i_t e^{\psi_t}, \mathcal{I}_{t+1}(\alpha_{t+1}^{(p)}, \beta_{t+1}^{(p)})) | \beta_t^{(p)}] &= -r_f \int_{\ln \bar{I} - \ln i_t}^{\infty} f_t^{(i)}(\psi_t) d\psi_t \\
&\quad + \int_0^{\ln \bar{I} - \ln i_t} \int_0^{\ln \bar{P}} V_{t+1}(p_t e^{\phi_t}, i_t e^{\psi_t}, \mathcal{I}_{t+1}(\alpha_{t+1}^{(p)}, \beta_{t+1}^{(p)})) f_t^{(p)}(\phi_t | \beta_t^{(p)}) f_t^{(i)}(\psi_t) d\phi_t d\psi_t.
\end{aligned}$$

Then for any (p, i) ,

$$\begin{aligned}
&\int_0^{\ln \bar{P}} V_{t+1}(p e^{\phi_t}, i, \mathcal{I}_{t+1}(\alpha_{t+1}^{(p)}, \beta_{t+1}^{(p)})) f_t^{(p)}(\phi_t | \beta_t^{(p)}) d\phi_t \\
&= \int_{-\alpha_t^{(p)}}^{\ln \bar{P} - \alpha_t^{(p)}} V_{t+1}(p' e^{\phi'_t}, i, \mathcal{I}_{t+1}(\alpha_{t+1}^{(p)}, \beta_{t+1}^{(p)})) f_t^{(p)}(\phi'_t | \beta_t^{(p)}) d\phi'_t \\
&\leq \int_{-\alpha_t^{(p)}}^{\ln \bar{P} - \alpha_t^{(p)}} V_{t+1}(p' e^{\phi'_t}, i, \mathcal{I}_{t+1}(\alpha_{t+1}^{(p)}, \beta_{t+1}^{(p)+})) f_t^{(p)}(\phi'_t | \beta_t^{(p)}) d\phi'_t \\
&= \int_0^{\ln \bar{P} - \alpha_t^{(p)}} V_{t+1}(p' e^{\phi'_t}, i, \mathcal{I}_{t+1}(\alpha_{t+1}^{(p)}, \beta_{t+1}^{(p)+})) f_t^{(p)}(\phi'_t | \beta_t^{(p)}) d\phi'_t \\
&\quad + \int_{-\alpha_t^{(p)}}^0 V_{t+1}(p' e^{\phi'_t}, i, \mathcal{I}_{t+1}(\alpha_{t+1}^{(p)}, \beta_{t+1}^{(p)+})) f_t^{(p)}(\phi'_t | \beta_t^{(p)}) d\phi'_t, \tag{32}
\end{aligned}$$

where the first equation holds by variable replacement $\phi'_t = \phi_t - \alpha_t^{(p)}$, so that $p' = pe^{\alpha_t^{(p)}}$, and

$$f_t^{(p)}(\phi'_t | \mathcal{X}_t) = \pi^{-1/2} \frac{\Gamma\left(\lambda_t^{(p)} + \frac{1}{2}\right)}{\Gamma(\lambda_t^{(p)})} \left[\frac{\nu_t^{(p)}}{2\beta_t^{(p)}(1 + \nu_t^{(p)})} \right]^{1/2} \left[1 + \frac{\nu_t^{(p)}\phi_t'^2}{2\beta_t^{(p)}(1 + \nu_t^{(p)})} \right]^{-\lambda_t^{(p)} - 1/2}.$$

In addition, $\beta_{t+1}^{(p)+} = \beta_t^{(p)+} + \frac{\nu_t^{(p)}\eta^2\phi_t'^2}{2\nu_{t+1}^{(p)}} \geq \beta_{t+1}^{(p)}$, with $\eta = \sqrt{\frac{\beta_t^{(p)+}}{\beta_t^{(p)}}} \geq 1$, the inequality (32) holds by induction assumption. Let $\phi_t'' = \eta\phi_t'$ and $\alpha_{t+1}^{(p)+} = \alpha_t^{(p)} + \frac{\eta\phi_t'}{\nu_{t+1}^{(p)}} \triangleq \alpha_t^{(p)} + \kappa^+\phi_t'$. Notice that $\alpha_{t+1}^{(p)} = \alpha_t^{(p)} + \frac{\phi_t'}{\nu_{t+1}^{(p)}} \triangleq \alpha_t^{(p)} + \kappa\phi_t'$, it is easy to see that $\kappa^+ > \kappa > 0$. Therefore,

$$\begin{aligned} & \int_0^{\ln \bar{P} - \alpha_t^{(p)}} V_{t+1}(p'e^{\phi_t'}, i, \mathcal{I}_{t+1}(\alpha_{t+1}^{(p)}, \beta_{t+1}^{(p)+})) f_t^{(p)}(\phi_t' | \beta_t^{(p)}) d\phi_t' \\ & \leq \int_0^{(\ln \bar{P} - \alpha_t^{(p)})/\eta} V_{t+1}(p'e^{\eta\phi_t'}, i, \mathcal{I}_{t+1}(\alpha_{t+1}^{(p)+}, \beta_{t+1}^{(p)+})) f_t^{(p)}(\phi_t' | \beta_t^{(p)}) d\phi_t' \\ & \leq \int_0^{\ln \bar{P} - \alpha_t^{(p)}} V_{t+1}(p'e^{\phi_t''}, i, \mathcal{I}_{t+1}(\alpha_{t+1}^{(p)+}, \beta_{t+1}^{(p)+})) f_t^{(p)}(\phi_t'' | \beta_t^{(p)+}) d\phi_t'', \end{aligned}$$

and

$$\begin{aligned} & \int_{-\alpha_t^{(p)}}^0 V_{t+1}(p'e^{\phi_t'}, i, \mathcal{I}_{t+1}(\alpha_{t+1}^{(p)}, \beta_{t+1}^{(p)+})) f_t^{(p)}(\phi_t' | \beta_t^{(p)}) d\phi_t' \\ & = - \int_0^{\alpha_t^{(p)}} V_{t+1}(p'e^{-\phi_t'}, i, \mathcal{I}_{t+1}(\alpha_t^{(p)} - \kappa\phi_t', \beta_{t+1}^{(p)+})) f_t^{(p)}(\phi_t' | \beta_t^{(p)}) d\phi_t' \\ & \leq - \int_0^{\alpha_t^{(p)}/\eta} V_{t+1}(p'e^{-\eta\phi_t'}, i, \mathcal{I}_{t+1}(\alpha_t^{(p)} - \kappa^+\phi_t', \beta_{t+1}^{(p)+})) f_t^{(p)}(\phi_t' | \beta_t^{(p)}) d\phi_t' \\ & \leq \int_{-\alpha_t^{(p)}}^0 V_{t+1}(p'e^{\phi_t''}, i, \mathcal{I}_{t+1}(\alpha_{t+1}^{(p)+}, \beta_{t+1}^{(p)+})) f_t^{(p)}(\phi_t'' | \beta_t^{(p)+}) d\phi_t'', \end{aligned}$$

where both inequalities hold because the value function $V_{t+1}(\cdot)$ is non-decreasing in protein level p_{t+1} and also the posterior mean of protein $\alpha_{t+1}^{(p)}$, and the final step holds by performing variable replacement $\phi_t'' = \eta \cdot \phi_t'$. Thus, combining the two parts, we have,

$$\mathbb{E}[V_{t+1}(p_t e^{\phi_t}, i_t e^{\psi_t}, \mathcal{I}_{t+1}) | \beta_t^{(p)}] \leq \mathbb{E}[V_{t+1}(p_t e^{\phi_t}, i_t e^{\psi_t}, \mathcal{I}_{t+1}) | \beta_t^{(p)+}].$$

Then, $V_t(p_t, i_t, \mathcal{I}_t(\beta_t^{(p)})) \leq V_t(p_t, i_t, \mathcal{I}_t(\beta_t^{(p)+}))$. On the other hand,

$$\begin{aligned} & \mathbb{E}[V_{t+1}(p_t e^{\phi_t}, i_t e^{\psi_t}, \mathcal{I}_{t+1}(\alpha_{t+1}^{(i)}, \beta_{t+1}^{(i)})) | \beta_t^{(i)}] = -r_f \int_{\ln \bar{I} - \ln i_t}^{\infty} f_t^{(i)}(\psi_t | \beta_t^{(i)}) d\psi_t \\ & + \int_0^{\ln \bar{I} - \ln i_t} \int_0^{\ln \bar{P}} V_{t+1}(p_t e^{\phi_t}, i_t e^{\psi_t}, \mathcal{I}_{t+1}(\alpha_{t+1}^{(i)}, \beta_{t+1}^{(i)})) f_t^{(p)}(\phi_t) f_t^{(i)}(\psi_t | \beta_t^{(i)}) d\phi_t d\psi_t. \end{aligned}$$

Following similar procedure, we have for any (p, i) ,

$$\begin{aligned} & \int_0^{\ln \bar{I} - \ln i_t} V_{t+1}(p, i e^{\psi_t}, \mathcal{I}_{t+1}(\alpha_{t+1}^{(i)}, \beta_{t+1}^{(i)})) f_t^{(i)}(\psi_t | \beta_t^{(i)}) d\psi_t \\ & \geq \int_0^{\ln \bar{I} - \ln i_t} V_{t+1}(p, i e^{\psi_t'}, \mathcal{I}_{t+1}(\alpha_{t+1}^{(i)+}, \beta_{t+1}^{(i)+})) f_t^{(i)}(\psi_t' | \beta_t^{(i)+}) d\psi_t'. \end{aligned}$$

Further,

$$\int_{\ln \bar{I} - \ln i_t}^{\infty} f_t^{(i)}(\psi_t | \beta_t^{(i)}) d\psi_t = \int_{\ln \bar{I} - \ln i_t - \alpha_t^{(i)}}^{\infty} f_t^{(i)}(\psi_t' | \beta_t^{(i)}) d\psi_t'$$

$$\leq \int_{(\ln \bar{I} - \ln i_t - \alpha_t^{(i)})/\eta}^{\infty} f_t^{(i)}(\psi'_t | \beta_t^{(i)}) d\psi'_t = \int_{\ln \bar{I} - \ln i_t - \alpha_t^{(i)}}^{\infty} f_t^{(i)}(\psi''_t | \beta_t^{(i)+}) d\psi''_t,$$

where $\psi'_t = \psi_t - \alpha_t^{(i)}$, $\eta = \sqrt{\frac{\beta_t^{(i)+}}{\beta_t^{(i)}}} \geq 1$, and $\psi''_t = \eta\psi'_t$. Therefore,

$$\mathbb{E}[V_{t+1}(p_t e^{\phi_t}, i_t e^{\psi_t}, \mathcal{I}_{t+1}) | \beta_t^{(i)}] \geq \mathbb{E}[V_{t+1}(p_t e^{\phi_t}, i_t e^{\psi_t}, \mathcal{I}_{t+1}) | \beta_t^{(i)+}],$$

so that $V_t(p_t, i_t, \mathcal{I}_t(\beta_t^{(i)})) \geq V_t(p_t, i_t, \mathcal{I}_t(\beta_t^{(i)+}))$. \square

D.3 Proof of Part (iii)

Proof. Here we consider the non-increasing in $\nu_t^{(p)}$, as the proof of the non-decreasing in $\nu_t^{(i)}$ can follow the similar procedure. Given the other hyper-parameters $(\alpha_t^{(p)}, \beta_t^{(p)}, \lambda_t^{(p)}, \alpha_t^{(i)}, \nu_t^{(i)}, \lambda_t^{(i)}, \beta_t^{(i)})$ to be the same at t , suppose $\nu_t^{(p)+} \geq \nu_t^{(p)} > 0$.

Notice at the stopping time T ,

$$V_T(p_T, i_T, \mathcal{I}_T) = \begin{cases} r_h(p_T, i_T), & i_T \neq I_f \\ -r_f, & i_T = I_f \end{cases}$$

which is non-increasing in $\nu_T^{(p)}$. Based on the Bellman's equation for value function, we can prove it through Dynamic programming or backward induction. Assume that $V_{t+1}(p_{t+1}, i_{t+1}, \mathcal{I}_{t+1})$ is non-increasing in $\nu_{t+1}^{(p)}$. Then, at any time t ,

$$V_t(p_t, i_t, \mathcal{I}_t) = \begin{cases} \max\{r_h(p_t, i_t), -c_u + \gamma \mathbb{E}[V_{t+1}(p_t e^{\phi_t}, i_t e^{\psi_t}, \mathcal{I}_{t+1})]\}, & i_t \neq I_f \\ -r_f, & i_t = I_f. \end{cases} \quad (33)$$

The difference in $\nu_t^{(p)}$ will impact the expectation through the predictive distribution $f_t^{(p)}(\phi_t | \nu_t^{(p)})$; and also the knowledge hyper parameters $\alpha_{t+1}^{(p)}, \nu_{t+1}^{(p)}, \beta_{t+1}^{(p)}$ through the knowledge states update, see eq.(6). Then,

$$\begin{aligned} \mathbb{E}[V_{t+1}(p_t e^{\phi_t}, i_t e^{\psi_t}, \mathcal{I}_{t+1}(\alpha_{t+1}^{(p)}, \nu_{t+1}^{(p)}, \beta_{t+1}^{(p)})) | \nu_t^{(p)}] &= -r_f \int_{\ln \bar{I} - \ln i_t}^{\infty} f_t^{(i)}(\psi_t) d\psi_t \\ &+ \int_0^{\ln \bar{I} - \ln i_t} \int_0^{\ln \bar{P}} V_{t+1}(p_t e^{\phi_t}, i_t e^{\psi_t}, \mathcal{I}_{t+1}(\alpha_{t+1}^{(p)}, \nu_{t+1}^{(p)}, \beta_{t+1}^{(p)})) f_t^{(p)}(\phi_t | \nu_t^{(p)}) f_t^{(i)}(\psi_t) d\phi_t d\psi_t. \end{aligned}$$

Then for any (p, i) ,

$$\begin{aligned} &\int_0^{\ln \bar{P}} V_{t+1}(p e^{\phi_t}, i, \mathcal{I}_{t+1}(\alpha_{t+1}^{(p)}, \nu_{t+1}^{(p)}, \beta_{t+1}^{(p)})) f_t^{(p)}(\phi_t | \nu_t^{(p)}) d\phi_t \\ &= \int_{-\alpha_t^{(p)}}^{\ln \bar{P} - \alpha_t^{(p)}} V_{t+1}(p' e^{\phi'_t}, i, \mathcal{I}_{t+1}(\alpha_{t+1}^{(p)}, \nu_{t+1}^{(p)}, \beta_{t+1}^{(p)})) f_t^{(p)}(\phi'_t | \nu_t^{(p)}) d\phi'_t \\ &\geq \int_{-\alpha_t^{(p)}}^{\ln \bar{P} - \alpha_t^{(p)}} V_{t+1}(p' e^{\phi'_t}, i, \mathcal{I}_{t+1}(\alpha_{t+1}^{(p)}, \nu_{t+1}^{(p)+}, \beta_{t+1}^{(p)})) f_t^{(p)}(\phi'_t | \nu_t^{(p)}) d\phi'_t \\ &= \int_0^{\ln \bar{P} - \alpha_t^{(p)}} V_{t+1}(p' e^{\phi'_t}, i, \mathcal{I}_{t+1}(\alpha_{t+1}^{(p)}, \nu_{t+1}^{(p)}, \beta_{t+1}^{(p)})) f_t^{(p)}(\phi'_t | \nu_t^{(p)}) d\phi'_t \\ &+ \int_{-\alpha_t^{(p)}}^0 V_{t+1}(p' e^{\phi'_t}, i, \mathcal{I}_{t+1}(\alpha_{t+1}^{(p)}, \nu_{t+1}^{(p)}, \beta_{t+1}^{(p)})) f_t^{(p)}(\phi'_t | \nu_t^{(p)}) d\phi'_t, \end{aligned} \quad (34)$$

where the first equation holds by variable replacement $\phi'_t = \phi_t - \alpha_t^{(p)}$ and $p' = p e^{\alpha_t^{(p)}}$. In addition, $\nu_{t+1}^{(p)+} = \nu_t^{(p)+} + 1 \geq \nu_{t+1}^{(p)}$, the inequality (34) holds by applying the induction assumption. Let $\phi''_t = \eta \cdot \phi'_t$, with $\eta = \sqrt{\frac{\nu_t^{(p)}(\nu_t^{(p)+} + 1)}{\nu_t^{(p)+}(\nu_t^{(p)} + 1)}} \leq 1$, $\beta_{t+1}^{(p)+} = \beta_t^{(p)} + \frac{\nu_t^{(p)+} \eta^2 \phi_t'^2}{2(\nu_t^{(p)+} + 1)} = \beta_t^{(p)} + \frac{\nu_t^{(p)} \phi_t'^2}{2(\nu_t^{(p)} + 1)} = \beta_{t+1}^{(p)}$, and $\alpha_{t+1}^{(p)+} = \alpha_t^{(p)} + \frac{\eta \phi_t'}{(\nu_t^{(p)+} + 1)} = \alpha_t^{(p)} +$

$\sqrt{\frac{\nu_t^{(p)}}{\nu_t^{(p)+}(\nu_t^{(p)}+1)(\nu_t^{(p)+}+1)}}\phi_t' \triangleq \alpha_t^{(p)} + \kappa^-\phi_t'$. Notice that $\alpha_{t+1}^{(p)} = \alpha_t^{(p)} + \frac{\phi_t'}{(\nu_t^{(p)}+1)} \triangleq \alpha_t^{(p)} + \kappa\phi_t'$, it is easy to see that $\kappa > \kappa^- > 0$. Therefore,

$$\begin{aligned} & \int_0^{\ln \bar{P} - \alpha_t^{(p)}} V_{t+1}(p'e^{\phi_t'}, i, \mathcal{I}_{t+1}(\alpha_{t+1}^{(p)}, \nu_{t+1}^{(p)+}, \beta_{t+1}^{(p)})) f_t^{(p)}(\phi_t' | \nu_t^{(p)}) d\phi_t' \\ & \geq \int_0^{(\ln \bar{P} - \alpha_t^{(p)})/\eta} V_{t+1}(p'e^{\eta\phi_t'}, i, \mathcal{I}_{t+1}(\alpha_{t+1}^{(p)+}, \nu_{t+1}^{(p)+}, \beta_{t+1}^{(p)+})) f_t^{(p)}(\phi_t' | \nu_t^{(p)}) d\phi_t' \\ & \geq \int_0^{\ln \bar{P} - \alpha_t^{(p)}} V_{t+1}(p'e^{\phi_t''}, i, \mathcal{I}_{t+1}(\alpha_{t+1}^{(p)+}, \nu_{t+1}^{(p)+}, \beta_{t+1}^{(p)+})) f_t^{(p)}(\phi_t'' | \nu_t^{(p)+}) d\phi_t'', \end{aligned}$$

and

$$\begin{aligned} & \int_{-\alpha_t^{(p)}}^0 V_{t+1}(p'e^{\phi_t'}, i, \mathcal{I}_{t+1}(\alpha_{t+1}^{(p)}, \nu_{t+1}^{(p)+}, \beta_{t+1}^{(p)})) f_t^{(p)}(\phi_t' | \nu_t^{(p)}) d\phi_t' \\ & = - \int_0^{\alpha_t^{(p)}} V_{t+1}(p'e^{-\phi_t'}, i, \mathcal{I}_{t+1}(\alpha_t^{(p)} - \kappa\phi_t', \nu_{t+1}^{(p)+}, \beta_{t+1}^{(p)+})) f_t^{(p)}(\phi_t' | \nu_t^{(p)}) d\phi_t' \\ & \geq - \int_0^{\alpha_t^{(p)}} V_{t+1}(p'e^{-\eta\phi_t'}, i, \mathcal{I}_{t+1}(\alpha_t^{(p)} - \kappa^-\phi_t', \nu_{t+1}^{(p)+}, \beta_{t+1}^{(p)+})) f_t^{(p)}(\phi_t' | \nu_t^{(p)}) d\phi_t' \\ & \geq \int_{-\alpha_t^{(p)}}^0 V_{t+1}(p'e^{\phi_t''}, i, \mathcal{I}_{t+1}(\alpha_{t+1}^{(p)+}, \nu_{t+1}^{(p)+}, \beta_{t+1}^{(p)+})) f_t^{(p)}(\phi_t'' | \nu_t^{(p)+}) d\phi_t'', \end{aligned}$$

where both inequalities hold because the value function $V_{t+1}(\cdot)$ is non-decreasing in protein level p_{t+1} and also the posterior mean of protein $\alpha_{t+1}^{(p)}$, and the final step holds by performing variable replacement $\phi_t'' = \eta \cdot \phi_t'$. Thus, combining the two parts, we have,

$$\mathbb{E}[V_{t+1}(p_t e^{\phi_t}, i_t e^{\psi_t}, \mathcal{I}_{t+1}) | \nu_t^{(p)}] \geq \mathbb{E}[V_{t+1}(p_t e^{\phi_t}, i_t e^{\psi_t}, \mathcal{I}_{t+1}) | \nu_t^{(p)+}].$$

Then, $V_t(p_t, i_t, \mathcal{I}_t(\nu_t^{(p)})) \geq V_t(p_t, i_t, \mathcal{I}_t(\nu_t^{(p)+}))$. On the other hand,

$$\begin{aligned} & \mathbb{E}[V_{t+1}(p_t e^{\phi_t}, i_t e^{\psi_t}, \mathcal{I}_{t+1}(\alpha_{t+1}^{(i)}, \nu_{t+1}^{(i)}, \beta_{t+1}^{(i)})) | \nu_t^{(i)}] = -r_f \int_{\ln \bar{I} - \ln i_t}^{\infty} f_t^{(i)}(\psi_t | \nu_t^{(i)}) d\psi_t \\ & + \int_0^{\ln \bar{I} - \ln i_t} \int_0^{\ln \bar{P}} V_{t+1}(p_t e^{\phi_t}, i_t e^{\psi_t}, \mathcal{I}_{t+1}(\alpha_{t+1}^{(i)}, \nu_{t+1}^{(i)}, \beta_{t+1}^{(i)})) f_t^{(p)}(\phi_t) f_t^{(i)}(\psi_t | \nu_t^{(i)}) d\phi_t d\psi_t. \end{aligned}$$

Following the similar procedure, we have for any (p, i) ,

$$\begin{aligned} & \int_0^{\ln \bar{I} - \ln i_t} V_{t+1}(p, i e^{\psi_t}, \mathcal{I}_{t+1}(\alpha_{t+1}^{(i)}, \nu_{t+1}^{(i)}, \beta_{t+1}^{(i)})) f_t^{(i)}(\psi_t | \nu_t^{(i)}) d\psi_t \\ & \leq \int_0^{\ln \bar{I} - \ln i_t} V_{t+1}(p, i e^{\psi_t'}, \mathcal{I}_{t+1}(\alpha_{t+1}^{(i)+}, \nu_{t+1}^{(i)+}, \beta_{t+1}^{(i)+})) f_t^{(i)}(\psi_t' | \nu_t^{(i)+}) d\psi_t'. \end{aligned}$$

Further,

$$\begin{aligned} & \int_{\ln \bar{I} - \ln i_t}^{\infty} f_t^{(i)}(\psi_t | \nu_t^{(i)}) d\psi_t = \int_{\ln \bar{I} - \ln i_t - \alpha_t^{(i)}}^{\infty} f_t^{(i)}(\psi_t' | \nu_t^{(i)}) d\psi_t' \\ & \geq \int_{(\ln \bar{I} - \ln i_t - \alpha_t^{(i)})/\eta}^{\infty} f_t^{(i)}(\psi_t' | \nu_t^{(i)}) d\psi_t' = \int_{\ln \bar{I} - \ln i_t - \alpha_t^{(i)}}^{\infty} f_t^{(i)}(\psi_t'' | \nu_t^{(i)+}) d\psi_t'', \end{aligned}$$

where $\psi_t' = \psi_t - \alpha_t^{(i)}$, $\eta = \sqrt{\frac{\nu_t^{(i)}(\nu_t^{(i)+}+1)}{\nu_t^{(i)+}(\nu_t^{(i)}+1)}} \leq 1$, and $\psi_t'' = \eta\psi_t'$. Therefore,

$$\mathbb{E}[V_{t+1}(p_t e^{\phi_t}, i_t e^{\psi_t}, \mathcal{I}_{t+1}) | \nu_t^{(i)}] \leq \mathbb{E}[V_{t+1}(p_t e^{\phi_t}, i_t e^{\psi_t}, \mathcal{I}_{t+1}) | \nu_t^{(i)+}],$$

and $V_t(p_t, i_t, \mathcal{I}_t(\nu_t^{(i)})) \leq V_t(p_t, i_t, \mathcal{I}_t(\nu_t^{(i)+}))$. □

D.4 Proof of Part (iv)

Proof. Here we prove the non-increasing in $\lambda_t^{(p)}$, as the proof of the non-decreasing in $\lambda_t^{(i)}$ can follow the similar procedure. Given the other hyper-parameters $(\alpha_t^{(p)}, \beta_t^{(p)}, \nu_t^{(p)}, \alpha_t^{(i)}, \nu_t^{(i)}, \lambda_t^{(i)}, \beta_t^{(i)})$ to be the same at t , suppose $\lambda_t^{(p)+} \geq \lambda_t^{(p)} > 0$. Notice at the stopping time T ,

$$V_T(p_T, i_T, \mathcal{I}_T) = \begin{cases} r_h(p_T, i_T), & i_T \neq I_f \\ -r_f, & i_T = I_f \end{cases}$$

which is non-decreasing in $\lambda_t^{(p)2}$. Based on the Bellman's equation for value function, we can prove it through Dynamic programming or backward induction. Assume that $V_{t+1}(p_{t+1}, i_{t+1}, \mathcal{I}_{t+1})$ is non-decreasing in $\lambda_{t+1}^{(p)2}$. Then, at any time t ,

$$V_t(p_t, i_t, \mathcal{I}_t) = \begin{cases} \max\{r_h(p_t, i_t), -c_u + \gamma E[V_{t+1}(p_t e^{\phi_t}, i_t e^{\psi_t}, \mathcal{I}_{t+1})]\}, & i_t \neq I_f \\ -r_f, & i_t = I_f \end{cases}. \quad (35)$$

The difference in $\lambda_t^{(p)}$ will impact the expectation through the predictive distribution $g_t^{(p)}(\phi_t | \lambda_t^{(p)2})$; and also the knowledge hyper parameters $\alpha_{t+1}^{(p)}, \lambda_{t+1}^{(p)}, \beta_{t+1}^{(p)}$ through the knowledge states update. Notice the approximate Gaussian predictive density,

$$g_t^{(p)}(\phi_t | \alpha_t^{(p)}, \tilde{\sigma}_t^{(p)2}) = \frac{1}{\tilde{\sigma}_t^{(p)} \sqrt{2\pi}} \exp\left\{-\frac{(\phi_t - \alpha_t^{(p)})^2}{2\tilde{\sigma}_{t+1}^{(p)2}}\right\}.$$

Then, based on the predictive distribution,

$$\begin{aligned} E[V_{t+1}(p_t e^{\phi_t}, i_t e^{\psi_t}, \mathcal{I}_{t+1}(\alpha_{t+1}^{(p)}, \lambda_{t+1}^{(p)}, \beta_{t+1}^{(p)})) | \lambda_t^{(p)}] &= -r_f \int_{\ln \bar{I} - \ln i_t}^{\infty} g_t^{(i)}(\psi_t) d\psi_t \\ &+ \int_0^{\ln \bar{I} - \ln i_t} \int_0^{\ln \bar{P}} V_{t+1}(p_t e^{\phi_t}, i_t e^{\psi_t}, \mathcal{I}_{t+1}(\alpha_{t+1}^{(p)}, \lambda_{t+1}^{(p)}, \beta_{t+1}^{(p)})) g_t^{(p)}(\phi_t | \lambda_t^{(p)}) g_t^{(i)}(\psi_t) d\phi_t d\psi_t. \end{aligned}$$

Then for any (p, i) ,

$$\begin{aligned} &\int_0^{\ln \bar{P}} V_{t+1}(p e^{\phi_t}, i, \mathcal{I}_{t+1}(\alpha_{t+1}^{(p)}, \lambda_{t+1}^{(p)}, \beta_{t+1}^{(p)})) g_t^{(p)}(\phi_t | \lambda_t^{(p)}) d\phi_t \\ &= \int_{-\alpha_t^{(p)}}^{\ln \bar{P} - \alpha_t^{(p)}} V_{t+1}(p' e^{\phi_t'}, i, \mathcal{I}_{t+1}(\alpha_{t+1}^{(p)}, \lambda_{t+1}^{(p)}, \beta_{t+1}^{(p)})) g_t^{(p)}(\phi_t' | \lambda_t^{(p)}) d\phi_t' \\ &\geq \int_{-\alpha_t^{(p)}}^{\ln \bar{P} - \alpha_t^{(p)}} V_{t+1}(p' e^{\phi_t'}, i, \mathcal{I}_{t+1}(\alpha_{t+1}^{(p)}, \lambda_{t+1}^{(p)+}, \beta_{t+1}^{(p)})) g_t^{(p)}(\phi_t' | \lambda_t^{(p)}) d\phi_t' \\ &= \int_0^{\ln \bar{P} - \alpha_t^{(p)}} V_{t+1}(p' e^{\phi_t'}, i, \mathcal{I}_{t+1}(\alpha_{t+1}^{(p)}, \lambda_{t+1}^{(p)}, \beta_{t+1}^{(p)})) g_t^{(p)}(\phi_t' | \lambda_t^{(p)}) d\phi_t' \\ &+ \int_{-\alpha_t^{(p)}}^0 V_{t+1}(p' e^{\phi_t'}, i, \mathcal{I}_{t+1}(\alpha_{t+1}^{(p)}, \lambda_{t+1}^{(p)}, \beta_{t+1}^{(p)})) g_t^{(p)}(\phi_t' | \lambda_t^{(p)}) d\phi_t', \end{aligned} \quad (36)$$

where the first equation holds by variable replacement $\phi_t' = \phi_t - \alpha_t^{(p)}$ and $p' = p e^{\alpha_t^{(p)}}$. In addition, $\lambda_{t+1}^{(p)+} = \lambda_t^{(p)+} + 1/2 \geq \lambda_{t+1}^{(p)}$, the inequality (36) holds by induction assumption. Let $\phi_t'' = \eta \cdot \phi_t'$ with $\eta = \sqrt{\frac{\lambda_t^{(p)} - 1}{\lambda_t^{(p)+} - 1}} \leq 1$,

$\beta_{t+1}^{(p)+} = \beta_t^{(p)} + \frac{\nu_t^{(p)} \eta^2 \phi_t'^2}{2\nu_{t+1}^{(p)}} \leq \beta_t^{(p)} + \frac{\nu_t^{(p)} \phi_t'^2}{2\nu_{t+1}^{(p)}} = \beta_{t+1}^{(p)}$, and $\alpha_{t+1}^{(p)+} = \alpha_t^{(p)} + \frac{\eta \phi_t'}{\nu_{t+1}^{(p)}} \triangleq \alpha_t^{(p)} + \kappa^- \phi_t'$. Notice that $\alpha_{t+1}^{(p)} = \alpha_t^{(p)} \frac{\phi_t'}{\nu_{t+1}^{(p)}} \triangleq \alpha_t^{(p)} + \kappa^- \phi_t'$, it is easy to see that $\kappa > \kappa^- > 0$. Therefore,

$$\int_0^{\ln \bar{P} - \alpha_t^{(p)}} V_{t+1}(p' e^{\phi_t'}, i, \mathcal{I}_{t+1}(\alpha_{t+1}^{(p)}, \lambda_{t+1}^{(p)+}, \beta_{t+1}^{(p)})) g_t^{(p)}(\phi_t' | \lambda_t^{(p)}) d\phi_t'$$

$$\begin{aligned}
&\geq \int_0^{(\ln \bar{P} - \alpha_t^{(p)})/\eta} V_{t+1}(p' e^{\eta \phi'_t}, i, \mathcal{I}_{t+1}(\alpha_{t+1}^{(p)+}, \lambda_{t+1}^{(p)+}, \beta_{t+1}^{(p)+})) g_t^{(p)}(\phi'_t | \lambda_t^{(p)}) d\phi'_t \\
&\geq \int_0^{\ln \bar{P} - \alpha_t^{(p)}} V_{t+1}(p' e^{\phi'_t}, i, \mathcal{I}_{t+1}(\alpha_{t+1}^{(p)+}, \lambda_{t+1}^{(p)+}, \beta_{t+1}^{(p)+})) g_t^{(p)}(\phi'_t | \lambda_t^{(p)+}) d\phi'_t,
\end{aligned}$$

and

$$\begin{aligned}
&\int_{-\alpha_t^{(p)}}^0 V_{t+1}(p' e^{\phi'_t}, i, \mathcal{I}_{t+1}(\alpha_{t+1}^{(p)}, \lambda_{t+1}^{(p)+}, \beta_{t+1}^{(p)})) g_t^{(p)}(\phi'_t | \lambda_t^{(p)}) d\phi'_t \\
&= - \int_0^{\alpha_t^{(p)}} V_{t+1}(p' e^{-\phi'_t}, i, \mathcal{I}_{t+1}(\alpha_t^{(p)} - \kappa \phi'_t, \lambda_{t+1}^{(p)+}, \beta_{t+1}^{(p)+})) g_t^{(p)}(\phi'_t | \lambda_t^{(p)}) d\phi'_t \\
&\geq - \int_0^{\alpha_t^{(p)}} V_{t+1}(p' e^{-\eta \phi'_t}, i, \mathcal{I}_{t+1}(\alpha_t^{(p)} - \kappa^- \phi'_t, \lambda_{t+1}^{(p)+}, \beta_{t+1}^{(p)+})) g_t^{(p)}(\phi'_t | \lambda_t^{(p)}) d\phi'_t \\
&\geq \int_{-\alpha_t^{(p)}}^0 V_{t+1}(p' e^{\phi'_t}, i, \mathcal{I}_{t+1}(\alpha_{t+1}^{(p)+}, \lambda_{t+1}^{(p)+}, \beta_{t+1}^{(p)+})) g_t^{(p)}(\phi'_t | \lambda_t^{(p)+}) d\phi'_t,
\end{aligned}$$

where both inequalities hold because the value function $V_{t+1}(\cdot)$ is non-decreasing in protein level p_{t+1} as well as the posterior mean of protein $\alpha_{t+1}^{(p)}$ and also scale parameter $\beta_{t+1}^{(p)}$, and the final step holds by performing variable replacement $\phi'_t = \eta \cdot \phi'_t$. Thus, combining the two parts, we have,

$$\mathbb{E}[V_{t+1}(p_t e^{\phi_t}, i_t e^{\psi_t}, \mathcal{I}_{t+1}) | \lambda_t^{(p)}] \geq \mathbb{E}[V_{t+1}(p_t e^{\phi_t}, i_t e^{\psi_t}, \mathcal{I}_{t+1}) | \lambda_t^{(p)+}].$$

Then, $V_t(p_t, i_t, \mathcal{I}_t(\lambda_t^{(p)})) \geq V_t(p_t, i_t, \mathcal{I}_t(\lambda_t^{(p)+}))$. On the other hand,

$$\begin{aligned}
&\mathbb{E}[V_{t+1}(p_t e^{\phi_t}, i_t e^{\psi_t}, \mathcal{I}_{t+1}(\alpha_{t+1}^{(i)}, \lambda_{t+1}^{(i)}, \beta_{t+1}^{(i)})) | \lambda_t^{(i)}] = -r_f \int_{\ln \bar{I} - \ln i_t}^{\infty} g_t^{(i)}(\psi_t | \lambda_t^{(i)}) d\psi_t \\
&+ \int_0^{\ln \bar{I} - \ln i_t} \int_0^{\ln \bar{P}} V_{t+1}(p_t e^{\phi_t}, i_t e^{\psi_t}, \mathcal{I}_{t+1}(\alpha_{t+1}^{(i)}, \lambda_{t+1}^{(i)}, \beta_{t+1}^{(i)})) g_t^{(p)}(\phi_t) g_t^{(i)}(\psi_t | \lambda_t^{(i)}) d\phi_t d\psi_t.
\end{aligned}$$

Following the similar procedure, we have for any (p, i) ,

$$\begin{aligned}
&\int_0^{\ln \bar{I} - \ln i_t} V_{t+1}(p, i e^{\psi_t}, \mathcal{I}_{t+1}(\alpha_{t+1}^{(i)}, \lambda_{t+1}^{(i)}, \beta_{t+1}^{(i)})) g_t^{(i)}(\psi_t | \lambda_t^{(i)}) d\psi_t \\
&\leq \int_0^{\ln \bar{I} - \ln i_t} V_{t+1}(p, i e^{\psi'_t}, \mathcal{I}_{t+1}(\alpha_{t+1}^{(i)+}, \lambda_{t+1}^{(i)+}, \beta_{t+1}^{(i)+})) g_t^{(i)}(\psi'_t | \lambda_t^{(i)+}) d\psi'_t.
\end{aligned}$$

Further,

$$\begin{aligned}
&\int_{\ln \bar{I} - \ln i_t}^{\infty} g_t^{(i)}(\psi_t | \lambda_t^{(i)}) d\psi_t = \int_{\ln \bar{I} - \ln i_t - \alpha_t^{(i)}}^{\infty} g_t^{(i)}(\psi'_t | \lambda_t^{(i)}) d\psi'_t \\
&\geq \int_{(\ln \bar{I} - \ln i_t - \alpha_t^{(i)})/\eta}^{\infty} g_t^{(i)}(\psi'_t | \lambda_t^{(i)}) d\psi'_t = \int_{\ln \bar{I} - \ln i_t - \alpha_t^{(i)}}^{\infty} g_t^{(i)}(\psi''_t | \lambda_t^{(i)+}) d\psi''_t,
\end{aligned}$$

where $\psi'_t = \psi_t - \alpha_t^{(i)}$, $\eta = \sqrt{\frac{\lambda_t^{(p)} - 1}{\lambda_t^{(p)+} - 1}} \leq 1$, and $\psi''_t = \eta \psi'_t$. Therefore,

$$\mathbb{E}[V_{t+1}(p_t e^{\phi_t}, i_t e^{\psi_t}, \mathcal{I}_{t+1}) | \lambda_t^{(i)}] \leq \mathbb{E}[V_{t+1}(p_t e^{\phi_t}, i_t e^{\psi_t}, \mathcal{I}_{t+1}) | \lambda_t^{(i)+}].$$

and that $V_t(p_t, i_t, \mathcal{I}_t(\lambda_t^{(i)})) \leq V_t(p_t, i_t, \mathcal{I}_t(\lambda_t^{(i)+}))$. □

E Proof of Theorem 4

Theorem 4: Given the perfect information on the underlying process model F^c , the optimal harvest policy obtained by MDP is: at any time period t during the exponential growth phase, the optimal harvest region is determined by

$\left\{ (p_t, i_t) : \min_{m=1,2,\dots,\bar{T}-t} h(p_t, i_t; m) \geq 0; p_0 \leq p_t \leq \bar{P}; i_0 \leq i_t \leq \bar{I} \right\}$, and

$$\begin{aligned}
h(p_t, i_t; m) &\equiv \frac{1-\gamma^m}{1-\gamma} c_u + c_0 \left[1 - \gamma^m \Phi \left(\frac{\ln \bar{I} - \ln i_t - m\mu_c^{(i)}}{\sqrt{m}\sigma_c^{(i)}} \right) \right] + \gamma^m r_f \left[1 - \Phi \left(\frac{\ln \bar{I} - \ln i_t - m\mu_c^{(i)}}{\sqrt{m}\sigma_c^{(i)}} \right) \right] \\
&+ c_2 i_t \left[\gamma^m e^{m\mu_c^{(i)} + m\sigma_c^{(i)2}/2} \Phi \left(\frac{\ln \bar{I} - \ln i_t - m\mu_c^{(i)} - m\sigma_c^{(i)2}}{\sqrt{m}\sigma_c^{(i)}} \right) - 1 \right] \\
&- c_1 \left\{ \gamma^m \bar{P} \Phi \left(\frac{\ln \bar{I} - \ln i_t - m\mu_c^{(i)}}{\sqrt{m}\sigma_c^{(i)}} \right) \left[1 - \Phi \left(\frac{\ln \bar{P} - \ln p_t - m\mu_c^{(p)}}{\sqrt{m}\sigma_c^{(p)}} \right) \right] \right. \\
&\left. + \gamma^m p_t e^{m\mu_c^{(p)} + m\sigma_c^{(p)2}/2} \Phi \left(\frac{\ln \bar{I} - \ln i_t - m\mu_c^{(i)}}{\sqrt{m}\sigma_c^{(i)}} \right) \Phi \left(\frac{\ln \bar{P} - \ln p_t - m\mu_c^{(p)} - m\sigma_c^{(p)2}}{\sqrt{m}\sigma_c^{(p)}} \right) - p_t \right\}, \quad (37)
\end{aligned}$$

where (p_0, i_0) are the starting conditions of the batch, $\Phi(\cdot)$ is the cumulative distribution function (CDF) of standard normal, and m is the number of possible future fermentation periods till harvest of this batch.

Proof. Suppose at certain time t during the growth phase, the physical states are $(p_t, i_t) \in [p_0, \bar{P}] \times [i_0, \bar{I}]$ (we ignore the batch failure since the decision will be harvest if failure happens). If we harvest at current time, despite the cost spent on this batch till time t , the additional total reward of this batch is,

$$r_0 = c_0 + c_1 p_t - c_2 i_t.$$

On the other hand, we could also choose to continue the fermentation for m ($1 \leq m \leq \bar{T} - t$) periods and then harvest, then the expected additional total reward of this batch could be computed by,

$$\begin{aligned}
r_m &= -\frac{1-\gamma^m}{1-\gamma} c_u + \gamma^m \Pr(i_{t+m} \leq \bar{I}) \Pr(p_{t+m} \leq \bar{P}) \mathbb{E} [c_0 + c_1 p_{t+m} - c_2 i_{t+m} | p_{t+m} \leq \bar{P}, i_{t+m} \leq \bar{I}] \\
&+ \gamma^m \Pr(i_{t+m} \leq \bar{I}) \Pr(p_{t+m} > \bar{P}) \mathbb{E} [c_0 + c_1 \bar{P} - c_2 i_{t+m} | p_{t+m} > \bar{P}, i_{t+m} \leq \bar{I}] \\
&- r_f \gamma^m \Pr(i_{t+m} > \bar{I}), \quad (38)
\end{aligned}$$

where $p_{t+m} = p_t e^{\sum_{k=1}^m \Phi_k}$ and $i_{t+m} = i_t e^{\sum_{k=1}^m \Psi_k}$, with $\Phi_k \sim \mathcal{N}(\mu_c^{(p)}, \sigma_c^{(p)2})$ and $\Psi_k \sim \mathcal{N}(\mu_c^{(i)}, \sigma_c^{(i)2})$. Therefore,

$$\Pr(i_{t+m} \leq \bar{I}) = \Pr \left(\sum_{k=1}^m \Psi_k \leq \ln \bar{I} - \ln i_t \right) = \Phi \left(\frac{\ln \bar{I} - \ln i_t - m\mu_c^{(i)}}{\sqrt{m}\sigma_c^{(i)}} \right),$$

similar results apply for $\Pr(p_{t+m} \leq \bar{P})$. Further, since $e^{\sum_{k=1}^m \Phi_k}$ and $e^{\sum_{k=1}^m \Psi_k}$ follow mutually independent log-normal distributions, we can compute the conditional expectations [39],

$$\begin{aligned}
&\mathbb{E} [c_0 + c_1 p_{t+m} - c_2 i_{t+m} | p_{t+m} \leq \bar{P}, i_{t+m} \leq \bar{I}] \\
&= c_0 + c_1 p_t \mathbb{E} \left[e^{\sum_{k=1}^m \Phi_k} \mid e^{\sum_{k=1}^m \Phi_k} \leq \bar{P}/p_t \right] - c_2 i_t \mathbb{E} \left[e^{\sum_{k=1}^m \Psi_k} \mid e^{\sum_{k=1}^m \Psi_k} \leq \bar{I}/i_t \right] \\
&= c_0 + c_1 p_t e^{m\mu_c^{(p)} + m\sigma_c^{(p)2}/2} \frac{\Phi \left(\frac{\ln \bar{P} - \ln p_t - m\mu_c^{(p)} - m\sigma_c^{(p)2}}{\sqrt{m}\sigma_c^{(p)}} \right)}{\Phi \left(\frac{\ln \bar{P} - \ln p_t - m\mu_c^{(p)}}{\sqrt{m}\sigma_c^{(p)}} \right)} \\
&\quad - c_2 i_t e^{m\mu_c^{(i)} + m\sigma_c^{(i)2}/2} \frac{\Phi \left(\frac{\ln \bar{I} - \ln i_t - m\mu_c^{(i)} - m\sigma_c^{(i)2}}{\sqrt{m}\sigma_c^{(i)}} \right)}{\Phi \left(\frac{\ln \bar{I} - \ln i_t - m\mu_c^{(i)}}{\sqrt{m}\sigma_c^{(i)}} \right)}.
\end{aligned}$$

Also,

$$\mathbb{E} [c_0 + c_1 \bar{P} - c_2 i_{t+m} | p_{t+m} > \bar{P}, i_{t+m} \leq \bar{I}]$$

$$\begin{aligned}
&= c_0 + c_1 \bar{P} - c_2 i_t \mathbb{E} \left[e^{\sum_{k=1}^m \Psi_k} \mid e^{\sum_{k=1}^m \Psi_k} \leq \bar{I}/i_t \right] \\
&= c_0 + c_1 \bar{P} - c_2 i_t e^{m\mu_c^{(i)} + m\sigma_c^{(i)2}/2} \frac{\Phi \left(\frac{\ln \bar{I} - \ln i_t - m\mu_c^{(i)} - m\sigma_c^{(i)2}}{\sqrt{m}\sigma_c^{(i)}} \right)}{\Phi \left(\frac{\ln \bar{I} - \ln i_t - m\mu_c^{(i)}}{\sqrt{m}\sigma_c^{(i)}} \right)}.
\end{aligned}$$

Plugging in those results, we have

$$\begin{aligned}
r_m &= -\frac{1-\gamma^m}{1-\gamma} c_u + \gamma^m c_0 \Phi \left(\frac{\ln \bar{I} - \ln i_t - m\mu_c^{(i)}}{\sqrt{m}\sigma_c^{(i)}} \right) - \gamma^m r_f \left[1 - \Phi \left(\frac{\ln \bar{I} - \ln i_t - m\mu_c^{(i)}}{\sqrt{m}\sigma_c^{(i)}} \right) \right] \\
&\quad + \gamma^m c_1 \bar{P} \Phi \left(\frac{\ln \bar{I} - \ln i_t - m\mu_c^{(i)}}{\sqrt{m}\sigma_c^{(i)}} \right) \left[1 - \Phi \left(\frac{\ln \bar{P} - \ln p_t - m\mu_c^{(p)}}{\sqrt{m}\sigma_c^{(p)}} \right) \right] \\
&\quad + \gamma^m c_1 p_t e^{m\mu_c^{(p)} + m\sigma_c^{(p)2}/2} \Phi \left(\frac{\ln \bar{I} - \ln i_t - m\mu_c^{(i)}}{\sqrt{m}\sigma_c^{(i)}} \right) \Phi \left(\frac{\ln \bar{P} - \ln p_t - m\mu_c^{(p)} - m\sigma_c^{(p)2}}{\sqrt{m}\sigma_c^{(p)}} \right) \\
&\quad - \gamma^m c_2 i_t e^{m\mu_c^{(i)} + m\sigma_c^{(i)2}/2} \Phi \left(\frac{\ln \bar{I} - \ln i_t - m\mu_c^{(i)} - m\sigma_c^{(i)2}}{\sqrt{m}\sigma_c^{(i)}} \right).
\end{aligned}$$

Therefore, given the current physical state (p_t, i_t) , the optimal decision is to harvest if and only if $r_0 \geq r_m$ for $m = 1, 2, \dots, \bar{T} - t$, otherwise the optimal decision is to continue the fermentation for this batch. Let $h(p_t, i_t; m) = r_0 - r_m$, then the optimal policy is to harvest in the region defined by $\left\{ (p_t, i_t) : \min_{m=1,2,\dots,\bar{T}-t} h(p_t, i_t; m) \geq 0; p_0 \leq p_t \leq \bar{P}; i_0 \leq i_t \leq \bar{I} \right\}$. \square

F Proof of Theorem 5

Theorem 5: Suppose the current knowledge state is $\mathcal{I}_t = (\alpha_t^{(p)}, \nu_t^{(p)}, \lambda_t^{(p)}, \beta_t^{(p)}, \alpha_t^{(i)}, \nu_t^{(i)}, \lambda_t^{(i)}, \beta_t^{(i)})$. The model based reinforcement learning has optimal policy: at any time period t , the optimal harvest region is determined by

$\left\{ (p_t, i_t) : \min_{m=1,2,\dots,\bar{T}-t} \tilde{h}(p_t, i_t; m) \geq 0; p_0 \leq p_t \leq \bar{P}; i_0 \leq i_t \leq \bar{I} \right\}$, and

$$\begin{aligned}
\tilde{h}(p_t, i_t; m) &\equiv \frac{1-\gamma^m}{1-\gamma} c_u + c_0 \left[1 - \gamma^m \Phi \left(\frac{\ln \bar{I} - \ln i_t - m\alpha_t^{(i)}}{\sqrt{m}\tilde{\sigma}_t^{(i)}} \right) \right] + \gamma^m r_f \left[1 - \Phi \left(\frac{\ln \bar{I} - \ln i_t - m\alpha_t^{(i)}}{\sqrt{m}\tilde{\sigma}_t^{(i)}} \right) \right] \\
&\quad + c_2 i_t \left[\gamma^m e^{m\alpha_t^{(i)} + m\tilde{\sigma}_t^{(i)2}/2} \Phi \left(\frac{\ln \bar{I} - \ln i_t - m\alpha_t^{(i)} - m\tilde{\sigma}_t^{(i)2}}{\sqrt{m}\tilde{\sigma}_t^{(i)}} \right) - 1 \right] \\
&\quad - c_1 \left\{ \gamma^m \bar{P} \Phi \left(\frac{\ln \bar{I} - \ln i_t - m\alpha_t^{(i)}}{\sqrt{m}\tilde{\sigma}_t^{(i)}} \right) \left[1 - \Phi \left(\frac{\ln \bar{P} - \ln p_t - m\alpha_t^{(p)}}{\sqrt{m}\tilde{\sigma}_t^{(p)}} \right) \right] \right. \\
&\quad \left. + \gamma^m p_t e^{m\alpha_t^{(p)} + m\tilde{\sigma}_t^{(p)2}/2} \Phi \left(\frac{\ln \bar{I} - \ln i_t - m\alpha_t^{(i)}}{\sqrt{m}\tilde{\sigma}_t^{(i)}} \right) \Phi \left(\frac{\ln \bar{P} - \ln p_t - m\alpha_t^{(p)} - m\tilde{\sigma}_t^{(p)2}}{\sqrt{m}\tilde{\sigma}_t^{(p)}} \right) - p_t \right\}. \quad (39)
\end{aligned}$$

Proof. When the underlying true parameters θ^c is unknown, at current time t , our beliefs of the protein and impurity growth kinetics are given by knowledge states $\mathcal{I}_t = (\alpha_t^{(p)}, \nu_t^{(p)}, \lambda_t^{(p)}, \beta_t^{(p)}, \alpha_t^{(i)}, \nu_t^{(i)}, \lambda_t^{(i)}, \beta_t^{(i)})$. Moreover, the specific growth rates during each period are modeled by posterior predictive distributions $\tilde{\Phi} \sim \mathcal{N} \left(\alpha_t^{(p)}, \tilde{\sigma}_t^{(p)2} \right)$, $\tilde{\Psi} \sim \mathcal{N} \left(\alpha_t^{(i)}, \tilde{\sigma}_t^{(i)2} \right)$. Notice the analysis procedure in proof of Theorem 4 can still be applied under model risk, by replacing the underlying true growth rates distribution with the predictive distribution. Then, the results in Theorem 5 just follow. \square

G Proof of Proposition 6

Theorem 6: As the amount of bioprocess historical data $J_t \rightarrow \infty$, we have $\alpha_t^{(p)} \xrightarrow{p} \mu_c^{(p)}$, $\alpha_t^{(i)} \xrightarrow{p} \mu_c^{(i)}$, and $\tilde{\sigma}_t^{(p)2} \xrightarrow{p} \sigma_c^{(p)2}$, $\tilde{\sigma}_t^{(i)2} \xrightarrow{p} \sigma_c^{(i)2}$, i.e., the asymptotic convergence to underlying true model coefficients in probability, so that for any $(p_t, i_t) \in [p_0, \bar{P}] \times [i_0, \bar{I}]$ and $m = 1, 2, \dots, \bar{T} - t$, $\tilde{h}(p_t, i_t; m) \xrightarrow{p} h(p_t, i_t; m)$. Thus, as the amount of process historical data goes to infinity, the harvest decision boundary under model risk will converge to the optimal boundary with the perfect information on the underlying process model F^c .

Proof. Since ϕ_j are i.i.d. samples from underlying true protein growth rate distribution $\mathcal{N}(\mu_c^{(p)}, \sigma_c^{(p)2})$. According to the properties of Gaussian sample mean and sample variance, we have $\bar{\phi} \sim \mathcal{N}(\mu_c^{(p)}, \frac{\sigma_c^{(p)2}}{J_t})$, $\frac{\sum_{j=1}^{J_t} (\phi_j - \bar{\phi})^2}{\sigma_c^{(p)2}} \sim \chi^2(J_t - 1)$, and they are independent of each other. According to weak law of large numbers (WLLN), we have sample mean converge to the true mean, i.e. $\alpha_t^{(p)} \xrightarrow{p} \mu_c^{(p)}$ as $J_t \rightarrow \infty$. In addition,

$$\mathbb{E} \left[\tilde{\sigma}_t^{(p)2} \right] = \frac{(J_t^2 - 1)\sigma_c^{(p)2}}{(J_t^2 - 2J_t)} = \sigma_c^{(p)2} + \frac{(2J_t - 1)\sigma_c^{(p)2}}{(J_t^2 - 2J_t)}, \quad \text{Var} \left[\tilde{\sigma}_t^{(p)2} \right] = \frac{2(J_t^3 + J_t^2 - J_t - 1)\sigma_c^{(p)4}}{J_t^4 - 4J_t^3 + 4J_t^2}. \quad (40)$$

As $J_t \rightarrow \infty$, we will have $\mathbb{E} \left[\tilde{\sigma}_t^{(p)2} \right] \rightarrow \sigma_c^{(p)2}$ and $\text{Var} \left[\tilde{\sigma}_t^{(p)2} \right] \rightarrow 0$, so that $\tilde{\sigma}_t^{(p)2} \xrightarrow{p} \sigma_c^{(p)2}$. Similar results also apply for impurity growth rate. That means we also have $\alpha_t^{(i)} \xrightarrow{p} \mu_c^{(i)}$ and $\tilde{\sigma}_t^{(i)2} \xrightarrow{p} \sigma_c^{(i)2}$. Thus, through the continuous mapping theorem, we have for any $(p_t, i_t) \in [p_0, \bar{P}] \times [i_0, \bar{I}]$ and $m = 1, 2, \dots, T - t$, $\tilde{h}(p_t, i_t; m) \xrightarrow{p} h(p_t, i_t; m)$ as $J_t \rightarrow \infty$. In other words, the harvest decision boundary under model risk will converge to the boundary with the perfect information on F^c . \square

References

- [1] McKinsey & Company. From science to operations: Questions, choices, and strategies for success in biopharma, 2014. <https://www.mckinsey.com/industries/pharmaceuticals-and-medical-products/our-insights/from-science-to-operations-questions-choices-and-strategies-for-success-in-biopharma>.
- [2] Lisa Mears, Stuart M Stocks, Gürkan Sin, and Krist V Gernaey. A review of control strategies for manipulating the feed rate in fed-batch fermentation processes. *Journal of Biotechnology*, 245:34–46, 2017.
- [3] Tugce Martagan, Ananth Krishnamurthy, and Christos T Maravelias. Optimal condition-based harvesting policies for biomanufacturing operations with failure risks. *IIE Transactions*, 48(5):440–461, 2016.
- [4] Jon C Gunther, Jeremy S Conner, and Dale E Seborg. Fault detection and diagnosis in an industrial fed-batch cell culture process. *Biotechnology progress*, 23(4):851–857, 2007.
- [5] Bernhard Henes and Bernhard Sonnleitner. Controlled fed-batch by tracking the maximal culture capacity. *Journal of biotechnology*, 132(2):118–126, 2007.
- [6] Patrick Wechslerberger, Patrick Sagmeister, Helge Engelking, Torsten Schmidt, Jana Wenger, and Christoph Herwig. Efficient feeding profile optimization for recombinant protein production using physiological information. *Bioprocess and biosystems engineering*, 35(9):1637–1649, 2012.
- [7] ZITA Soons, JA Voogt, G Van Straten, and AJB Van Boxtel. Constant specific growth rate in fed-batch cultivation of bordetella pertussis using adaptive control. *Journal of biotechnology*, 125(2):252–268, 2006.
- [8] Marco Jenzsch, Stefan Gnoth, Martin Kleinschmidt, Rimvydas Simutis, and Andreas Lübbert. Improving the batch-to-batch reproducibility of microbial cultures during recombinant protein production by regulation of the total carbon dioxide production. *Journal of biotechnology*, 128(4):858–867, 2007.
- [9] MA Hussain, KB Ramachandran, et al. Design of a fuzzy logic controller for regulating substrate feed to fed-batch fermentation. *Food and Bioprocess Processing*, 81(2):138–146, 2003.
- [10] Liang Chang, Xinggao Liu, and Michael A Henson. Nonlinear model predictive control of fed-batch fermentations using dynamic flux balance models. *Journal of Process Control*, 42:137–149, 2016.
- [11] Stephen Craven, Jessica Whelan, and Brian Glennon. Glucose concentration control of a fed-batch mammalian cell bioprocess using a nonlinear model predictive controller. *Journal of Process Control*, 24(4):344–357, 2014.

- [12] Jiansheng Peng, Fanmei Meng, and Yuncan Ai. Time-dependent fermentation control strategies for enhancing synthesis of marine bacteriocin 1701 using artificial neural network and genetic algorithm. *Bioresource technology*, 138:345–352, 2013.
- [13] Carlos A Duran-Villalobos, Barry Lennox, and David Lauri. Multivariate batch to batch optimisation of fermentation processes incorporating validity constraints. *Journal of Process Control*, 46:34–42, 2016.
- [14] Tugce Martagan, Ananth Krishnamurthy, Peter A Leland, and Christos T Maravelias. Performance guarantees and optimal purification decisions for engineered proteins. *Operations Research*, 66(1):18–41, 2017.
- [15] TG Martagan, A Krishnamurthy, and P Leland. Managing trade-offs in protein manufacturing: How much to waste? *Manufacturing & Service Operations Management*, 2018.
- [16] Neythen J Treloar, Alex JH Fedorec, Brian Ingalls, and Chris P Barnes. Deep reinforcement learning for the control of microbial co-cultures in bioreactors. *PLOS Computational Biology*, 16(4):e1007783, 2020.
- [17] Saxena Nikita, Anamika Tiwari, Deepak Sonawat, Hariprasad Kodamana, and Anurag S. Rathore. Reinforcement learning based optimization of process chromatography for continuous processing of biopharmaceuticals. *Chemical Engineering Science*, 230:116171, 2021.
- [18] Hua Zheng, Wei Xie, and M. Ben Feng. Green simulation assisted reinforcement learning with model risk for biomanufacturing and control. *2020 Winter Simulation Conference (WSC)*, 2020. accepted.
- [19] Mohammad Ghavamzadeh, Shie Mannor, Joelle Pineau, and Aviv Tamar. Bayesian reinforcement learning: A survey. *arXiv preprint arXiv:1609.04436*, 2016.
- [20] Michael O Duff. *Optimal learning: Computational procedures for Bayes-adaptive Markov decision processes*. PhD thesis, University of Massachusetts Amherst, 2002.
- [21] Pascal Poupart, Nikos Vlassis, Jesse Hoey, and Kevin Regan. An analytic solution to discrete bayesian reinforcement learning. In *Proceedings of the 23rd international conference on Machine learning*, pages 697–704, 2006.
- [22] Ian Osband, Daniel Russo, and Benjamin Van Roy. (more) efficient reinforcement learning via posterior sampling. In *Advances in Neural Information Processing Systems*, pages 3003–3011, 2013.
- [23] Stephane Ross, Brahim Chaib-draa, and Joelle Pineau. Bayesian reinforcement learning in continuous pomdps with application to robot navigation. In *2008 IEEE International Conference on Robotics and Automation*, pages 2845–2851. IEEE, 2008.
- [24] Raphael Fonteneau, Lucian Buşoniu, and Rémi Munos. Optimistic planning for belief-augmented markov decision processes. In *2013 IEEE Symposium on Adaptive Dynamic Programming and Reinforcement Learning (ADPRL)*, pages 77–84. IEEE, 2013.
- [25] John Asmuth and Michael L Littman. Approaching bayes-optimality using monte-carlo tree search. In *Proc. 21st Int. Conf. Automat. Plan. Sched., Freiburg, Germany*, 2011.
- [26] John Asmuth, Lihong Li, Michael L Littman, Ali Nouri, and David Wingate. A bayesian sampling approach to exploration in reinforcement learning. *arXiv preprint arXiv:1205.2664*, 2012.
- [27] J Zico Kolter and Andrew Y Ng. Near-bayesian exploration in polynomial time. In *Proceedings of the 26th annual international conference on machine learning*, pages 513–520, 2009.
- [28] Pauline M Doran. *Bioprocess Engineering Principles*. Elsevier, Amsterdam, 1995.
- [29] Amos E. Lu, Joel A. Paulson, and Richard D. Braatz. ph and conductivity control in an integrated biomanufacturing plant. *Proceedings of the American Control Conference*, pages 1741–1746, 2016.
- [30] Amos E. Lu, Joel A. Paulson, Nicholas J. Mozdierz, Alan Stockdale, Ashlee N. Ford Versypt, Kerry R. Love, J. Christopher Love, and Richard D. Braatz. Control systems technology in the advanced manufacturing of biologic drugs. In *Proceedings of the IEEE Conference on Control Applications*, pages 1505–1515, 2015.
- [31] Moo Sun Hong, Kristen A. Severson, Mo Jiang, Amos E. Lu, J. Christopher Love, and Richard D. Braatz. Challenges and opportunities in biopharmaceutical manufacturing control. *Computers & Chemical Engineering*, 110:106–114, 2018.
- [32] Matthew C Coleman and David E Block. Retrospective optimization of time-dependent fermentation control strategies using time-independent historical data. *Biotechnology and bioengineering*, 95(3):412–423, 2006.
- [33] A. Gelman, J. B. Carlin, H. S. Stern, and D. B. Rubin. *Bayesian Data Analysis*. Taylor and Francis Group, LLC, New York, 2nd edition, 2004.
- [34] Kevin P Murphy. Conjugate bayesian analysis of the gaussian distribution. *def*, 1($2\sigma^2$):16, 2007.

- [35] Panayiotis Theodossiou. Financial data and the skewed generalized t distribution. *Management Science*, 44(12-part-1):1650–1661, 1998.
- [36] Tao Wang, Daniel Lizotte, Michael Bowling, and Dale Schuurmans. Bayesian sparse sampling for on-line reward optimization. In *Proceedings of the 22nd international conference on Machine learning*, pages 956–963, 2005.
- [37] Stéphane Ross and Joelle Pineau. Model-based bayesian reinforcement learning in large structured domains. In *Uncertainty in artificial intelligence: proceedings of the... conference. Conference on Uncertainty in Artificial Intelligence*, volume 2008, page 476. NIH Public Access, 2008.
- [38] Michael Kearns, Yishay Mansour, and Andrew Y Ng. A sparse sampling algorithm for near-optimal planning in large markov decision processes. *Machine learning*, 49(2-3):193–208, 2002.
- [39] Log-normal distribution. Log-normal distribution — Wikipedia, the free encyclopedia, 2021. [Online; accessed 10-Jan-2021].